Now where was I? Cortical function during ocular and oculo-manual pursuit

Lénaïc Borot

A thesis submitted in partial fulfilment of the requirements of Liverpool John Moors University for the degree of Doctor of Philosophy

August 2024

à Pierric,

à Loïc

Table of Contents

List of Figures

Abstract:

Coordinated eye and hand movements are often performed when carrying out daily activities. When executed concurrently with the goal of pursuing the same slow-moving moving object, the resulting smooth pursuit eye movement is facilitated by the available limb efference and afference. This is particularly evident when retinal input from the moving object is temporarily unavailable (e.g., during a transient occlusion), with concurrent limb movement providing extra-retinal input to the oculomotor system. Studies have shown that several cortical areas are involved in the control of smooth pursuit eye movement, and that their activity is mediated by factors that influence predictability of the object trajectory. However, the study of brain activity and functional connectivity between cortical areas has been limited to simple pursuit tasks, typically performed with eyes alone. The aim of the current thesis was to examine the impact of concurrent upper limb movement on cortical activity and network organisation in tasks of varying complexity and cognitive demand, which thus have greater fidelity with pursuit tasks performed when interacting with a complex and dynamic environment. In Chapter 2, a series of experiments was conducted using the Gorilla.sc online testing platform to examine the behavioural effects of performing a secondary change-detection task (colour or form stimulus array) concurrently (experiments 1-3) or consecutively (experiment 4) with a primary spatial prediction motion task. The primary task was performed with eyes alone (i.e., ocular pursuit) or with eyes and concurrent right upper limb movement (i.e., oculo-manual pursuit) in order to determine the impact of afferent and efferent signals. In Chapter 3, a lab-based version of the dual-task pursuit protocol was conducted that included a combination of eye tracking (i.e., video-oculography) and neuroimaging (Near InfraRed Spectroscopy - NIRS) of prefrontal cortical activity. In Chapter 4 a second lab-based experiment examined cortical activity within a wider network using a 24 by 24 NIRS optode array during ocular and oculo-manual pursuit of sinusoidal object motion (0.1Hz). This was done in a pre-test and post-test, which were separated by an adaptation phase in which participants pursued a continuously

visible object in the oculo-manual condition. Across the two lab-based experiments, it was found that differences existed in cortical activity and network organisation between ocular and oculo-manual tracking, and that these were most evident in areas of prefrontal cortex. There was also evidence that smooth pursuit eye movement was facilitated by concurrent upper limb movement, although this was greater when the task involved pursuit of sine-wave object motion (Chapter 4) compared to step-ramp motion (Chapter 3). These results bring new insight to understanding the cortical basis of oculo-manual facilitation during smooth pursuit eye movement, and could provide a basis for future study of populations with acute and chronic neurological conditions, who exhibit changes in cognitive and/or oculomotor function.

Declaration

I, Lenaic Borot, declare that no portion of the work referred to in the thesis has been submitted in support of an application for another degree or qualification of this or any other university or other institute of learning.

I, Lenaic Borot, hereby declare that this PhD thesis includes an original publication that has not been submitted for any other degree or qualification:

Borot, L., Ogden, R., & Bennett, S. J. (2024). Prefrontal cortex activity and functional organisation in dual-task ocular pursuit is affected by concurrent upper limb movement. *Scientific Reports*, *14*(1), 9996.

This project was funded by the Doctoral Training Alliance (DTA) Applied Biosciences for Health programme, which is supported by Horizon 2020 Marie Curie-Skłodowska Action funding.

Acknowledgments

I would like to thank first my supervision team, Professor Simon Bennett and Professor Ruth Ogden for their expertise and support, without which this PhD would not have been possible. Simon, from the biggening of this journey, when I arrived in Liverpool, a little lost in this new country, until the end of this 4 year-long work, you were just amazing. I have been very lucky to have a supervisor like you.

I also would like to thank my jury members, because you have turned an experience that I really apprehended, the viva, into a positive moment and a good memory. A huge thank you for that.

Thanks as well to the *Doctoral Training Alliance (DTA)* Applied Biosciences for Health programme, which is supported by Horizon 2020 Marie Curie-Sklodowska Action funding, for funding this project and without whom nothing would have been possible.

Je tiens aussi à remercier mes amis de Liverpool et d'ailleurs pour leur soutien indéfectible, pour toutes ces discussions, tous ces moments passés ensemble, certains sérieux et d'autres beaucoup moins, mais qui ont toujours réussi à me remonter le moral quand il le fallait.

Je tiens à remercier aussi mon ancien laboratoire de recherche, Euromov, ou j'ai toujours été accueillie les bras ouverts lors de mes séjours à Montpellier.

Merci aussi à ma famille qui, malgré la distance qui nous a séparés durant ces années de PhD, m'a toujours accompagnée dans mes pensées, et m'a toujours soutenue.

Pour finir je tiens à te remercier toi, Grégoire. Il n'y a pas assez de mots pour décrire tout ce que tu m'as apporté durant cette longue route qu'est le PhD et plus globalement durant toutes ces années depuis que nous nous connaissons.

Chapter 1: General Introduction

1.1 General background

In our daily lives, we are constantly interacting with a complex and dynamic environment comprising of people, objects and surfaces that can each move within the field of view. In order to perform simple actions such as eating, walking, climbing stairs, or more complex actions such as cycling or driving in the city centre, it is important to perceive accurate and reliable information about our relationship with the visual scene. Due to the physiology of the human eye and the associated neural pathways to the visual cortex and beyond, the location of eye gaze impacts upon the perception of the required information. For example, rod photoreceptor cells of the peripheral retina, which project to the parietal cortex via the magnocellular layers of the lateral geniculate nucleus (LGN), are sensitive to low-spatial, high-temporal frequency inputs that are typically associated with the perception of visual motion stimuli. Conversely, cone photoreceptor cells within the fovea of the retina, which project to the temporal cortex via the parvocellular layers of the LGN, are primarily sensitive to high-spatial, low-temporal frequency inputs that support perception of high acuity visual information (Merigan et al., 1991). Accordingly, stabilising (i.e., Vestibulo-Ocular Reflex or Optokinetic Nystagmus) or orienting (e.g., saccade, smooth pursuit or vergence) eye gaze on an object of interest (e.g., a coffee cup) is necessary to enable an individual to perceive characteristics such as shape, form and colour through foveal vision, while at the same time perceiving the motion of another object (e.g., the limb as it approaches a coffee cup) through peripheral vision: for a description of the different stabilising and orienting eye movements (see Box 1). Studies using microstimulation, neuroimaging or targeted lesions have identified several cortical areas involved in the control of gaze orienting eye movements (for a review see Krauzlis, 2004; Lencer et al., 2019), as well as how these are influenced by a transient loss of vision of an object of interest, such as if it were occluded (Lencer et al., 2004; Nagel et al., 2006). In addition, behavioural (Vercher et al., 1997) studies have shown that gaze orientation can be facilitated by extra-retinal input from concurrent upper limb movement, which can offset the loss of drive from

visual input when the object is occluded (Gauthier & Hofferer, 1976). However, only very recently have researchers started to examine the functional connectivity between these cortical areas, and to date only when performing simple ocular pursuit compared to fixation tasks (Schröder et al., 2020).

Box 1: Eye Movement (Pouget, 2019; Lencer et al., 2019)

- ***Saccades:*** are rapid and brief eye movements allowing to abruptly change the fixation point. Saccades can be elicited voluntarily, but also occur reflexively to the sudden appearance of an object whenever the eyes are open, even when fixated on an object.
- ***Vergence:*** makes it possible to direct the fovea of each eye towards a single object of interest, thus facilitating binocular fusion and the perception of depth. This requires moving the eyes in opposite (i.e., disconjugate) directions.
- ***Smooth pursuit eye movements:*** are rather slow eye tracking movements allowing to keep an object moving on the fovea. These movements are under voluntary control.
- ***Vestibulo-ocular reflex:*** stabilise the eyes in relation to the outside world, allowing accurate compensation for head movements, particularly during locomotion, and thus enabling precise vision to be maintained.
- ***Optokinetic Nystagmus:*** are slow compensatory eye movement to stabilise the gaze when large environmental models move in relation to the eyes.
- ***Fixation:*** This is not strictly considered as a type of eye movement. It is a period during which the eye remains relatively motionless (i.e., eye stationary interspersed with microsaccades), allowing extraction of detailed information around the point of fixation.

Therefore, the overall aim of the current thesis is to extend understanding of functional organisation in oculo-manual pursuit tasks that vary in complexity and cognitive demand, and thus have greater fidelity with everyday tasks requiring coordination between gaze orientation and upper limb movement. To this end, the following sections in this chapter will provide a general background on smooth pursuit eye movement, the role of cognitive processes such as working memory and attention, possible brain regions involved in smooth pursuit and how these may be measured and modelled, followed by an overview of work on facilitation of smooth pursuit by concurrent upper limb movement. A rationale is then provided that links each of the subsequent chapters and gives a brief description of the work conducted.

1.2 Smooth pursuit eye movement

While the stabilisation of eye movements is required to compensate for head movements when interacting with fixed objects in our surrounds, it is often necessary to voluntarily maintain one's gaze on moving objects. In the absence of head movement, this is done primarily through smooth pursuit eye movements (SPEM), which attempt to match eye speed to object speed, thus maintaining the retinal image of the moving object in the foveal zone (Lencer & Trillenberg, 2008). If there is a sufficient mismatch in velocity between the eye and object, the visual system perceives the resulting positional and velocity error (de Brouwer et al., 2002) and realigns the eye with very rapid saccadic movements (i.e., catch-up saccades). This same velocity error signal, traditionally known as retinal slip, was once thought to be the main driver of both the amplitude and timing of SPEM. However, such a simple control model would be limited by the neural delay in processing the velocity error signal, as well as the small fluctuations that occur continuously during SPEM. As a result, it is now well accepted that extra-retinal input also makes an important contribution during the two distinct phases of SPEM: initiation and maintenance.

In situations where the movement of the object cannot be anticipated (i.e., time of appearance) and/or predicted (i.e., velocity), initiation corresponds to the first 50 to 100ms after the object moves and is an open-loop control process in which SPEM is driven by the velocity error signal (Lencer et al., 2019). However, if participants have an expectation about the imminent movement of the object, whether based on previous experience (Barnes, 2008) or external cues (Jarrett & Barnes, 2005), they will voluntarily generate SPEM based on extra-retinal input. After an additional 100-150ms, the initiation phase gives way to the maintenance phase, during which SPEM is driven by a combination of extra-retinal and retinal inputs (Lencer et al., 2019). As well as maintaining gain near unity during this phase, extra-retinal input, such as an internal representation formed from experiencing a previous trajectory, enables participants to predict a change direction of SPEM in accord with cues in the environment (Kowler, 1989, Dallos & Jones, 1963; Barnes, 2008), and to cope with the loss of retinal input when the pursuit object is transiently occluded by another surface/object (Bennett & Barnes, 2003). In the latter situation, SPEM decays rapidly following object occlusion (Becker & Fuchs, 1985), but is maintained at a reduced gain if participants try to pursue an imagined moving object (Pola & Wyatt, 1997) or if the object is expected to reappear (Bennett & Barnes, 2003; 2004; see Figure 1.1). There is also a saccadic response that works in combination with reduced gain SPEM in order to locate the eyes close to the unseen position of the occluded object (Orban de Xivry et al., 2006). However, depending on the length of time for which the moving object is not visible, it inevitably follows that there will be a velocity error when the object reappears. Importantly, this error can be reduced through an anticipatory and predictive increase in eye velocity towards the object velocity to coincide with the time of object reappearance.

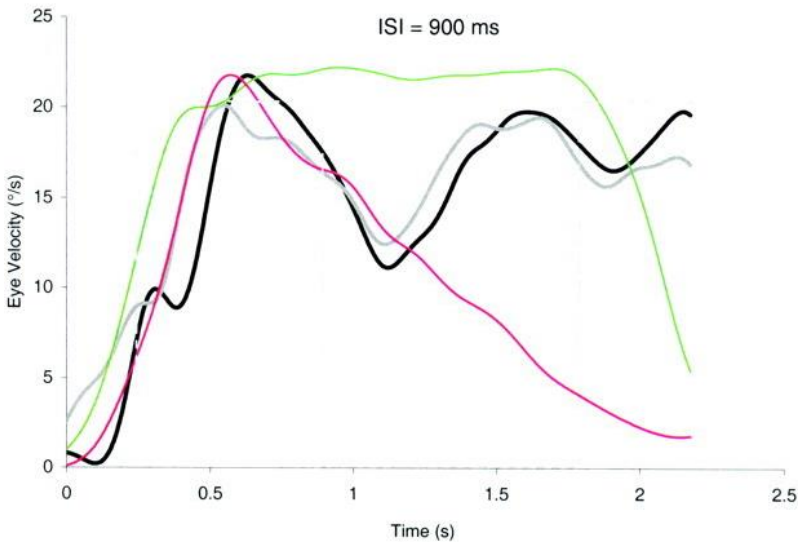

Figure 1.1: *Representation of eye velocity during pursuit of a momentarily occluded object (copied with permission from Bennett, S. J., & Barnes, G. R. (2003). Human ocular pursuit during the transient disappearance of a visual target. Journal of Neurophysiology, 90(4), 2504-2520. Figure page 2510). The black line represents eye velocity during pursuit with a random occlusion duration. Grey line represents eye velocity during pursuit with a blocked occlusion duration. In comparison, the green line represents eye velocity when the object remains visible, and the magenta line represents eye velocity when the object is not expected to reappear after occlusion.*

The SPEM control system can be studied using sinusoidal stimuli. This type of stimulus makes it possible to demonstrate that SPEM is not solely controlled by a linear feedback system. Indeed, if the system was purely linear, the periodic stimuli would always induce an oculomotor response that is sinusoidal and corresponds closely to the stimulus in terms of magnitude (or gain) and temporal characteristics (or phase). Although this phenomenon occurs when the stimulus is of low frequency (<0.4Hz), at higher frequencies there is an increased phase delay. Importantly, this is lower than the expected phase delay duration for a linear feedback system (Barnes, 2008). This may be explained by the inclusion of a predictive mechanism, which would form in the early cycle(s) of the ocular response. Another model using eye velocity and acceleration as an input regulating gain and phase lag during smooth pursuit has also been proposed (see Krauzlis & Lisberger, (1989). This extra-

retinal input was traditionally conceived as an efferent copy of the oculomotor command (Robinson et al., 1986), but it is now widely accepted that factors such as expectation, attention and memory must also be taken into account (see Barnes, 2008 for a model and Figure 1.2).

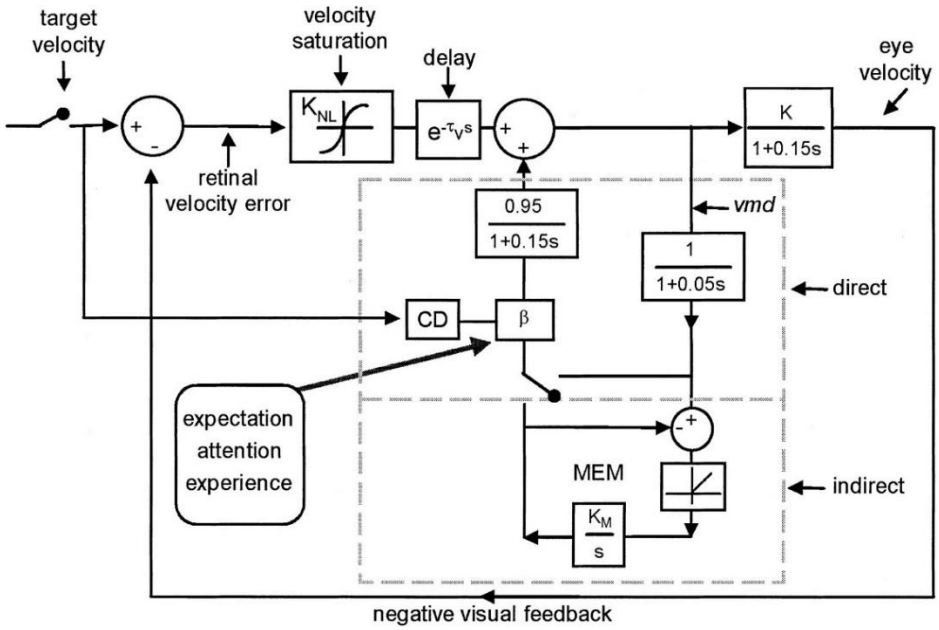

Figure 1.2: *Model of ocular pursuit (copied with permission from Bennett, S. J., & Barnes, G. R. (2004). Predictive smooth ocular pursuit during the transient disappearance of a visual target. Journal of neurophysiology, 92(1), 578-590. Figure page 587). This model includes extra-retinal input from a direct or indirect (predictive) loop (within the grey dashed line). If the participant has no expectation of the future object motion (e.g. no prediction), the indirect loop is activated. Conversely, if there is prediction, the indirect loop is activated, which engages the use of a short-term memory (MEM) of previous events (expectation, experience and attention). The indirect loop allows for a longer storage of velocity information and can be used to anticipate the movement of the object (i.e., in the absence of retinal input). The direct loop simply maintains eye velocity, although at less than unity gain in absence of retinal input. Indeed, when an object is occluded, a conflict detector (CD) temporarily reducing the gain β. When the object becomes visible again, the gain β is reinstated thus enabling eye velocity to increase back to pre-occlusion levels (see Figure 1.1). The input to both direct and indirect loop comes from a copy of the visuomotor drive signal (vmd). K = open-loop gain, and internal dynamics are controlled by low pass filters (time constant 100–150ms).*

1.3 Smooth pursuit, attention and working memory

As described above, to maintain an object of interest moving in a fronto-parallel plane in foveal vision, participants exhibit a combination of SPEM and catch-up saccades. This oculomotor response facilitates the perception of object characteristics such as shape and texture, and concurrently enables covert visual attention to be directed to low acuity input in the peripheral visual field on the layout, motion, and colour of surrounding objects. Interestingly, although it is well accepted that greater attentional resource is allocated to a pursuit object than background objects (Khurana & Kowler, 1987), thus enhancing gain by reducing the impact of an optokinetic effect, there has been much debate about exactly where and how (i.e., spatial extent) covert attention is located during SPEM, and whether it impacts upon performance of SPEM per se.

Based on the assumption that the control of SPEM requires expectation about a moving object's future trajectory, Lovejoy et al., (2009) examined the hypothesis that covert attention should be located ahead of a moving object's current (i.e., veridical) location (see Tanaka et al., 1998; van Donkelaar & Drew, 2002). Using a letter discrimination task, it was found that performance was more accurate when the probe stimulus (i.e., number 3 or letter E) was presented at a location coincident with the cue (e.g., pursuit object). Specifically, performance accuracy deteriorated when the probe was presented at ±0.6deg of the cue and was not significantly different from chance when the probe was presented at ±1.2deg of the cue. Analysis of eye movements indicated that overt attention (i.e., gaze location) was close to the cue (average offset of 0.24deg for 16deg/s ramp), and that variations in the magnitude of offset did not influence discrimination performance. The authors suggested that previous evidence for covert attention being located ahead of the pursuit object was most likely due to conditions that created attentional capture following the abrupt onset in motion or luminance of a probe stimulus (e.g., sudden appearance of a saccade target during smooth pursuit of a moving object). The finding that covert attention is coincident

with a pursuit object in the letter discrimination task was replicated by Watamaniuk & Heinen, (2015). In addition, when the stimulus array formed the shape of a plus sign, it was found that the spatial extent of covert attention was dependent on the spacing between characters, as well the total number of characters. For example, with stimulus arrays of the same maximum eccentricity (4deg), discrimination performance deteriorated from approximately 80% to 60% with an increase from 5 to 9 characters. It was suggested that these effects were not caused by crowding between characters, which were separated by at least 2deg, and instead were related to limits in serial processing within the 200ms probe presentation. Importantly, though, discrimination performance of 60-80% was well above chance, thus indicating that covert attention during pursuit has a symmetrical spatial extent of at least 4deg relative to gaze location.

To reconcile these equivocal findings, it has been suggested that by default covert attention is located slightly ahead (1.5deg) of a pursuit object (for a novel EEG tagging method see Chen et al., 2017), but can be flexibly allocated to different eccentric locations when this offers a potential advantage (see also Heinen et al., 2011). Watamaniuk & Heinen, (2015) found that this flexible allocation of covert attention task did not impair SPEM even at the most difficult level of their secondary identification task. In addition, there was no difference in performance of the identification task between pursuit and fixation conditions, thus indicating that pursuit did not require additional attentional resource. In fact, SPEM was enhanced (i.e., higher steady-state gain and fewer catch-up saccades) compared to a control condition in which participants pursued a single moving object. The authors suggested that this could simply have been a result of participants trying harder, or that performing the identification task was facilitated by maintaining gaze at the centre of the stimulus array, which thereby led to enhanced SPEM. The latter explanation is consistent with the finding that pursuit of a large stimulus comprising several individual elements requires less attention than pursuit of a single small object (Heinen et al., 2011), which then frees-up attention for the performance of secondary tasks (Jin et al., 2013; 2014).

Others, however, have found interference between SPEM and performance of a secondary working memory task requiring covert attention (Kerzel & Ziegler, 2005; Yue et al., 2017). Across a series of studies, Kerzel & Ziegler, (2005) found that visual short-term memory (VSTM) capacity (i.e., ability to identify change in spatial layout between a memory and probe array comprising 3, 6 or 12 elements with an overall size of 17deg wide x 20.4deg high) was consistently worse in conditions involving pursuit than fixation. The deleterious effect of SPEM on VSTM was no longer present when the stimulus array was maintained in foveal vision (1deg wide x 1deg high), or when the secondary task involved identification of a change in colour rather than spatial layout of elements in the stimulus array. The authors concluded that SPEM requires attentional resource in order to monitor differences between the fovea and pursuit object, and that this limits availability of covert attention to concurrently process and encode into VSTM the spatial layout of elements in peripheral vision. The finding of no such limitation for colour elements (n = 8), even though they spanned the same extent as the spatial stimulus array, was suggested to be a result of covert attention for processing colour elements being unrelated to attention directed to pursuit of the moving object, and thus not causing any conflict when encoding and storing the elements in VTSM (i.e., processing across different attentional dimensions).

Although Kerzel & Ziegler, (2005) found no effect of SPEM on colour VSTM (i.e., synonymous with colour working memory), evidence of a mutual interference has been reported by Yue et al., (2017). In their change-detection task, colour working memory was impaired when participants performed SPEM compared to fixation in the cue-probe interval, whereas SPEM was impaired when participants performed pursuit plus the colour working memory task vs pursuit alone. The authors proposed that the interference between SPEM and colour change detection task in their study could be the result of competition for resources processed in a fronto-parietal network. Indeed, the fronto-parietal network (FPN), which includes dorsolateral PFC (BA 9/46), pre-motor cortex (BA 6), the supramarginal gyrus (BA 40) and posterior parietal cortex, is suggested to have a central role in cognitive

functions such as working memory (Menon & D'Esposito, 2022), which is known to be involved in SPEM.

1.4 Brain involvement in SPEM

Neuroimaging research and studies in people with brain lesions, highlights several cortical areas involved in SPEM that seem to have a functional architecture very similar to that of the saccadic system (for a detailed review see Krauzlis, 2004; Lencer et al., 2019). These are discussed below, although an exhaustive account of all cortical and sub-cortical areas is not provided as this falls outside the scope of the current thesis. In addition, neuroimaging of adult humans performing SPEM has typically involved fMRI, which provides an indirect indication of neural activity based on neurovascular coupling.

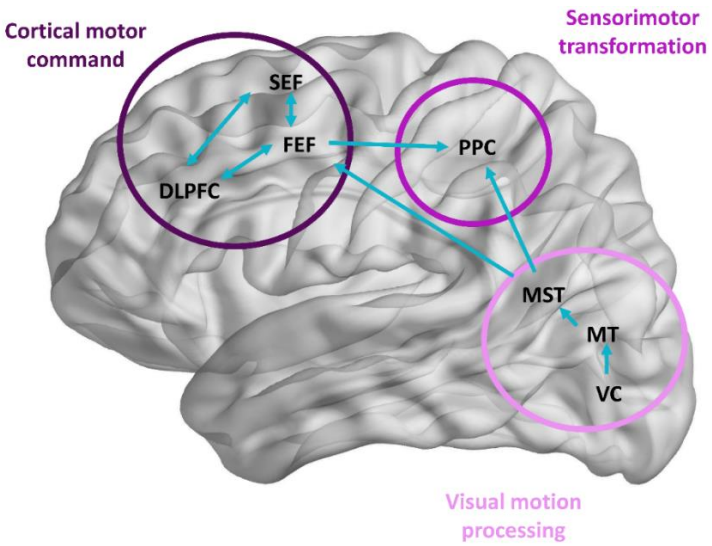

Figure 1.3: *Hypothetical scheme for the smooth pursuit network (inspired by Krauzlis, 2004, Lencer & Trillenberg, 2008 and Lencer et al., 2019). Visual cortex (VC) projects to visual area V5 (MT and MST) and seems to be involved during visual motion processing. From there, signals are transmitted to the posterior parietal cortex (PPC) for sensorimotor transformation and to frontal areas (FEF). Further frontal smooth pursuit regions in humans involve the supplementary eye field (SEF) and dorsolateral prefrontal cortex (DLPFC), which together are involved in higher cognitive control and cortical motor command.*

Visual cortex to V5/V5a – MT/MST

The processing of image motion involves the primary visual cortex (V1), which projects directly and indirectly to the human extra-striate visual area V5/V5a. In the primate cortex, V5/V5a corresponds to the middle temporal visual area (MT, assumed to correspond to Brodmann area 19, 37 and 39 in human cortex) and the medial superior temporal visual area (MST, assumed to be in occipito-temporal-parietal junction adjacent to MT in human), which share strong projections (Lencer et al., 2019). Barton et al., (1996), who studied brain activity by fMRI showed a greater signal intensity in the lateral occipito-temporal cortex during pursuit of the moving object than during a motion perception task (e.g. fixed eyes, unattended task), however this difference is reduced when participants had to carry out motion perception task while they were asked to count the number of times a marker stripe appeared (e.g., attended task). The authors suggest that the lateral occipito-temporal cortex receives extra-retinal signals during SPEM including potentially attentional input, corollary eye movement information or pursuit command. The authors also proposed that the presence of extra-retinal signals suggest that the lateral occipito-temporal cortex may contain a human counterpart of MT, as well as MST (Barton et al., 1996). However, while MT seems to encode the first-order elements of movement (i.e., speed, direction, acceleration), MST appears to have higher-order movement processing capabilities (Lencer et al., 2019). For example, Ilg & Thier, (2003) demonstrated a dissociation between MT and MST in an eye tracking task involving visual and non-visual stimuli (e.g., imaginary object). In fact, unlike MT, MST seems to respond to non-visual stimulus presentation, implying it receives extra-retinal inputs. In addition, MT lesions produce deficits in the initiation of SPEM, while MST lesions appear to produce particularly pronounced directional deficits. These results highlight a general distinction between the two cortical areas. MT is thought to be more widely involved in initiating SPEM, while MST is thought to be more important in maintaining SPEM (Krauzlis, 2004). These visual areas also appear to receive extra-retinal input from other cortical areas such as FEF and IPS (Figure 1.3).

Posterior Parietal Cortex (PPC)

V5/V5a neurons (equivalent to MT and MST in human) project visual information about moving objects for perceptual analysis to the intraparietal sulcus (IPS) of the posterior parietal cortex (PPC) and frontal areas (FEF). In general, the PPC is involved in shifting attention during eye movement tasks, including the maintenance of foveal fixation (Lencer et al., 2019), either by saccades or SPEM. Indeed, Tian & Lynch, (1996) described how separate subregions of the FEF areas associated with saccades and SPEM (see below) receive inputs from adjacent and non-overlapping sub-regions of lateral intraparietal area (LIP) of PPC. A similar functional organisation of the human and monkey IPS was described by Konen & Kastner, (2008). Specifically, the authors showed that the human PPC contains six topographically organised zones along the intraparietal sulcus (IPS1-IPS5) and the superior parietal lobule 1 (SPL1). Consistent with the functional organisation of monkey PPC, there was shift in eye movement representation along the IPS, with a greater preference for saccades in SPL1 and SPEM in the IPS5. This seems to be confirmed by the study of eye tracking in patients with a lesion in the right PPC, who show a bidirectional deficiency of SPEM with lower gain than healthy subjects in both horizontal directions (Heide et al., 1996). Activity in the PPC, particularly at the IPS has often been related to saccade planning, but it also appears to be related to saccade suppression during SPEM, as well as in the representation of eye position as part of the extra-retinal mechanism (e.g. efference copy) (Nagel et al., 2006; Lencer et al., 2019). Indeed, this suggestion seems to be consistent with Lencer et al., (2004) who also show the role of PPC in SPEM maintenance during occlusion. Specifically, there was an increased BOLD response in SPL, and IPS during pursuit with object occlusion compared to continuous object presentation. Also, while not activated in smooth pursuit of a continuously presented object, they found that the supramarginal gyrus seemed to be involved in control of SPEM when the object is occluded.

Frontal Eye Field (FEF) and supplementary eye field (SEF)

The frontal eye field region (FEF) is well known to be the main cortical region involved in control of initiation and maintenance of SPEM (Krauzlis, 2004). This can be seen in the work of Heide et al., (1996), who showed greater directional deficits of SPEM in patients with lesions in the right FEF. This was particularly evident for SPEM in the right direction, which had a low gain with frequent interruptions by catch-up saccades. Moreover, this phenomenon was more pronounced with predictable periodic stimuli, thus indicating that predictive gain of SPEM was more sensitive to damage induced by FEF lesions. Interestingly, it has also been shown that while the command generated by FEF contributes to maintenance of SPEM, it has a greater impact on initiation and prediction (Lencer et al., 2019). Fukushima et al., (2002) studied the activity of FEF by registering individual units in monkeys during an object occlusion pursuit task. Their results show that several FEF neurons are involved in the prediction of object trajectories. However, other frontal regions, namely the supplementary eye field (SEF), which is located in the dorsal medial frontal lobe in close proximity to the supplementary motor area (SMA), and has connections with FEF, seems to be involved in immediate motor planning and prediction (Lencer et al., 2019). Heinen, (1995) have studied the activity of SEF neurons (e.g. dorsal medial frontal lobe) in monkey during pursuit. Their results show that SEF neurons show some preference for pursuit direction and can maintain their activity in the absence of a visual object, indicating that their responses are influenced by both retinal and extra-retinal inputs. For example, in a study by Shichinohe et al., (2009) who trained macaques to perform a SPEM task based on memory and decision making (e.g., go, no-go task), it was found that SEF was involved in signal and memory coding of the visual direction of movement, the decision whether or not to track the object and the preparation of the movement.

Prefrontal cortex

The PFC is associated with working memory and is suggested to be involved in higher-order control of SPEM pursuit, such as short-term learning of

sequences (Burke & Barnes, 2008) and predicting the onset and trajectory of a moving object during transient blanking/occlusion (Lencer et al., 2019; Bennett & Barnes, 2004). There is evidence that DLPFC provides extra-retinal input related to prediction in SPEM, especially when the object is occluded. Indeed, Nagel et al., (2006) suggested that predictive processes operating in DLPFC provide extra-retinal input, and that the DLPFC appears to be involved in compensatory mechanisms when the speed of SPEM decreases. This was particularly evident during maintenance of SPEM in the absence of a visual object. Indeed, Ding et al., 2009 also reported an increased activity in DLPFC during a task requiring tracking and predicting the location of an occluded moving object compared to a task where the object was always visible. This is consistent with neurophysiological and neuroimaging studies that have highlighted the involvement of DLPFC in higher order cognitive processes. Indeed, DLPFC is well known to be part of the fronto-parietal network known to play an important role in working memory (Menon & D'Esposito, 2022). Another part of PFC, the medial PFC (BA10) is also suggested to be involved in in cognitive processes. More specifically, Mansouri et al., (2017) and Koechlin et al., (1999) suggest that this area is acting in cognitive branching and would be involved when it's required to keep information in order to maintain the goal of a primary or main task while allocating simultaneously attention to perform a secondary task goal.

Functional connectivity in SPEM

Schröder et al., (2020) studied, using fMRI, the functional connectivity *in vivo* of human brain areas known to be activated in SPEM with different object frequencies compared to a fixation task. Their results showed a task-dependent functional connectivity (fixation vs. SPEM) involving visual, frontal and parietal regions. However, a higher object frequency, although leading to a deterioration in performance, did not seem to influence functional connectivity. Ding et al., (2009) also studied the changes in functional link between cortical areas involved in pursuit of a continuously presented object and when the object was momentarily occluded. Their results show that the

correlation between cortical areas is modified with occlusion. More precisely, during SPEM of a continuously visible moving object there a strong correlation between the bilateral FEF and DLPFC. Conversely, SPEM in a condition with a momentary occlusion of the object resulted in a strong connectivity between left and right FEF and left and right DLPFC, as well as strong connectivity in the right hemisphere between DLPFC and FEF compared to the left hemisphere.

As mentioned above, several brain networks involving PFC, as well as other cortical areas that are part of the SPEM network, are known to be involved in cognitive control and executive function (Menon & D'Esposito, 2022). As reported previously, some cortical regions tend to show a higher activation during SPEM of an occluded object (Lencer et al., 2004; Nagel et al., 2006), which is a more attention-demanding task requiring working memory to represent the unseen object trajectory. While the strength of the functional link between two cortical areas can help identify the SPEM brain network, to understand fully the relationship between those cortical areas, it is necessary to determine the pattern of connections between multiple cortical areas (network topology). Changes in network topology can be investigated using Graph theory metrics, calculated and compared between rest and performance of motor or cognitive tasks as developed in the following paragraph.

1.5 Activation, connectivity and topology

As detailed above, human brain activity during SPEM has been studied in terms of the function served by a specific region, or how several regions may be involved concurrently. These two approaches are different but complementary (Horien et al., 2020). One of the first interests in neurosciences was to identify the cerebral area involved in a specific cognitive or behavioural function. This approach was based on the assumption that a function was localized in a specific region of the brain (e.g. localizationism) and originated from Gall's phrenology, which argued that mental faculties were localised in a specific brain region and that this region could be identified in relation to the bumps on the skull. Later, in the 1900s

(e.g. work on brain parcellation by Brodmann in 1909), a major scientific contribution helped to map distinct regions of the brain and assign them specific functions. For example, Broca in 1861, associated the inability to articulate words to a lesion of the left frontal lobe. This was followed by Wernicke's work in 1873, which associated damage to the left posterior superior temporal gyrus with a deficit in language comprehension (Nasios et al., 2019). Latter evidence started to show that several brain areas could be activated for the same cognitive or behavioural function. Building on this early pioneering work, the advent of modern brain imaging techniques has resulted in huge advances in understanding. Functional activation of the brain regions involved in the performance of a task relative to a baseline can now be quantified with varying temporal and spatial precision by the change in BOLD signal for magnetic resonance imaging (fMRI), electrical activity for electroencephalography, or oxy-haemoglobin (O_2Hb) concentration combined with a concomitant decrease in deoxy-haemoglobin (HHb) concentration for near infrared spectroscopy (fNIRS).

Importantly, however, a relative change in activation of brain regions does not provide information on the nature of the links and (statistical) dependence between these different regions. Indeed, two brain regions may be activated during the task but not be statistically linked/dependent on each other (the reverse may also be true). It is therefore becoming increasingly evident that functional brain networks are necessary to understand simple behaviours, as well as those involving higher cognitive function (Reijneveld et al., 2007). Wernicke and Brodmann were aware of the importance of connectivity and networks in the understanding of brain function (Fornito et al., 2016), but did not have the neuroimaging methods available to measure and visualize brain organization. With the growth in the science of networks and technological improvement of neuroimaging methods, the study of brain functional networks has become an important focus of neuroscience in the twenty-first century (Fornito et al., 2016). In addition, methods such as DTI (diffusion tension imaging) have provided better understanding of the white matter composition and thus how this provides the means for structural connectivity between different parts of the brain. Together, this has resulted in researchers

studying the communication between brain areas and how this communication can contribute to a specific cognitive or behavioural function. An important concept was that communication between different brain areas may play an important role in a cognitive/behavioural function, even if those areas were not activated in the traditional sense (Ito et al., 2020).

A seminal study reported by Biswal et al., (1995), recorded participants brain activity while they performed a task (finger tapping) and during rest. Surprisingly, while Biswal et al., aimed to find a method to remove the physiological noise in the signal (cardiac rhythm, respiration), they discovered that even after having remove this noise in the rest condition time series, a functional pattern was still present in the data. Specifically, after having defined a seed region in left motor cortex, they obtained a strong correlation between bilateral motor cortices, and not a random correlation that would be expected if the rest condition resulted in no "structured" signal fluctuations (Lowe, 2010). This result suggested that bilateral motor cortices have a functional activity even at rest and paved the way for researchers to study the resting state functional connectivity between other bilateral cortical areas, as well as inter-hemispheric and intra-hemispheric connectivity between multiple cortical areas.

Brain connectivity can be defined from a primary point of view by the link between neurons (i.e., structural connectivity via white matter tracts), and can be investigated globally via diffusion tensor imaging (DTI). However, estimating the location and role of these connections does not answer the question of how they are involved in the task. Accordingly, other methods of analysis have been developed, such as effective connectivity and functional connectivity. The former is linked to structural connectivity but is based on strong a priori hypotheses and models of causal interactions between neural nodes (i.e., channels for fNIRS systems which correspond to the measurement zone comprised between the source and detector optodes). Functional connectivity (fMRI, EEG, fNIRS) reflects the statistical dependence between two or more time series associated with neural nodes. To date, there has been a focus on resting state connectivity, which has resulted in the identification of several intrinsic brain networks (Seitzman et al., 2019; Van Den Heuvel &

Pol, 2010), such as the default mode network, FPN, DAN, visual network and more. Another important reason for measuring resting state functional connectivity is the possibility to study both task positive and negative networks, as well as their coordination. Impaired task positive and negative network organisation has been reported in specific populations (Liu et al., 2012; Mills et al., 2018), as well as being used to study brain activity of people with altered motor or cognitive function without having to complete cognitive or motor tasks.

To date, there are many methods to quantify functional connectivity, with the choice depending on the underlying research question. In a very simple way, one can imagine brain activity in two nodes being represented by perfect sinusoids, which are then analysed to determine what characterises the statistical link between these two time series. In this example, the link can be understood in terms of measures such as phase locking (i.e., in phase and antiphase), amplitude difference, correlation, and coherence (for a review see Bastos & Schoffelen, 2016). These methods are also dependent on the domain in which they are located (time domain, frequency domain or both). Network organisation can be understood as a compromise between two properties: functional integration and segregation (Sporns, 2013; see Figure 1.4). Segregation refers to clustered communities of nodes that are highly connected (functional coupling) with each other and support functional specialisation but have little connection with other communities. Integration refers to a globally strong functional coupling (information sharing) of a network, including within and between communities (Sporns, 2013). Because of its intrinsic organisation, the brain is considered to be the complex system "par excellence" (Sporns et al., 2004). This complex spatial organisation of the brain enables an economical network organisation (locally and globally efficient), which is neither completely lattice nor completely random, thus reflecting a compromise between efficient information transfer and low cost (Achard & Bullmore, 2007). Indeed, a completely lattice like brain network will have a low-cost in terms of supporting connection but does not favour efficiency in term of integration of information processing. Conversely, a random organisation will favour efficiency with more long-distance

connections, but this will also lead to a high-cost network organisation (Bullmore & Sporns, 2012). It has been suggested that task demands can result in oscillations between more lattice (more segregated) or random (more integrated) network organisation (Fornito et al., 2016; Cohen & D'Esposito, 2016). For example, increased cognitive demand would lead to a more globally efficient brain organisation and less clustered network, with more long-distance connections between brain regions, leading to efficient transfer of information but less economical network organisation. Conversely, a return to low cognitive task demand would be associated with a less globally efficient but more locally efficient (clustered) organisation, which has a more economical network organisation. Importantly, the authors also highlighted that these changes in network organisation are related to task performance. The implication is that brain network organisation, conceived as a balance between integration and segregation, is adaptively modified as a function of task demand (Cohen & D'Esposito, 2016).

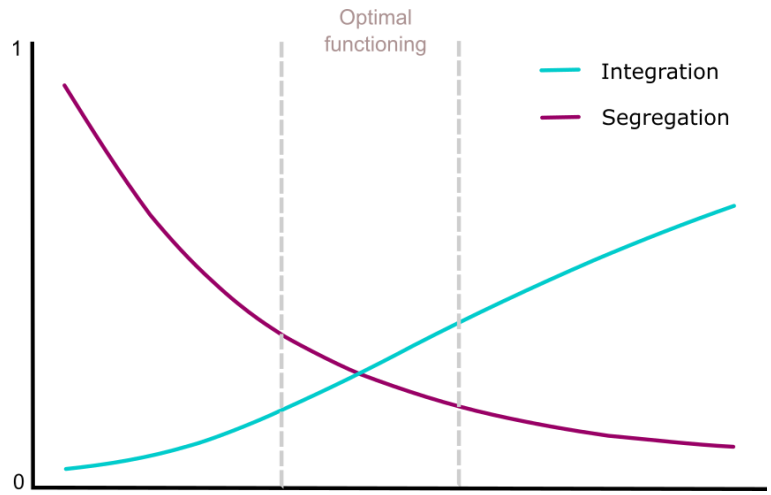

Figure 1.4*: Schematic curve of integration and segregation (Wang et al., 2021), where optimal functioning (complex network organisation, Lord et al., 2017) occurs between the grey lines and corresponds to a brain network that is neither completely lattice (left part of the curve with high segregation and low integration) nor completely random (right part of the curve with high integration and low segregation.*

A property of a network, like topology or information transfer, can be studied using Graph Theory (for common properties of Graphs see Box 2). This method originated from the mathematical work of Euler in the 1700's, whose theorizing about "the bridges of Konigsberg" problem involved trying to find a walking path that crossed all seven bridges on the two sides of the river Pregel, but only a single time. By representing the problem as an abstract network (e.g. a Graph), Euler was able to prove that the problem cannot be resolved (Reijneveld et al., 2007; Sporns, 2016). Moreover, he showed that the exact positions of the seven bridges (i.e., size and distance from each other) was not the key information, and instead that it was necessary to understand their topology (i.e., which bridges connect to which islands or riverbanks). The non-reliance on exact geometry in Graph theory has made it a widely used tool for studying brain network organisation. Indeed, a brain graph can be constructed from connectivity matrices (correlation between time series from two brain regions), where each brain region is a node (channel for fNIRS) and the correlation value between each node is an edge (see box 2 and Figure 1.5) (Fornito et al., 2016). From a brain graph, characteristics of the network topology such as for example local and global efficiency can then be extracted.

Box 2: Graphs properties (Sporns, 2016; Rubinov & Sporns, 2010; Fornito et al., 2016)

- ***Node:*** neurones, brain regions (e.g. channels for fNIRS) (Figure 1.5C)

- ***Edges:*** connection, pathway between nodes (e.g. functional link) (Figure 1.5C)

- ***Path:*** sequences of linked nodes that visit a node only ones.

- ***Shortest path length:*** reflects the minimal number of links that have to be crossed to go from one node to another.

- ***Global efficiency:*** the average of inverse shortest path lengths in the network. Reflect the efficiency of information exchange in the network. Measure of network integration (Figure 1.5).

- ***Local efficiency:*** the global efficiency computed on node neighbourhoods. Reflect the integration between the neighbour of a node when this node and edges are removed. Measure of network segregation (Figure 1.5).

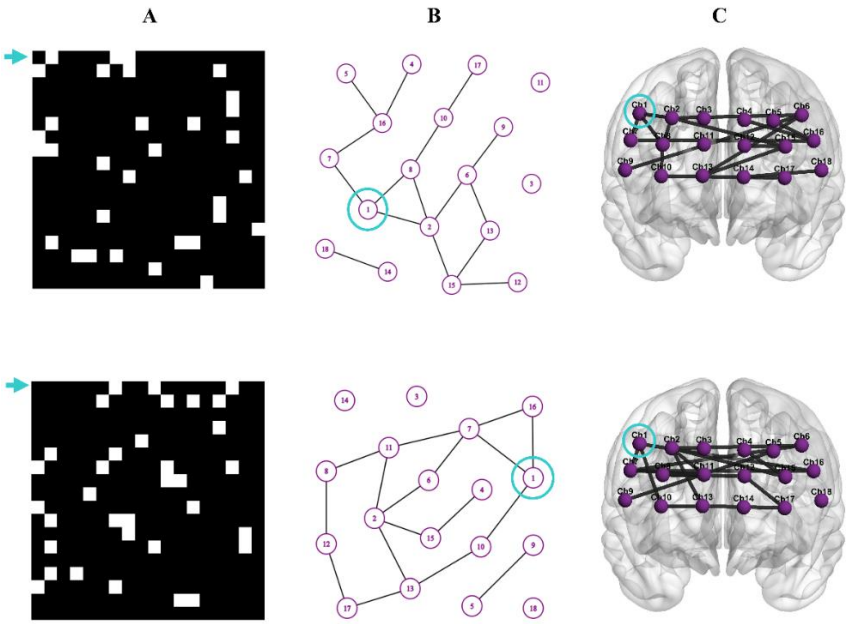

Figure 1.5: *A) Example of two unweighted symmetrical connectivity matrices generated using matlab comprising (black = 0: no connections; white = 1: connection exists) 18 nodes with an edge density of 16 (top) and 17 (bottom). The matrices comprised different connections but were generated in order to set an identical local efficiency of node 1 in the top and the bottom (LE= 0.333), as well as identical Global efficiency of the two networks (0.2615). B) Optimised representation of the graph generated using Graph Editor (csacademy.com), where each node is represented as a purple circle and edges (connection = 1 in the matrices A) as black lines. C) Representation of the networks on the brain with channel (Ch, purple dots) corresponding to nodes and edges (black lines). While Local efficiency of node 1 and Global efficiency are identical between the two networks, one can see that the individual network connections are quite different.*

1.6 Oculo-manual coordination

Previous studies have reported improved performance of SPEM, such as increased maximum velocity and gain, and reduced latency of pursuit onset, when object movement is related to simultaneous upper limb movement (Bennett et al., 2012; Gauthier et al., 1988; Koken & Erkelens, 1992; Gauthier & Hofferer, 1976). The most comprehensive work on this

issue can be traced back to Vercher, Gauthier and colleagues, who conducted experimental studies involving neurotypical adults (i.e., humans and baboons), deafferented baboons, and humans with ischaemic nerve block, performing oculo-manual tasks (i.e., finger, upper arm) of internally-generated and externally-generated moving objects. The results of the experimental studies, as well as simulations and modelling, showed that the eye movement system and the hand movement system could share a common input (i.e., interdependence), although not necessarily a common command (i.e., dependence). According to the coordination-control model described by Vercher et al., (1997), there is an exchange of information from non-visual signals (afference, efference copy) between the arm motor system and the oculomotor system, which permits oculo-manual facilitation, as well as adaptation when the arm and eye move with different direction, delay and/or gain. The integration of this extra-retinal information from upper limb movement is thought to occur within the cerebellum (Vercher & Gauthier, 1988), which is involved in integrating inputs from multiple cortical regions for the purpose of timing and learning visuo-motor skills (see Miall, et al., 2001).

Another key outcome from their series of elegant experiments in monkey and human, was the suggestion by Vercher, Gauthier and colleagues that efference copy of the moving arm plays a key role in synchronisation with eye movements at motion onset, while afference (i.e., proprioception) from the arm accounts for increased smooth pursuit accuracy (i.e., gain and phase). The role of arm efference copy in oculo-manual coordination was demonstrated by comparing SPEM during active and passive arm movement (Vercher et al., 1996). For example, when the arm was actively moved by the participant, the latency of SPEM was on average -5ms before object motion onset. However, when the arm was moved by the experimenter (passive condition), the latency of SPEM was on average 130ms after object motion onset. Similar effects were found in two deafferented patients, who exhibited an average SPEM latency of -8ms in the active condition. Therefore, it was suggested that in the absence of arm proprioception, efference copy

associated with active arm movement is sufficient to synchronise the oculomotor and arm motor systems.

The role of arm afference (i.e., proprioception) in smooth pursuit was shown in a study by Gauthier and Mussa Ivaldi (1988), where baboons were trained to track different visual and imagined stimuli (e.g., step ramp, sine and square wave) with eyes alone or eyes and hand. After training, the baboons underwent surgery (dorsal root rhizotomy - cutting the nerve roots) inducing a loss of afferent information from the right arm. After surgery, the baboons were unable the to track the slow-moving externally-generated object with their right arm, or track smoothly with their eyes the imaginary object displaced by the deafferented limb in total darkness. Similar evidence for the contribution of arm afference to SPEM was found in human deafferented participants (e.g., people without proprioception) and participants with an ischaemic block applied to the biceps (e.g., temporary interruption of proprioception). For example, Vercher et al., (1996) found that in deafferented participants, the lack of information from proprioception did not negatively impact upon the temporal synchronisation between arm motion and smooth pursuit onset. However, arm proprioception did appear to be necessary for the parametric adjustment between arm and eye motor control during the maintenance phase.

As said previously, the integration of this extra-retinal information from upper limb movement was suggested to involve the cerebellum (Vercher & Gauthier, 1988), but oculo-manual coordination is complex, and this function is not confined to a single area. Indeed, Rizzo et al., (2020), suggest that the cerebellum would be predominantly involved in the temporal prediction processes of eye and hand movements, while a fronto-parietal network (e.g., FEF and PPC) would be indispensable to the spatial prediction process, both of which are critical aspects of functional movement control. This involvement of a wider network comprising frontal and parietal cortex is also suggested by Battaglia-Mayer & Caminiti, (2018). Indeed, the authors highlighted the major role of parietal cortex and suggested oculo-manual coordination emerged from parietal operations while interacting with more frontal regions. More specifically the SPL and IPL via intraparietal

connection, would be the first stage of oculo-manual coordination, while longer connections between frontal (e.g. supplementary motor area, dorsal premotor cortex and motor cortex) and parietal cortex would be the domains of eye and hand motor output.

1.7 Outline and Rationale

As detailed previously, SPEM involves processes such as attention, working memory and prediction, and even more so when the object is momentarily occluded. The inclusion of a secondary task that also involves working memory increases the overall cognitive demand and can impact negatively on SPEM. Conversely, a positive impact on SPEM can occur when it is performed with concurrent upper limb movement. As described above, oculo-manual coordination involves an interdependent coordination where information is shared between ocular and motor systems, thereby influencing performance of both in a positive way (Vercher & Gauthier, 1988; Gauthier et al., 1988; Maioli et al., 2007). This raises the interesting question of whether at a behavioural level, and how at a cortical level, performing SPEM in conditions of increased cognitive demand, for example in the presence of a secondary working memory task (Chapter 3) or with object visible vs. occluded (Chapter 4) is influenced by concurrent upper limb movement. To better understand this issue, the current thesis used a combination of perceptual, ocular, motor and/or neurophysiological measures. However, given the novelty of this work, it was first necessary to examine in a series of online studies some of the factors that influence motion extrapolation during an occlusion (Chapter 2). Although not part of the experimental work per se, it was also necessary to examine the potential crosstalk between eye movement (i.e., Eyelink 1000) and brain imaging (i.e., Brainsight, NIRSport2) devices. This work is presented in Appendix I. Below, a brief overview of these four chapters is provided.

Chapter 2: Development of a novel dual-task pursuit protocol

In Chapter 2, a novel dual-task pursuit protocol was designed to systematically examine the impact of primary and secondary task difficulty on judgment accuracy and response time in ocular and oculo-manual conditions. A series of four online studies was conducted in which a secondary change-detection task was performed concurrently (experiments 1-3) or consecutively (experiment 4) with a primary spatial prediction motion task.

Chapter 3: Prefrontal cortex activity and functional organisation in dual-task ocular pursuit is affected by concurrent upper limb movement

Having developed a suitable protocol, a lab-based experiment was conducted to determine the impact of concurrent upper limb movement during dual-task pursuit on measures of SPEM and prefrontal cortex activity and organisation. This required a combination of video-oculography (Eyelink 1000) and neurophysiological (fNIRS) devices, and permitted a more controlled testing environment in which participants adherence to the task protocol could be verified. In order to ensure the quality of fNIRS data recording, the same randomized-block protocol was followed as Chapter 2, but with additional time included before trial onset for the purpose of signal normalisation, as well as additional time after trial completion adjusted for differences in occlusion interval. Prefrontal activity (changes in mean O_2Hb and HHb) and network organisation (local and global efficiency) was then calculated across conditions. In Addition, in Appendix I, a detailed account of how crosstalk with an eye movement recording device was measured and minimised. Data were recorded during a series of 18 resting state acquisitions, on a single participant in three conditions conducted with a single video-oculography device (EyeLink 1000) and the 2 different fNIRS devices used for neuroimaging in Chapters 3 (Brainsight) and 4 (NirSport2). Three conditions were examined in order to investigate the potential noise induced by the infrared illuminator of the eye tracking on fNIRS data, and the effectiveness of a method to minimise that potential noise.

Chapter 4: Cortical activity and network organisation during oculo-manual vs ocular pursuit: The impact of task adaptation.

The second lab-based experiment examined the wider cortical network in oculo-manual facilitation, and whether this is influenced by a period of adaptation. In order to measure the wider cortical network using fNIRS, a 24 by 24 optode array was used, which resulted in a total of 79 long distance channels and 8 short distance channels. To provide the best opportunity for facilitation of SPEM by concurrent upper limb movement, the stimulus involved sinusoidal object motion (0.1Hz) for a duration of 35 seconds. At pre-test and post-test, participants pursued a continuously visible or momentarily occluded object with eyes alone (ocular condition) or with eyes and hand (oculo-manual condition). During adaptation, they pursued a continuously visible object in the oculo-manual condition.

Chapter 2: Dual-task pursuit

2.1 Introduction

Smooth pursuit is a voluntary response to track a moving object, which is often performed in a context of static and/or dynamic stimuli comprising multiple elements with different spatial layout, shape and/or colour. It typically involves participants selecting and then choosing from several options which moving object to track (Ferrera & Lisberger, 1995), and/or which direction a moving object will take as it progresses along its trajectory (Kowler, 1989). Therefore, as well as demanding attention to monitor a visually-based error signal (position and velocity) between the fovea and a moving object, it is necessary to allocate covert attention to processing of stimuli in peripheral vision. Rather than covert attention simply being located closely ahead of a moving object (Tanaka et al., 1998; van Donkelaar & Drew, 2002), it is now recognised that the allocation (i.e., location and amount) of covert attention depends on the characteristics of the object being tracked, as well as the surrounding elements (e.g., shape, colour, location). For example, it is more attentionally demanding to track a small, single object than a large stimulus comprising several individual elements (Heinen et al., 2011), which thus impacts upon the allocation of covert attention for the performance of a secondary task (Jin et al., 2013; 2014). In addition, when the pursuit task and secondary task compete for the same processing resource (i.e., visual-spatial short-term memory), participants exhibit a limited ability to allocate covert attention to eccentric locations (Kerzel & Ziegler, 2005).

The impact of competing attentional demands can be even greater when tracking a moving object that is not continuously visible. In Jonikaitis et al., (2009), participants performed a spatial prediction motion task in which they made a judgement about the reappearance location (i.e., ahead or behind the correct location) of a moving object (2, 3 or 4deg/s) after a period of transient occlusion. In control trials, two small grey circles were presented at ±2deg of the either side of the horizontal trajectory of the pursuit object, which participants were told to ignore. In experimental trials, one of the grey circles could change colour to green during the occlusion, which then acted as the target for a pro-saccade. Alternatively, if a grey circle changed colour to red,

participants were required to make an anti-saccade to the other grey circle. As would be expected, performing a pro-saccade disrupted pursuit of the occluded object (i.e., mean eye position across trials and participants), but it also impaired performance of the spatial prediction motion task. More interestingly, however, the same effect but with a lesser magnitude was found in the control condition where participants were instructed not to make an anti-saccade when one of the grey circles turned red. The authors suggested that a covert shift of attention in a dual-task context (i.e., to simply determine the colour of a single peripheral object) was sufficient to interfere with the processes involved in spatial prediction motion (i.e., extrapolation of the occluded trajectory of the moving object).

Competing attentional demands of a primary task involving smooth pursuit and secondary tasks involving visual working memory can also occur when the two tasks are performed consecutively (Yue et al., 2017). In their change-detection task, colour working memory (2 or 4 elements) was impaired when participants performed smooth pursuit compared to fixation in the cue-probe interval, whereas smooth pursuit was impaired when participants performed pursuit plus the colour working memory task vs pursuit alone. Moreover, while colour working memory performance benefited when smooth pursuit was consistent vs inconsistent with the direction of the cued elements of the colour stimulus array, the opposite effect was found for smooth pursuit. It was suggested that these findings can be explained by reliance on a limited attentional resource that is shared between the pursuit and the colour working memory task, with demand persisting across the cue-probe interval (i.e., retention period). Dependence between the two tasks was suggested to result from a common reliance on spatial information, and thus activation of a similar fronto-parietal network. That is, despite there being no change in the spatial layout of the colour elements between the cue-probe interval, participants still encoded their spatial location in the left or right peripheral visual field, which then interfered with the processes involved in smooth pursuit. This is consistent with Jiang et al., (2000), who showed that the spatial configuration of elements in a stimulus array acts as an important

source of relational information encoded in working memory, which then facilitates identification of a change in spatial location, colour or shape.

It is clear, then, that performing a secondary task requiring covert attention to process spatial layout and/or colour of surrounding elements, has the potential to interfere with a primary pursuit task, particularly when it involves a transient occlusion. In the latter situation, pursuit eye movements are associated with activation of different cortical areas compared to fixation or pursuit of a continuously visible object (Lencer et al., 2004; Nagel et al., 2006; Ding et al., 2009), and in particular dorsolateral prefrontal cortex (DLPFC). This is a key cortical area involved in higher-order cognitive processes such as attention, working memory and prediction, and would likely be involved in both a secondary change-detection task, as well as representing an occluded object trajectory. Medial prefrontal cortex (MPFC) is also involved in many cognitive processes (Braver & Bongiolatti, 2002; Ramnani & Owen, 2004), and is known to monitor other areas of PFC (Mansouri et al., 2017). As such, it can be expected that MPFC plays a key role in dual-task contexts requiring the maintenance/monitoring of a primary task goal while simultaneously allocating attention to a secondary task goal (Christoff et al., 2001). At present, however, it first remains to be determined at a behavioural level if the spatial configuration and colour of elements within a secondary task impact upon the predictive processes involving visual-spatial working memory, which are key to spatial prediction motion.

In the current chapter, a series of studies are reported that examine a secondary change-detection task comprising a colour or form stimulus array that is performed concurrently (experiments 1-3) or consecutively (experiment 4) with a primary spatial prediction motion task. In addition, it is examined if afferent and efferent signals from performing concurrent upper limb (i.e., arm) movement, which are known to enhance smooth pursuit (Koken & Erkelens, 1992), particularly when the moving object undergoes a momentary occlusion (Gauthier & Hofferer, 1976; Bennett et al., 2012), influences performance of the primary and/or secondary task. For example, if afferent and efferent signals from upper limb and eye movements are integrated to form a dynamic predictive model of a moving object's trajectory

(Vercher et al., 1997), this might benefit the primary task and also free-up attentional resource for completion of the secondary change-detection task. Conversely, if oculo-manual tracking requires greater attentional resource than tracking with the eye alone, it follows that performance of the secondary change-detection task may be impaired. For example, Li et al., (2023) studied the impact of secondary motor task (e.g. pressing a keyboard to identify time of collision) on a primary motion prediction task (e.g. participants had to judge if a moving object reappeared behind or ahead the correct location after having undergone an occlusion). Their results indicate that participants underestimate the object reappearance (primary task) when concurrent upper limb movement is performed during the occlusion, suggesting that concurrent upper limb movement could interfere with prediction motion.

2.2 Materials and Methods

General considerations for online testing

A series of online studies was conducted, each using a variation of a novel dual-task pursuit. Each study lasted approximately 45 minutes and was implemented using the Gorilla.sc platform within the web browser on the participant's desktop computer or laptop (NB. not permitted to use a tablet or mobile phone). As reported by Anwyl-Irvine et al., (2021), this web-based platform provides reasonable accuracy and precision for display duration (Mean delay = 13.44 ± 15.41ms) and manual response time (Mean delay = 78.53 ± 8.25ms) and performs to a similar level as other platforms (i.e., jsPsych, Lab.js, PsychoJS). Importantly, absolute timing delays in these web-based platforms are not problematic if only making within-study comparisons (i.e., not comparing to lab-based findings). In such situations, which was the case in the current series of studies, the precision of presentation timing and response measurements are more meaningful and can be further controlled by minimizing the number online programming steps. To this end, here, visual stimuli (i.e., static images and videos) were rendered offline and pre-loaded

prior to testing. Videos depicting the visual stimuli of dual-task pursuit were generated in Matlab® (MATLAB 2020b, The MathWorks, USA) by drawing a figure, which was then saved to a video object using the VideoWriter function each time the figure was updated. In addition, to ensure that the visual stimuli were shown at a similar visual angle on each participant's screen, a calibration was performed before starting the task. Participants were instructed to put a standard size credit card or store card on the location indicated on the screen, and then to drag a slider so the image on the screen matched the size of their card. To ensure participants were seated comfortably and could maintain their position relative to the screen, they were asked to sit with their elbows at approximately 90 degrees, with arms resting on the desk in front of them and fingers on the keyboard. An image was shown on their screen to help participants with the positioning instructions.

2.3 Study A

Participants

Thirty-two participants (15 males/ 17 females) with a mean age of 29.09 (± 6.98) years took part in the ***study A***. Participants were recruited using reverse snowball sampling (n = 14), as well as a third-party recruitment service (Prolific.co) that provided a monetary recompense (£8.21/h on average across the four studies) for participation (n = 18). All participants self-declared to be right-handed, with normal or corrected vision and no neurological impairment. Participants provided informed consent prior to participation in the study. The study was approved by the local ethics committee (21/SPS/008a) and was conducted in accordance with the ethical standards specified by the Declaration of Helsinki.

Task and Procedure

Participants performed a novel dual-task pursuit comprising a primary task of spatial prediction motion, and a secondary change-detection task (see Figure 2.1). They received written instructions regarding the protocol, and practiced

the task until they achieved 6/20 correct responses. At the start of each trial, a grey circular object (0.5 degrees diameter) was presented at -8.5 degrees to the left of screen centre (white background) for 500ms. The object then disappeared for 300ms, and reappeared moving horizontally to the right at constant velocity of 5deg/s. After 600ms, the object disappeared behind an invisible occluder and continued to move to the right, with the same velocity, but not visible to the participant. At the end of the occlusion, the object reappeared but always in a position that was either 2 or 4 degrees behind (e.g. 2B and 4B) or ahead (e.g. 2A and 4A) of where it should have been given no change in its velocity. In order to minimize anticipation of object reappearance, occlusion time on each trial was randomly selected from five possibilities (1700, 1800, 1900, 2000 and 2100ms). Having reappeared, the object continued moving to the right for an additional 400ms. Participants were instructed to pursue the object through the visible and occluded parts of the trial and then to estimate whether it reappeared behind or ahead of the correct position. Participants gave their answer by pressing the z or v key of their computer keyboard with the ring or index finger of their left hand. Importantly, the primary task did not end until the z or v key had been pressed, meaning participants were always faced with a forced, 2-choice response. The primary task was completed with either the eyes alone (ocular condition, OC) or with the eyes and right hand (oculo-manual condition, OM). For the OC condition, participants were instructed to place their right hand on their desk to the right of the keyboard, and then to maintain this position throughout the block of trials. For the OM condition, participants were given the same instructions about where to place their right hand, but in addition they were instructed to move their hand such that it matched the speed of the moving circular object. No feedback was provided regarding the movement of the right hand.

For the secondary change-detection task, an array of four squares (each 0.25deg) was presented to the participant for 500ms, centred to the spatial and temporal midpoint of the occlusion of the moving object in the primary task. The array was presented again after participants gave their response to the primary task, at a location coincident with the final position of the moving

object (i.e., not the reappearance location). Participants were given 3s to judge whether the squares had changed form or colour between the cue and probe presentation by pressing the z (no change) or the v (change) key of the computer keyboard with the ring or index finger of their left hand. The array of four squares was designed to give three different conditions. In the *Control* stimulus array, participants were informed that there would be no change between the cue and probe presentation of four black squares, which were each assigned an x and y location to coincide with the four corners of a larger square of 1deg. For the *Form* stimulus array, each of the four squares of the control stimulus array were randomly shifted by -0.25, 0 or +0.25deg. For the probe presentation, the four squares were either assigned the same location or randomly shifted again by -0.25, 0 or +0.25deg, with the caveat that none of the four squares have an overlapping location. For the *Colour* stimulus array, the four squares had the same spatial layout as the *Control* stimulus array, but each was randomly assigned a colour (red, magenta, blue and green) with no repetition. For the probe presentation, the four squares were either assigned the same colour or the colours were randomly assigned a second time with no repetition.

There were 6 unique combinations of Stimulus Array (*Control, Colour, Form*) and Tracking (*OC, OM*), which were presented as 6 separate blocks of 24 trials. The order of *OC* and *OM* tracking was counterbalanced, with participants performing each of the 3 blocks of Stimulus Array in one tracking mode before completing those same blocks of Stimulus Array in the other tracking mode. For both tracking modes, the 3 blocks of Stimulus Array were randomized. In blocks with the *Control* stimulus array, participants performed 24 randomly-ordered trials, with 6 trials for each Position Step. For blocks with the *Colour* or *Form* stimulus array, there was a randomly-ordered change between cue and probe in 12 of the 24 trials. Position Step was interleaved in these blocks, such that there was an equal distribution for trials with a change or no change in the stimulus array. Occlusion time on each trial was randomly selected from five possibilities (1700, 1800, 1900, 2000 and 2100ms). Participants performed 144 trials in total, resulting of a testing duration of approximately 45min.

For each trial, judgement accuracy (1 = correct; 0 = incorrect) and response time of both the primary and secondary tasks was measured. Judgment data were analysed using generalized linear mixed modelling with a logit link function, whereas response time data were analysed using linear mixed modelling (lme4 package in RStudio, v1.1-31). An iterative, top-down process was followed in order to find the simplest model (i.e., random and fixed effects) that best fit the data. The initial, full model included all main and interaction effects for the fixed factors of Step (4B, 2B, 2A and 4A), Stimulus Array (*Control, Colour and Form*) and Tracking (*OC and OM*), and a random intercept for each participant. For all significant interaction effects, a custom contrast was set in order to generate only relevant pairwise comparisons (i.e., a change in only 1 level of a single factor while keeping levels of other factors constant), which were then subject to Bonferroni correction (EMMEANS package v1.7.2).

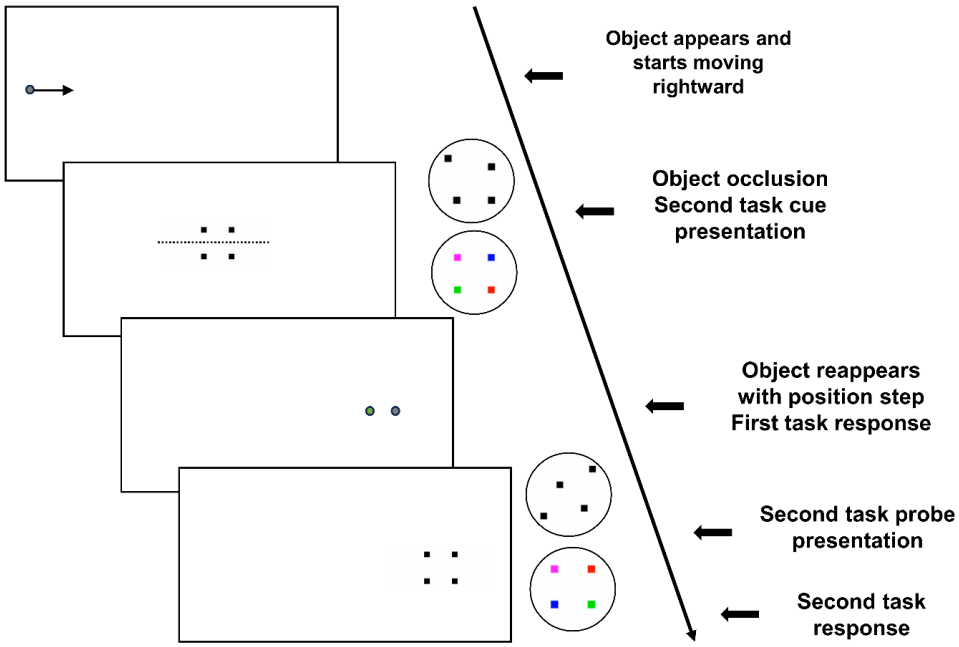

Figure 2.1: *Schematic diagram of an experimental trial for* ***study A*** *with the Control stimulus array (Form and Colour stimulus arrays are represented within the circle to the right of the white boxes). Black arrow (box 1) represents direction when the target was in motion and the dashed line (box 2) represents when the target is not visible to the participant.*

Results

Prediction Motion

Judgement accuracy: The reduced model (AIC = 2361.0; conditional R^2 = 0.46) indicated a significant main effect of Step [χ^2 (3) = 211.39; $p < 0.0001$], Stimulus Array [χ^2 (2) = 10.74; $p < 0.01$] and Tracking [χ^2 (1) = 8.79; $p < 0.01$]. These effects were superseded by significant interactions for Step x Stimulus Array [χ^2 (6) = 13.45; $p = 0.036$] and Step x Tracking [χ^2 (3) = 9.43; $p < 0.024$] (see Figure 2.2 panel A). For the Control stimulus array, judgements were less accurate when the object reappeared with a small negative step (-2deg: 0.814) compared to all other steps (+2deg: 0.932, $p < 0.0001$; +4deg: 0.995, $p < 0.0001$; -4deg: 0.978, $p < 0.0001$). Judgement accuracy was also lower when the object reappeared with a small positive step (+2deg) compared to the two larger steps (+4deg: $p = 0.0005$; -4deg: $p = 0.0165$). For the other two stimulus arrays, judgements were less accurate ($p < 0.001$) when the object reappeared with a small step (Form: -2deg: 0.848; +2deg: 0.880; Colour: -2deg: 0.792; +2deg: 0.865) compared to larger steps (Form: +4deg: 0.993; -4deg: 0.967; Colour: -4deg: 0.969 and +4deg: 0.978). Finally, judgement accuracy was lower in the Colour (0.865) than Control (0.932; $p = 0.04$) stimulus array when the object reappeared with a small positive step.

As can be seen in Figure 2.2 panel A, for OC tracking, judgement accuracy was lower when the object reappeared with a small negative step (-2deg: 0.781) compared to all other steps (+2deg: 0.891, $p < 0.0001$; +4deg: 0.994, $p < 0.0001$; -4deg: 0.959, $p < 0.0001$). Judgement accuracy was also lower when the stimulus reappeared with a small positive step (+2deg) compared to the two larger steps (+4deg: $p < 0.0001$; -4deg: $p = 0.0001$), and when the object reappeared with a large negative step (-4deg) compared to a large positive step (+4deg; $p = 0.0007$). For OM tracking, judgement accuracy was lower ($p < 0.0001$) when the object reappeared with a small step (+2deg: 0.902; -2deg: 0.852) than a larger step (+4deg: 0.987; -4deg: 0.981). Finally, for the most difficult condition where the object reappeared with a small negative step (-2deg), judgement accuracy was higher in OM tracking (0.852) than OC tracking (0.781; $p = 0.043$).

Response time: The reduced model (AIC = 66707; conditional R^2 = 0.22) indicated a significant main effect of Step [χ^2 (3) = 122.09; $p < 0.0001$] and Stimulus Array [χ^2 (2) = 17.77; p = 0.00014], as well as a significant Step x Stimulus array interaction [χ^2 (6) = 15.59; p = 0.016] (see Figure 2.2 panel C). With the Form stimulus array, response time was longer ($p < 0.001$) for the two small steps (-2deg: 1095ms; +2deg: 1123ms) than the two larger steps (-4deg: 854ms; +4deg: 767ms). With the Control stimulus array, response time was longer ($p < 0.0001$) when the object reappeared with a small negative step (-2deg: 1268ms) than the two larger steps (-4deg: 934ms; +4deg: 830ms), and when the object reappeared with a small positive step (+2deg: 1088ms) than a large positive step (+4deg: 830ms, p = 0.0003). There were no significant differences between steps for the Colour stimulus array. Finally, when the object reappeared with a large positive step (+4deg) response time was longer in Colour (998ms) than Form (767ms; p = 0.0025) stimulus array.

Change Detection

Judgement accuracy: The reduced model (AIC = 2559.9; conditional R^2 = 0.22) indicated a significant main effect of Stimulus Array [χ^2 (2) = 84.25; $p < 0.0001$], which was superseded by a significant Step x Stimulus Array interaction [χ^2 (6) = 15.66; $p < 0.05$] (see Figure 2.2 panel B). For all four levels of step, judgement accuracy was higher in the Control (-2deg: 0.961, $p < 0.0001$; +2deg: 0.965, p = 0.0023; -4deg: 0.985, p = 0.0001; +4deg: 0.967) than Form (-2deg: 0.819, $p < 0.0001$; +2deg: 0.886, p = 0.0023; -4deg: 0.891, p = 0.0001; +4deg: 0.885, p = 0.0008) stimulus array. Judgement accuracy was also higher in the Control (-4deg: 0.985; +4deg: 0.967) than Colour stimulus array for the two larger steps (-4deg: 0.874, $p < 0.0001$; +4deg: 0.903, p = 0.011). Finally, when the object reappeared with a small negative step, judgement accuracy was higher in Colour (-2deg: 0.913) than Form (-2deg: 0.819, p = 0.0046) stimulus array. Within each stimulus arrays, there were no significant difference between the four step levels.

Response time: The reduced model (AIC = 66950; conditional R^2 = 0.12) indicated a significant main effect of Stimulus Array [χ^2 (2) = 57.84; $p < 0.0001$], as well as a significant Stimulus Array x Tracking interaction [χ^2

(2) = 9.08; p = 0.01] (see Figure 2.2 panel D). For OC tracking, response time was longer in the Colour (828ms) than Form (692ms; p = 0.0001) and Control (721ms; p = 0.004) stimulus arrays, which did not differ from each other. For OM tracking, response time was shorter in the Form (647ms) than Control (804ms; p < 0.0001) and Colour (832ms; p < 0.0001) stimulus arrays, which did not differ from each other. Within each stimulus array, there were no significant difference between OC and OM tracking.

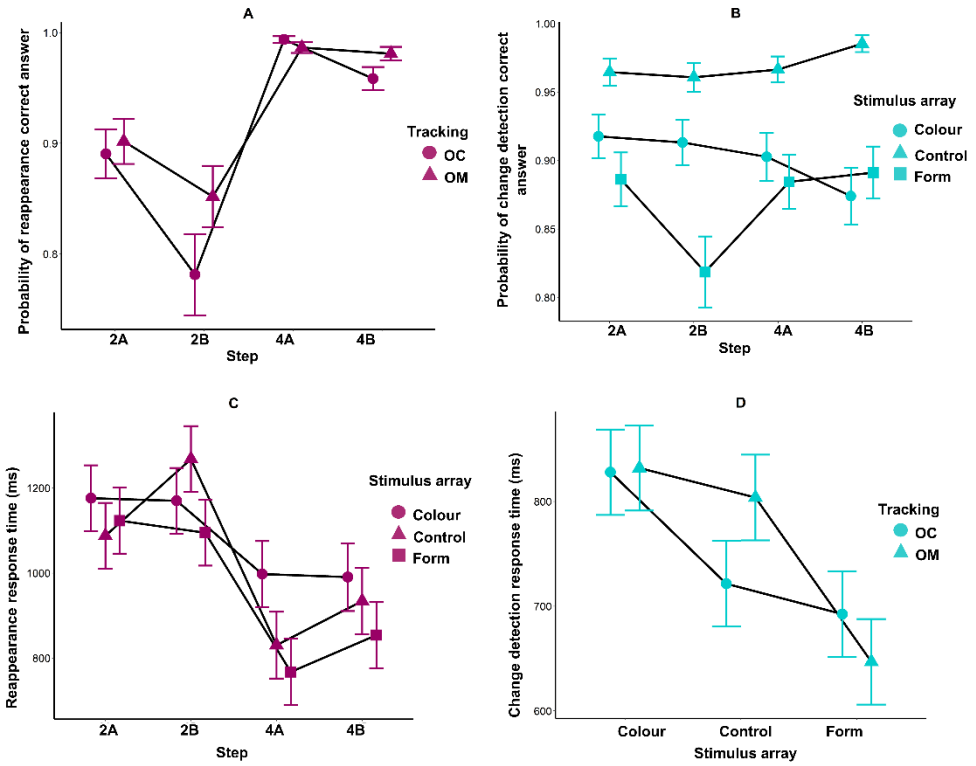

Figure 2.2: *A) Probability of correct response in the prediction motion task as a function of Step (2A, 2B, 4A and 4B) and Tracking (OC represented by filled circles; OM represented by filled triangles). B) Probability of correct response in the change detection task as a function of Step (2A, 2B, 4A and 4B) and Stimulus Array (Colour represented by filled circles, Control represented by filled triangles, and Form represented by filled squares. C) Response time in the prediction motion task as a function of Step (2A, 2B, 4A and 4B) and Stimulus Array. D) Response time in the change detection task as a function of Stimulus Array (Colour, Control, Form) and Tracking. Estimated marginal means and standard errors are shown from the accepted model.*

2.4 Study B

Participants

Twenty-two participants (19 males/3 females) with a mean age of 24.23 (± 6.78) years took part. Participants were recruited from the staff and student population of the host University (n = 17), as well as a third-party recruitment service (Prolific.co) that provided a monetary reimbursement (£8.21/h on average across the four studies) for volunteering (n = 5). All participants self-declared to be right-handed, with normal or corrected vision and no neurological impairment. Participants provided informed consent prior to participation in the study. The study was approved by the local ethics committee (21/SPS/008a) and was conducted in accordance with the ethical standards specified by the Declaration of Helsinki.

Task and Procedure

The task and procedure were the same as study A, except that there were *six squares* in the secondary change-detection task (see Figure 2.3). In the *Control* stimulus array, the six black squares were each assigned an x and y location such that they created 2 rows of 3 squares (1deg width), with 1 row located 0.5deg above and the other 0.5deg below the vertical location of the moving object. For the *Form* stimulus array, each of the six squares of the *Control* stimulus array were randomly shifted by -0.25, 0 or +0.25deg. For the probe presentation, the six squares were either assigned the same location or randomly shifted again by -0.25, 0 or +0.25deg, with the caveat that none of the four squares have an overlapping location. For the *Colour* stimulus array, the six squares had the same spatial layout as the *Control* stimulus array, but each was randomly assigned a colour (red, magenta, blue, green, yellow, cyan) with no repetition. For the probe presentation, the six squares were either assigned the same colour or the colours were randomly assigned a second time with no repetition. Participants were asked to determine whether the *six squares array* had changed between the first and second presentation by pressing the z or the v key with their left hand.

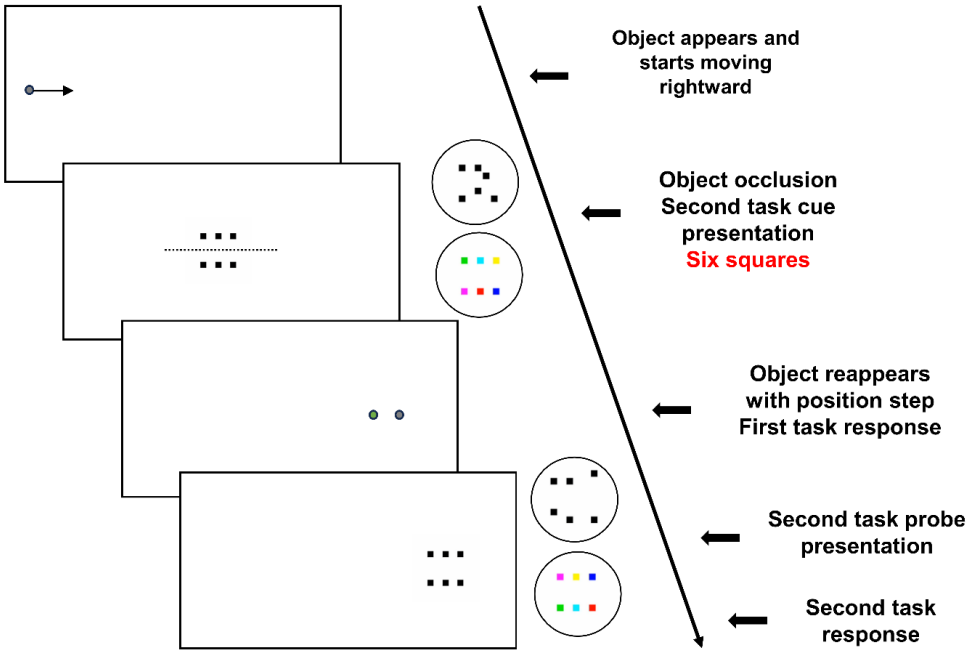

Figure 2.3: *Schematic diagram of an experimental trial for* ***study B*** *with the Control stimulus array (Form and Colour stimulus arrays are represented within the circle to the right of the white boxes). Black arrow (box 1) represents direction when the target was in motion and the dashed line (box 2) represents when the target is not visible to the participant. To the right of the boxes, red text highlights the change between this study and study A.*

Results

Prediction Motion

Judgement accuracy: The reduced model (AIC = 1601.1; conditional R^2 = 0.46) indicated a significant main effect of Step [χ^2 (3) = 281.82; $p < 0.001$] (see Figure 2.4 panel A). Judgments were less accurate ($p < 0.0001$) when the object reappeared with a small negative step (-2deg: 0.657) compared to all other steps (+2deg: 0.915; +4deg: 0.978; -4deg: 0.955). Judgments were also less accurate when the object reappeared with a small positive step (+2deg: 0.915) compared to large positive (+4deg: 0.978; $p < 0.0001$) and negative (-4deg: 0.955; $p = 0.01$) step.

Response time: The reduced model (AIC = 42941; conditional R^2 = 0.22) indicated a significant main effect of Step [χ^2 (3) = 66.84; $p < 0.0001$]

and Tracking [χ^2 (1) = 6.20; p = 0.013] (see Figure 2.4 panel C), as well as a significant Stimulus Array x Tracking interaction [χ^2 (2) = 11.86; p = 0.0027]. Response time was longer when the object reappeared with a small negative step (-2deg: 1343ms) than all other steps (+2deg: 1187ms, p = 0.0024; -4deg: 1115ms, p < 0.0001; +4deg: 989ms, p < 0.0001). Response time was shorter when the object reappeared with a large positive step (+4deg) than a large negative step (-4deg, p = 0.027) and small positive step (+2deg: p = 0.0001). Response time was also longer with the Control stimulus array in the OM (1283ms) than OC tracking (1075ms, p = 0.0016) condition. Finally, during OM tracking, response time was longer with the Control (1283ms) than Form (1093ms, p = 0.0047) stimulus array.

Change Detection

Judgement accuracy: The reduced model (AIC = 1718.2; conditional R^2 = 0.48) indicated a significant main effect of Step [χ^2 (3) = 18.49; p < 0.001] and Stimulus Array [χ^2 (2) = 89.03; p < 0.0001]. There were also significant interactions for Stimulus Array x Tracking [χ^2 (2) = 7.48; p = 0.024] (see Figure 2.4 panel B), and Step x Stimulus Array [χ^2 (6) = 22.53; p < 0.001]. During both OC and OM tracking, judgement accuracy was lower in the Form (OC: 0.7967; OM: 0.8088) than Colour (OC: 0.8882, p = 0.0012; OM: 0.9131, p < 0.0001) and Control (OC: 0.9971, p < 0.0001; OM: 0.9813, p < 0.0001) stimulus arrays. Again, for both tracking conditions, judgement accuracy was lower in the Colour than Control stimulus array. For each level of step, judgement accuracy was higher in the Control (-2deg: 0.985; +2deg: 0.997; -4deg: 0.986; +4deg: 0.995) than Colour (-2deg: 0.861, p = 0.0003; +2deg: 0.925, p = 0.037; -4deg: 0.889, p = 0.0041; +4deg: 0.919, p = 0.011) and Form (-2deg: 0.832, p < 0.0001; +2deg: 0.680, p < 0.0001; -4deg: 0.781, p < 0.0001; +4deg: 0.880, p = 0.0009) stimulus arrays. Judgement accuracy was also higher in the Colour than Form stimulus array when the object reappeared with a small positive step (+2deg, p < 0.0001) and a large negative step (-4deg, p = 0.047). Finally, there were no significant differences between each level of step except for the Form Stimulus array, where judgement accuracy was lower when the object reappeared with a small positive step

(+2deg) compared with a small negative step (-2deg; p = 0.0056) and large positive step (+4deg; p < 0.0001).

Response time: The reduced model (AIC = 43788; conditional R^2 = 0.083) indicated a significant main effect of Stimulus Array [χ^2 (2) = 27.345; p < 0.0001] (see Figure 2.4 panel D). Response time was longer in the Colour (753ms) than Control (674ms, p = 0.007) and Form (617ms, p < 0.0001) stimulus arrays.

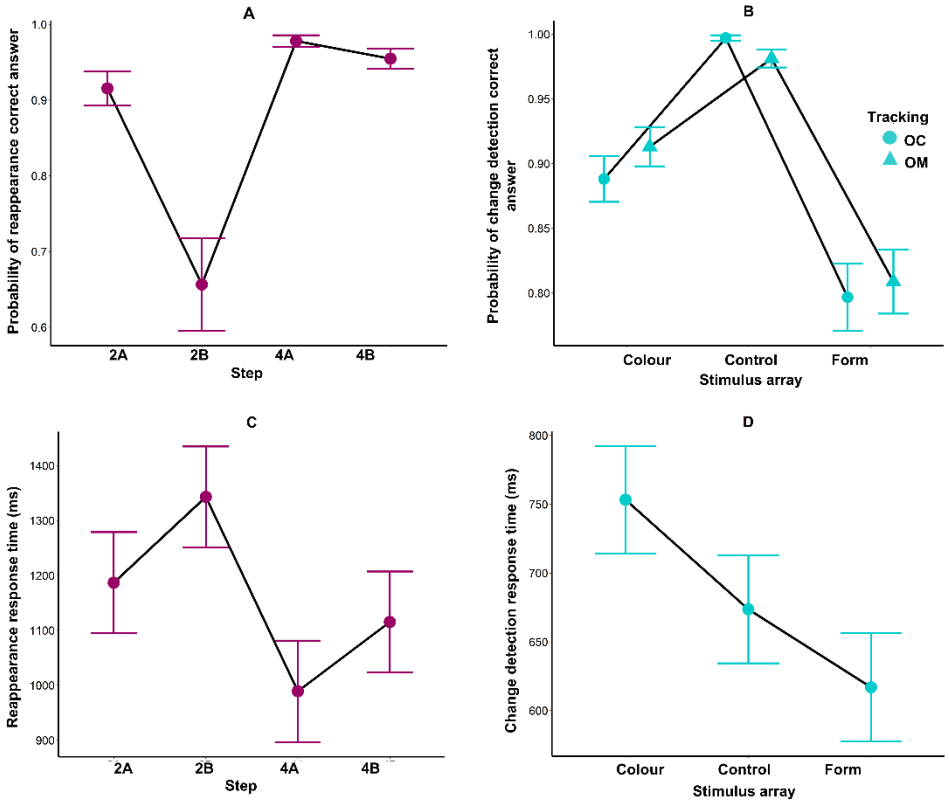

Figure 2.4: *A) Probability of correct response in the prediction motion task as a function of Step (2A, 2B, 4A and 4B). B) Probability of correct response in the change detection task as a function of Stimulus Array (Colour, Control, Form) and Tracking (OC represented as filled circles and OM represented as filled triangles). C) Response time in the prediction motion task for each level of Step (2A, 2B, 4A and 4B). D) Response time in the change detection task for each level of Stimulus Array (Colour, Control, Form). Estimated marginal means and standard error are shown from the accepted model.*

2.5 Study C

Participants

Twenty-three participants (13 males/ 10 females) with a mean age of 23.96 (± 4.94) years took part. Participants were recruited from the Staff and Student population of the host University (n = 17), as well a third-party recruitment service (Prolific.co) that provided a monetary recompense (£8.21/h on average across the four studies) for participation (n = 6). All participants self-declared to be right-handed and self-declared with normal or corrected vision and no neurological impairment. Participants provided informed consent prior to participation in the study. The study was approved by the local ethics committee (21/SPS/008a) and was conducted in accordance with the ethical standards specified by the Declaration of Helsinki.

Task and Procedure

The task and procedure were the same as study A except that the moving object of the primary task reappeared 1 or 3 degrees behind (e.g. 1B and 3B) or ahead (e.g. 1A and 3A) of where it should have been given no change in its velocity during occlusion (see Figure 2.5).

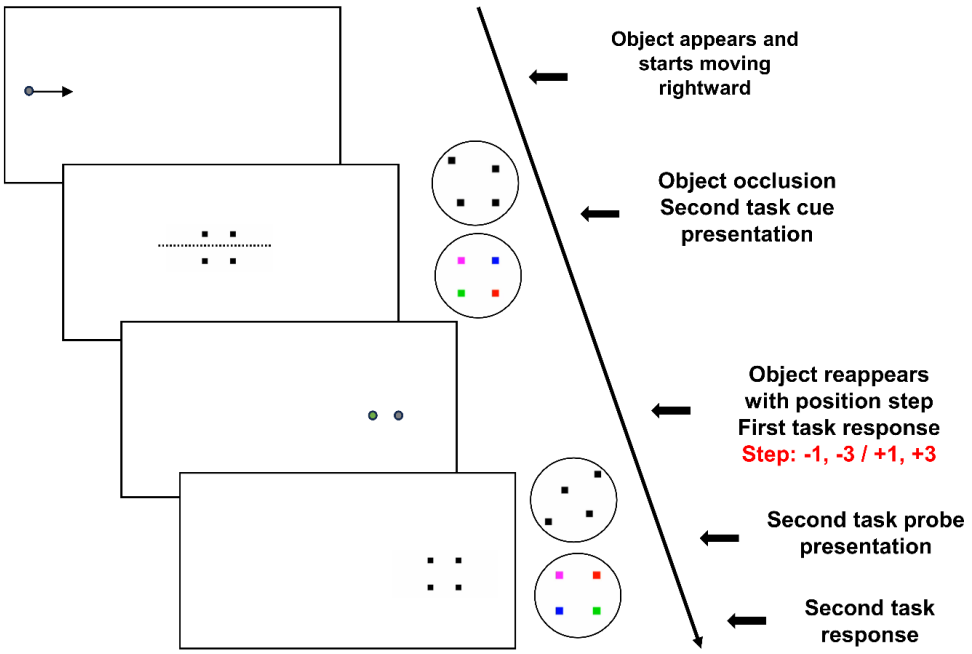

Figure 2.5: *Schematic diagram of an experimental trial for* ***study C*** *with the Control stimulus array (Form and Colour stimulus arrays are represented within the circle to the right of the white boxes). Black arrow (box 1) represents direction when the target was in motion and the dashed line (box 2) represents when the target is not visible to the participant. To the right of the white boxes, red text highlights the change between this study and the study A.*

Results

Prediction Motion

Judgement accuracy: The reduced model (AIC = 2716.9; conditional R^2 = 0.34) indicated a significant main effect of Step [χ^2 (3) = 138.51; $p < 0.0001$], which was superseded by a Step x Tracking interaction [χ^2 (3) = 22.67; $p < 0.0001$] (see Figure 2.6 panel A). For OC tracking, judgement accuracy was lower when the object reappeared with a small negative step (-1deg: 0.556, $p < 0.0001$) compared to all the other steps (+1deg: 0.805; -3deg: 0.808; +3deg: 0.934). Judgement accuracy was also lower when the object reappeared with a small positive step (+1deg) than the large positive step (+3deg, $p < 0.0001$), and for the large negative step (-3deg) than large positive step (+3deg, $p < 0.0001$). For OM tracking, judgement accuracy was lower when the object reappeared with a small negative step (-1deg: 0.663)

compared to the two larger steps (-3deg: 0.811, p = 0.0002; +3deg: 0.867, p < 0.0001). Judgement accuracy was lower when the object reappeared with a small positive step (+1deg: 0.714) than large positive step (+3deg: p < 0.0001), and approached significance when compared to the large negative step (-3deg: p = 0.0502). Finally, when the object reappeared with a large positive step (+3deg) judgement accuracy was lower in OM than OC (p = 0.028).

Response time: The reduced model (AIC = 46842; conditional R^2 = 0.29) indicated a significant main effect of Step [χ^2 (3) = 60.01; p < 0.0001] (see Figure 2.6 panel C), Stimulus Array [χ^2 (2) = 16.17; p < 0.001] and Tracking [χ^2 (1) = 16.22; p < 0.0001], as well as a significant Stimulus Array x Tracking interaction [χ^2 (2) = 8.18; p = 0.017]. Response time was longer when the object reappeared with a small negative step (-1deg: 1284ms) than the two larger steps (-3deg: 1144ms, p = 0.0023; +3deg: 981ms, p < 0.0001). Response time was also shorter when the object reappeared with a large positive step (+3deg) than a small positive step (+1deg: 1189ms, p < 0.0001) and a large negative step (-3deg: p = 0.0003). In OC tracking, response time was longer with the Colour (1225ms) than Control (1008ms, p = 0.0001) and Form (1041ms, p = 0.0019) stimulus arrays. No significant differences in response time were found between the stimulus arrays in OM tracking. Finally, response time was longer (p = 0.0002) in OM (1216ms) than OC tracking with the Control stimulus array.

Change Detection

Judgement accuracy: The reduced model (AIC = 1804.4; conditional R^2 = 0.27) indicated a significant main effect of Step [χ^2 (3) = 13.44; p = 0.0038] and Stimulus Array [χ^2 (2) = 87.06; p < 0.0001] (see Figure 2.6 panel B). Judgement accuracy was higher when the object reappeared with a small positive step (+1deg: 0.950) than small negative (-1deg: 0.919, p = 0.036) and large positive step (+3deg: 0.909, p = 0.0025). Judgement accuracy was lower with the Form (0.855) than Colour (0.896, p = 0.0136) and Control (0.978, p < 0.0001) stimulus arrays. Judgement accuracy was also lower with the Colour than Control (p < 0.0001) stimulus array.

Response time: The reduced model (AIC = 46557; conditional $R^2 = 0.1$) indicated a significant main effect of Stimulus Array [χ^2 (2) = 28.94; $p < 0.0001$] (see Figure 2.6 panel D). Response time was shorter with the Form (673ms) than Colour (819ms, $p < 0.0001$) stimulus array, and approached significance with the Control (739ms, $p = 0.0505$) stimulus array. Response time was also significantly longer with the Colour than Control ($p = 0.01$) stimulus array.

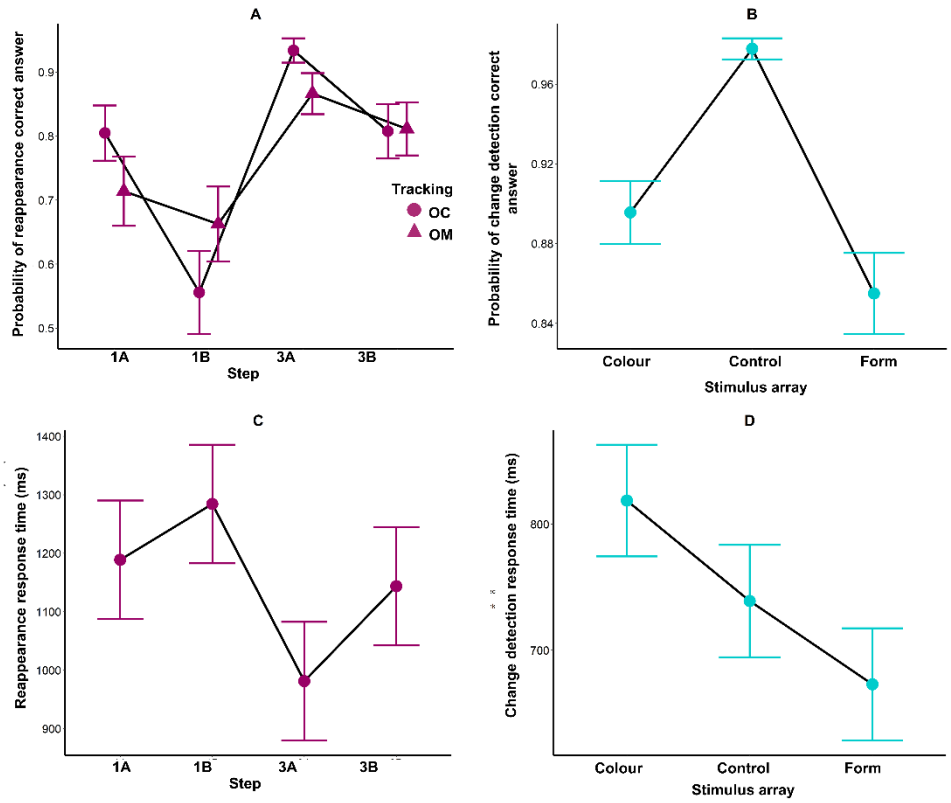

Figure 2.6: *A) Probability of correct response during prediction motion task for the significant Step (1A, 1B, 3A and 3B) by Tracking interaction (OC represented as filled circles and OM represented as filled triangles). B) Probability of correct response during change detection task for significant main effect of Stimulus Array (Colour, Control, Form). C) Response time during prediction motion task for significant main effect of Step (1A, 1B, 3A and 3B). D) Response time during change detection task for the significant main effect of Stimulus Array (Colour, Control, Form). Estimated marginal means (shaped and coloured points) and standard errors are shown from the accepted model. Interactions are represented with black lines.*

2.6 Study D

Participants

Twenty-five (11 males/ 13 females/1 does not answer) with a mean age of 30.64 (± 7.31) were recruited using a third-party recruitment service (Prolific.co) that provided a monetary recompense for participation (£8.21/h on average across the four studies). All participants self-declared to be right-handed and self-declared with normal or corrected vision and no neurological impairment. Participants provided informed consent prior to participation in the study. The study was approved by the local ethics committee (21/SPS/008a) and was conducted in accordance with the ethical standards specified by the Declaration of Helsinki.

Task and Procedure

The task and procedure were the same as study A, except that the four squares of the secondary change-detection task were initially presented at the start of the trial for 500ms, such that they surrounded the grey circular object of the primary task as it remained stationary at -8.5 degrees to the left of screen centre. After 500ms, the four squares disappeared, and the circular object remained stationary for a further 500ms. It the then disappeared for 300ms and reappeared moving horizontally to the right at constant velocity of 5deg/s (see Figure 2.7).

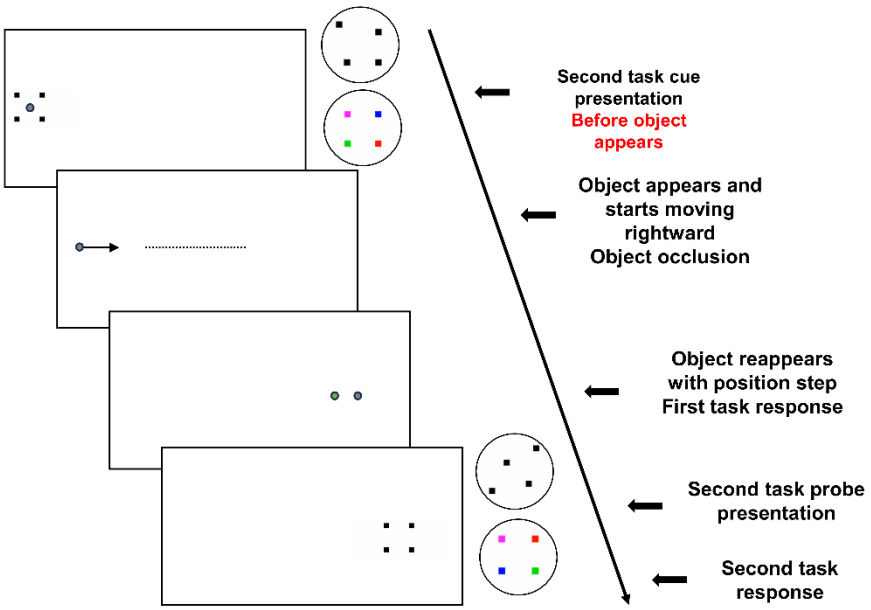

Figure 2.7: *Schematic diagram of an experimental trial for* ***study D*** *with the Control stimulus array (Form and Colour stimulus arrays are represented within the circle to the right of the white boxes). Black arrows (box 2) represent direction when the target was in motion and the dashed line represents when the target is not visible to the participant. To the right, red text highlights the change between this study and the study A.*

Results

Prediction Motion

Judgement accuracy: The reduced model (AIC = 1236.7; conditional R^2 = 0.67) indicated a significant main effect of Step [χ^2 (3) = 248.97; $p < 0.0001$], and a Step x Tracking interaction [χ^2 (3) = 11.73; $p = 0.0084$] (see Figure 2.8 panel A). In OC tracking, judgement accuracy was lower when the object reappeared with a small negative step (-2deg: 0.628, $p < 0.0001$) than all other steps (+2deg: 0.963; -4deg: 0.977; +4deg: 0.996). In OM tracking, judgement accuracy was also lower when the object reappeared with a small negative step (-2deg: 0.700, $p < 0.0001$) than all other steps (+2deg: 0.918; -4deg: 0.972; +4deg: 0.980). In addition. judgement accuracy in OM tracking was lower when the object reappeared with a small positive step (+2deg) than the larger steps (-4deg, $p = 0.015$; +4deg, $p = 0.0046$). Across all levels of step, no significant differences were found between OC and OM tracking.

Response time: The reduced model (AIC = 36964; conditional R^2 = 0.16) indicated a significant main effect of Step [χ^2 (3) = 37.93; $p < 0.0001$] (see Figure 2.8 panel C), Stimulus array [χ^2 (2) = 10.58; $p = 0.005$], and Tracking [χ^2 (1) = 11.42; $p = 0.0007$]. Response time was longer when the object reappeared with a small negative step (-2deg: 840ms) compared to a large step (+4deg: 636ms, $p < 0.0001$; -4deg: 699ms, $p = 0.0003$). Response time was also longer when the object reappeared with a small positive step (+2deg: 777ms) than a large positive step (+4deg: 636ms). Response time was longer with the Control (792ms) than Colour (692ms, $p = 0.0043$) stimulus array, and also in OM (781ms) than OC (694, $p = 0.0007$) tracking.

Change Detection

Judgement accuracy: The reduced model (AIC = 1955.5; conditional R^2 = 0.57) indicated a significant main effect of Stimulus Array [χ^2 (2) = 97.63; $p < 0.0001$] and a significant Stimulus Array x Tracking interaction [χ^2 (2) = 6.35; $p < 0.05$] (see Figure 2.8 panel B). In OC tracking, judgement accuracy was higher with the Control (0.9974) than Colour (0.8688; $p < 0.0001$) and Form (0.8233; $p < 0.0001$) stimulus arrays. In OM tracking, judgement accuracy was lower with the Form (0.8018) than Colour (0.9132; $p < 0.0001$) and Control (0.9973; $p < 0.0001$) stimulus arrays, and with the Colour than Control ($p < 0.0001$) stimulus array. No significant differences were found between OC and OM tracking for all stimulus arrays.

Response time: The reduced model (AIC = 51492; conditional $R^2 = 0.1$) indicated a significant main effect of Stimulus Array [χ^2 (2) = 53.08; $p < 0.0001$] and Tracking [χ^2 (1) = 3.94; $p < 0.05$], and a Stimulus Array x Tracking interaction [χ^2 (2) = 10.77; $p = 0.0046$] (see Figure 2.8 panel D). For OC tracking, response time was longer with the Colour (808ms) than Form (625ms; $p < 0.0001$) and Control (682ms; $p = 0.0005$) stimulus arrays. For OM tracking, response time was longer with the Colour (824ms) than Form (743ms, $p < 0.0001$) stimulus array. Finally, response time was higher in OM tracking (743ms) than OC tracking (625ms, $p = 0.0018$) with the Form stimulus array.

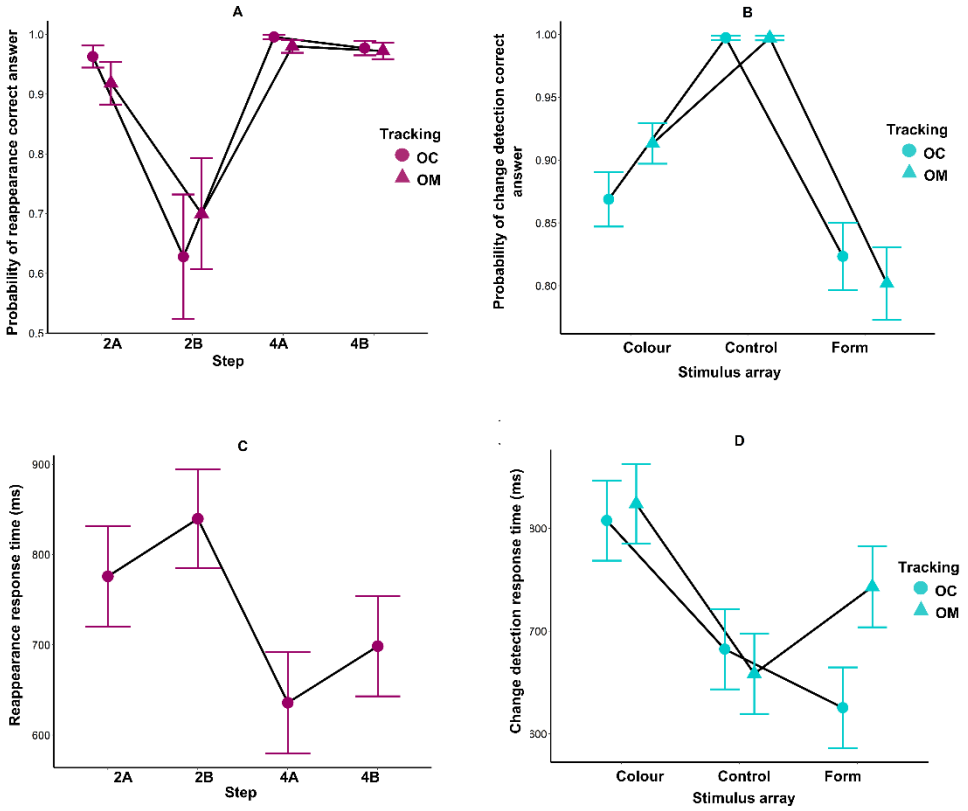

Figure 2.8: *A) Probability of correct response in the prediction motion task as a function of Step (2A, 2B, 4A and 4B) and Tracking (OC - circles; OM - triangles). B) Probability of correct response in the change detection task as a function of Stimulus Array (Colour, Control, Form) and Tracking. C) Response time in the prediction motion task for each level of Step (2A, 2B, 4A and 4B). D) Response time in the change detection task as a function of Stimulus Array (Colour, Control, Form) and Tracking. Estimated marginal means and standard errors are shown from the accepted model.*

2.7 Discussion

As well as determining what we see from tracking a moving object, pursuit eye movements influence where we allocate attention and what we perceive from the surrounding environment. Although voluntary and seemingly effortless, they require overt attention to process a visually-based error signal between the fovea and moving object, as well as the allocation of covert attention to other stimuli located at eccentric locations in the peripheral visual field. Depending on the object being pursued (Heinen et al., 2011) and

the demands on covert attention (Kerzel & Ziegler, 2005; Watamniuk & Heinen, 2015), there may be a deterioration in performance of pursuit eye movements or a secondary visual working-memory task. The potential for interference between competing attentional demands may be even greater when the pursuit task involves a transient occlusion (Jonikaitis et al., 2009), which increases the demand on predictive processes involving visual-spatial working memory. Here, a series of four studies was conducted that required a secondary change-detection task to be performed concurrently (experiments 1-3) or consecutively (experiment 4) with a primary spatial prediction motion task. Borrowing from the work of Yue et al., (2017), the secondary task required participants to determine if there was a change between a cue and probe presentation in the spatial layout or colour of individual elements within a stimulus array. Spatial prediction motion required a judgement about the reappearance location of a transiently occluded moving object. Although pursuit eye movements were not recorded due to the use of an online testing platform, it was expected that spatial prediction motion would benefit from being instructed to pursue the moving object (Bennett et al., 2010). In a separate tracking condition, participants were instructed to pursue the moving object with their eyes and upper limb. This provided the opportunity to determine whether performance of the primary and/or secondary tasks is influenced by the presence of limb afference and efference, which is known to facilitate smooth pursuit of a moving object that undergoes a transient occlusion (Gauthier & Hofferer, 1976; Bennett et al., 2012).

Consistent with previous work on spatial prediction motion (Bennett & Benguigui, 2016), across all studies judgments were least accurate and took longer to respond when the object reappeared with a small negative position step. The next most difficult reappearance location was a small positive step, whereas the two larger steps were consistently judged more quickly and accurately, often in excess of 96% correct. Reducing the magnitude of reappearance step in Study C (i.e., -1deg) reduced judgment accuracy compared to Studies A, B and D (i.e., -2deg). These findings are consistent with the suggestion that participants tend to underestimate object location along the occluded trajectory (Lyon & Waag, 1995; Tanaka et al., 2009),

which results in gaze being more closely aligned to an object that reappears just behind the moving object, thus making judgments more difficult (Bennett & Benguigui, 2016; Wexler & Klam, 2001). However, there was no reduction in judgment accuracy in Study B where there were 6 elements in the stimulus array of the secondary change-detection task compared to 4 elements in Studies A, C and D. Also, while there was some interactive influence of stimulus array of the secondary change-detection task in Study A, this was not present in the other 3 studies. Therefore, it would seem that performance of the primary spatial prediction motion task was not impaired by the demands placed on attention and working memory by the secondary change-detection task. Similarly, there was some evidence of an interaction between Step and Tracking in Studies A, C and D, but there was no consistent oculo-manual facilitation. Irrespective of tracking condition, participants still had more difficulty judging the reappearance location of an object that reappeared close but behind the correct location.

The findings for the secondary change-detection task indicated across all studies that judgment accuracy was lowest for the form stimulus array and highest for the control stimulus array. Judgment accuracy did not appear to be associated with response time, which was in fact longest for the colour stimulus array. This may be indicative of a speed-accuracy relationship whereby participants took longer to achieve a high level of accuracy for the colour stimulus array. This could have been a consequence of processing both spatial configuration and colour of the elements in the stimulus array. For instance, Jiang et al., (2000) showed that the spatial configuration of elements in a stimulus array acts as an important source of relational information encoded in working memory, which then facilitates identification of a change in spatial location, colour or shape. The magnitude of reappearance step exerted some effect on change-detection accuracy but this was not consistent across studies. For example, there was no evidence that the increased difficulty of judging a reappearance just behind the true location was associated with worse performance of the secondary change-detection task. Similarly, while there some differences in judgement accuracy between the control, form and colour stimulus arrays in the ocular and oculo-manual

conditions, there was no evidence of oculo-manual facilitation. Together, these findings indicate that performance of the secondary change-detection task was not impaired by the demands placed on attention and working memory to extrapolate the occluded moving object of the primary spatial prediction task, nor was it enhanced by the presence of extra-retinal signals from upper limb movement.

The finding that oculo-manual tracking did not facilitate performance of either the primary or secondary tasks was counter to initial expectations. Although upper limb movement was not recorded, meaning it is not possible to be sure that participants followed instructions, the finding of some interaction effects involving tracking condition would seem to suggest this was the case. A more plausible explanation is that participants were not given sufficient opportunity to develop a coupling between the object and upper limb motion, which then limited the sharing of information between ocular and motor control centres. Due to the nature of the online testing, participants were instructed to place their right hand on their desk to the right of the keyboard, and then to move their hand such that it matched the speed of the moving object. They were given familiarisation trials, but at no point were there provided with visual feedback on their display regarding the movement of the right hand relative to the object. As such, they may have experienced difficulty determining with accuracy if the upper limb movement was well matched to the discrete, short duration, externally-generated object motion of the spatial prediction motion task. Notably, oculo-manual facilitation in previous work was particularly evident when performing large amplitude (e.g., 20-40deg), cyclical upper limb movement in which the object to be tracked was attached to the finger of moving limb (Gauthier & Hofferer, 1976; Gauthier et al., 1988; Vercher & Gauthier, 1988). Performing a less familiar coupling between eye and finger movements resulted in lower smooth pursuit gain (0.5) of a non-visible object than arm movements (0.7), which did not respond as well to training. That said, Mailoi et al., (2007) reported that simply holding the arm in a congruent postural configuration (i.e., pronated forearm) while performing pursuit eye movement results in active inhibition (i.e., reduced cortical excitability as determined by the

magnitude of MEPs) of the motor response. The authors concluded that pursuit of a moving object always entails a coordinated motor plan (i.e., common drive), which involves both eye and hand movements. The implication, therefore, is that more careful consideration of the impact of concurrent upper limb movement on attention-demanding tasks during pursuit eye movement is required. In addition, given that pursuit of an occluded object has been shown to involve several areas of prefrontal cortex (Lencer et al., 2004; Nagel et al., 2006; Ding et al., 2009), it will be relevant to determine if cortical activity in these areas is influenced by the difficulty of primary and secondary tasks performed during smooth pursuit, and whether the availability of extra-retinal input from upper limb mediates any effects.

In the next chapter, a lab-based experiment will be presented that uses the same dual pursuit task as Study A in this chapter. As well as giving a more controlled environment, a combination of video-oculography (Eyelink 1000) and neurophysiological (fNIRS) devices was used to record eye movement and cortical activity. However, this combination of devices first required some subsidiary analysis, which are presented in Appendix I. This Appendix was focused on methods and was primarily aimed at determining, and then minimizing, the impact of IR light from video-oculography on the fNIRS signal recorded from PFC. The general recommendation from manufacturers of fNIRS devices is to cover the optode array in order to minimise the impact of ambient light or other near-infrared light sources. This approach was adopted by Urakawa et al., (2015) and Shi et al., (2020), who combined fNIRS measurement (using Shadzu OM3000 and NIRSportTM, respectively) with eye tracking measurement (Tobii X120 eye tracker and Tobii Pro VR integration, respectively). Although not empirically verified, NIRx report that the EyeLink 1000 eye tracker does not interfere with the signal from their NIRSport device. Accordingly, it was expected that covering the NIRS optode would not be necessary for the NIRsport2, and would minimise the potential noise induced within the Brainsight NIRS.

Chapter 3: Prefrontal cortex activity and functional organisation in dual-task ocular pursuit is affected by concurrent upper limb movement.

This chapter, except for necessary changes to align with the thesis general formatting and the amendments requested by the examiners, is as published in Scientific Reports:

Borot, L., Ogden, R., & Bennett, S. J. (2024). Prefrontal cortex activity and functional organisation in dual-task ocular pursuit is affected by concurrent upper limb movement. *Scientific Reports*, *14*(1), 9996.

3.1 Introduction

Smooth pursuit and saccades are complementary but different functional outcomes of a similar cortico-ponto-cerebellar network (Krauzlis, 2004; Ilg & Their, 2008). Together, they ensure that gaze, and hence overt attention, is directed towards the object of interest, thus facilitating the processing of high acuity input from the central visual field, while at the same time enabling covert attention to process low acuity input from the peripheral visual field; for the spatial extent of covert attention during smooth pursuit (see Lovejoy et al., 2009; Watamaniuk & Heinen, 2015; Chen et al., 2017). Importantly, smooth pursuit is not simply a reflexive response to retinal input (Robinson et al., 1986; Krauzlis & Lisberger, 1989) and often involves cognitive processes such as attention, working memory and prediction (Barnes, 2008). Consequently, smooth pursuit may involve similar neural resources as secondary tasks presented at peripheral locations that require visual-spatial (Kerzel & Ziegler, 2005) or colour (Makovski & Jiang, 2009; Yue et al., 2017) working memory.

Specific areas of prefrontal cortex (PFC) are involved in the control of smooth pursuit, with activation varying between conditions where a moving object remains visible or is occluded. In the latter condition, participants exhibit a reduction in smooth pursuit velocity with the loss of retinal input (Becker & Fuchs, 1985), followed by an anticipatory increase if the object reappears (Bennett & Barnes, 2003; Churchland et al., 2003, Orban de Xivry et al., 2006). This is associated with increased activation of dorsolateral prefrontal cortex (DLPFC) (Lencer et al., 2004), which exhibits a negative correlation with the reduction in smooth pursuit velocity (Nagel et al., 2006). Findings of increased bilateral DLPFC activation during occlusion have also been reported (Ding et al., 2009), although this was mediated by additional cues that influenced predictability of the occluded object trajectory. The authors suggested that activation of different areas of PFC during ocular pursuit depends on the requirement for higher-order cognitive processes. This is consistent with the areas of PFC (DLPFC, medial PFC – MPFC) being differentially activated by demands on attention, working memory and

prediction (Schmid et al., 2001; Pierrot-Deseilligny et al., 2003; Burke & Barnes, 2008).

Here, we examined the impact of a secondary change-detection task (visual-spatial or colour working memory) embedded within a spatial prediction motion task, on DLPFC and MPFC measured using functional Near InfraRed Spectroscopy (fNIRS). These two areas of PFC have been implicated in working memory and related executive functions (Braver & Bongiolatti, 2002), and are involved in pursuit tasks (Nagel et al., 2006; Ding et al., 2009). Consistent with previous studies on prediction motion (Bennett & Benguigui, 2016), we expected participants to exhibit a decrease in judgment accuracy when the object reappeared close but behind the correct location. For the secondary change-detection task, we expected a decrease in judgement accuracy as a function of demand on working memory. Moreover, we expected that the increased demand on working memory in the change-detection task would result in changes in PFC activity and organisation.

Extending previous imaging work described above, we required participants to pursue the moving object of the prediction motion task with eyes alone, or eyes and upper limb. Afferent and efferent signals from the upper limb have been shown to facilitate smooth pursuit (Koken & Erkelens, 1992), even when the moving object undergoes an occlusion (Gauthier & Hofferer, 1976; Bennett et al., 2012). Modelling of behavioural data indicates a sharing of afferent and efferent signals between the oculomotor and motor systems, which act interdependently to achieve the task goal (Vercher et al., 1997). Accordingly, we expected that smooth pursuit would benefit from concurrent and congruent upper limb movement. It is less clear, however, whether afferent and efferent signals from the upper limb would facilitate prediction motion (Wexler & Klam, 2001) and change-detection judgment accuracy. Investigating whether upper limb tracking mediates the demand on attention and working memory, and how this affects PFC activity and efficiency of organisation, could help in understanding cortical control of pursuit tasks that are representative of everyday behaviours (e.g. driving, handwriting, drawing).

3.2 Materials and Methods

Participants

Nineteen participants (10 males, 9 females) with a mean age of 26.9 (± 4.6) years from the staff and student population of the host University took part in the study. All participants were right-handed and self-declared with normal or corrected vision and no neurological impairment. Participants provided written informed consent prior to participation in the study. The study received ethics clearance through the Liverpool John Moores University Research Ethics Committee (20/SPS/014), and was conducted in accordance with the ethical standards specified by the Declaration of Helsinki 2008.

Task and Procedure

Participants were invited to come to the laboratory to carry out a test session of about two hours. They were seated on a height-adjustable chair at a worktop, such that their eyes were 915mm away from a 24-inch LCD screen (ViewPixx EEG) operating at a resolution of 1280 x 1024 pixels and 100Hz refresh rate. The head was supported by a chin rest in order to minimize head movement (during blocks of experimental trials). An EyeLink 1000 (250Hz sampling rate) with remote optics was located beneath the lower edge of the LCD screen. Participants' gaze location was calibrated relative to the LCD screen using a 9-point grid: for one participant the calibration could only be achieved using 3 equidistant horizontal points centred on the mid-point of the display. The task was verbally explained to participants, and they were given the opportunity to familiarise with the protocol by performing 8 randomly-selected trials in both the ocular and oculo-manual tracking conditions before commencing the experimental phase of the study.

Participants performed a novel, dual-task pursuit protocol that placed specific demands on visual-spatial and colour working memory (Figure 3.1). The stimulus was generated using the Cogent toolbox v1.33 in Matlab® (MATLAB R2013b, The MathWorks, USA). Each trial started with 6000ms fixation, where a cross was displayed at -8.5 degrees to the left of screen

centre (grey background). This coincided with the start location of object motion and ensured that participants did not have to relocate the eye before the start of each trial. The fixation cross then changed to a white circular object (0.5 degrees diameter) with a black dot at its centre. After 500ms, the object disappeared for 300ms and then reappeared moving horizontally to the right with a constant velocity of 4deg/s. After 600ms, the moving object disappeared for a random duration of 1700, 1800, 1900, 2000 or 2100ms, and then reappeared for a further 400ms. Importantly, the moving object reappeared on each trial with a position step that was -4, -2, +2 or +4 degrees from the correct position had the object continued to move with constant velocity. Participants were informed that their primary task was to judge whether the moving object reappeared behind or ahead of the correct location (i.e., prediction motion). This judgement had to be made within a 3000ms interval after the moving object reappeared and required participants to press the z (behind) or v (ahead) key of the computer keyboard with their left hand. During each trial, participants pursued the moving object with either the eyes alone (ocular condition, *OC*) or with the eyes and right upper limb (oculo-manual condition, *OM*). For oculo-manual pursuit, movement of a stylus held in the right hand was measured with a Wacom A3 wide digitising tablet (250Hz), located between the participant and the LCD screen. The recorded x-axis position data of the hand-held stylus was scaled such that there was a 1:1 gain relationship between movement on the tablet and movement of the object on the screen. In order to ensure a natural coupling, participants were made aware of the correspondence between their hand and the object movement, but no visual feedback was provided on the LCD screen. This should have helped participants focus attention on the object motion, as well as to minimise ongoing corrective movements that occur when vision on the hand and object are continuously available.

For the secondary task, participants were required to judge whether there was a change in the form or colour between successive (cue and probe) presentations of a stationary stimulus array. Four squares (each 0.25deg) were initially presented for 500ms (cue) on the LCD display, centred to the spatial and temporal midpoint of the disappearance of the moving object. After

participants had given their response to the primary task, the four squares were presented again (probe) at a location coincident with the final position of the moving object (i.e., not the reappearance location). Participants were given 3000ms to judge whether the squares had changed form or colour between the cue and probe presentation by pressing the z (no change) or the v (change) key of the computer keyboard with their left hand.

In the *Form* stimulus array, the four squares were each initially assigned an x and y location to coincide with the four corners of a larger square of 1 deg. Each of the four squares were then randomly shifted by -0.25, 0 or +0.25deg. For the probe presentation, the four squares were either assigned the same location or all were randomly shifted again by -0.25, 0 or +0.25deg. For the *Colour* stimulus array, the four squares were each assigned an x and y location to coincide with the four corners of a larger square of 1deg, and then randomly assigned a colour (red, magenta, blue and green) with no repetition. For the probe presentation, the four squares were either assigned the same colour or the colour of all four squares were randomly assigned a second time with no repetition. In the *Control* stimulus array, participants were informed that there would be no change between the cue and probe presentation of four back squares, which were each assigned an x and y location to coincide with the four corners of a larger square of 1deg. Having given their response to the secondary change-detection task, participants were presented with a rest period, adjusted according to the occlusion duration, during which time the grey screen remained blank between 6000ms and 6400ms.

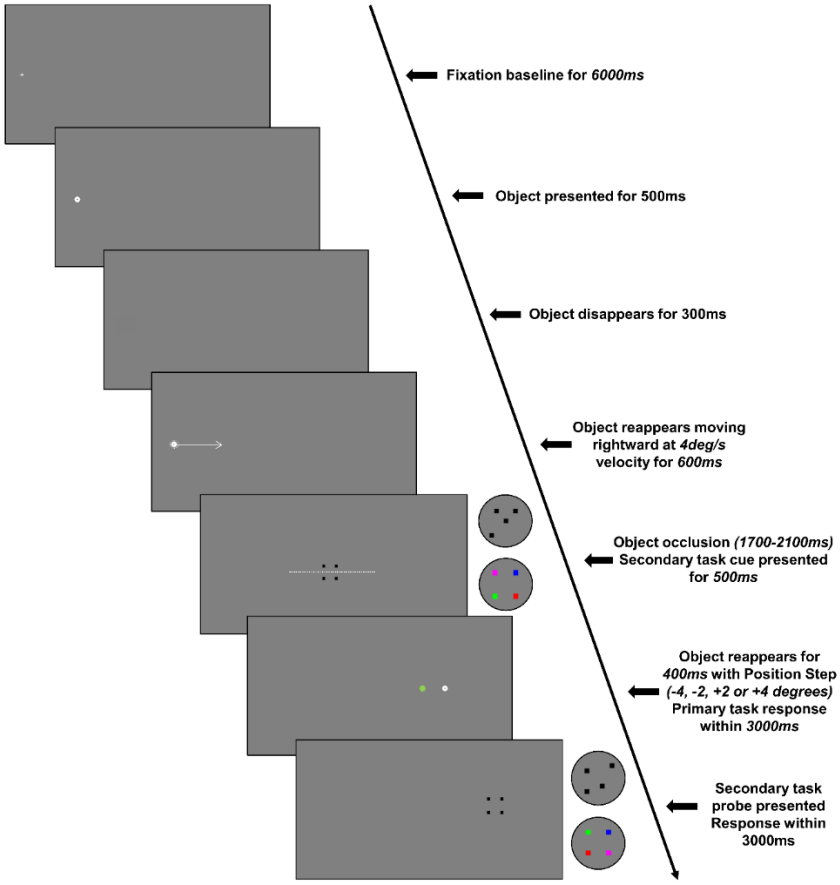

Figure 3.1: *Schematic diagram showing the timeline of a trial for the control stimulus array (enlarged examples of a form and colour stimulus array are shown within the circle to the right of the grey boxes). Nb. White arrow depicting direction of object motion and white broken line depicting occluded object trajectory were not visible to participants.*

There were 6 unique combinations of Stimulus Array (*Control, Colour, Form*) and Tracking (*OC, OM*), which were presented in a randomised block order. In blocks with the *Control* stimulus array, participants performed 24 randomly-ordered trials, with 6 trials for each Position Step (-4, -2, +2, +4deg). For blocks with the *Colour* or *Form* stimulus array, there was a randomly-ordered change between cue and probe in 12 of the 24 trials. Position Step was interleaved in these blocks, such that there was an equal distribution for trials with a change or no change in the stimulus array. For each trial, we evaluated the judgement accuracy of both the primary and secondary tasks, as well as the response time for the secondary task.

Data Acquisition and Analysis

Ocular pursuit

Eye position (relative to display reference system) and eye velocity (relative to head reference system) signals were exported using the Eyelink parser software. In addition, the software identified and labelled saccades and blinks in the x-axis and -y-axis eye position data. The criteria for saccade identification were a velocity threshold of 30deg/s, acceleration threshold of 8000deg/s^2, and a motion threshold of 0.15deg. Using routines written in Matlab® (MATLAB 2020b, The MathWorks, USA), we then derived desaccaded smooth eye velocity. To this end, identified saccades and blinks in the eye velocity trace, plus 5 additional data points at the beginning and end of the saccade/blink trajectory, were replaced by linear interpolation. Saccades were generally of small amplitude and short duration, making linear interpolation a simple and adequate method of signal restoration (Bennett & Barnes, 2003). The desaccaded eye velocity data were then filtered with a zero-phase, low-pass (20Hz) auto-regressive filter. From the resulting smooth eye velocity, we calculated for each trial, the average over 6 frames (i.e., 24ms) prior to occlusion (*T1*), 128-152ms after occlusion (*T2*), and 228-252ms after occlusion (*T3*).

fNIRS

Relative change in oxy (O_2Hb) and deoxy (HHb) haemoglobin while performing dual-task pursuit was quantified with a continuous wave NIRS system (BrainSight V2.3 system) that used two NIR wavelengths (705 and 830nm) and a sampling rate of 10 Hz. The optodes (receivers and transmitters) were placed on the head of each participant using a cap (EasyCap) with holes cut at predetermined locations. The cap was placed by the same experienced researcher and was located relative to standard head landmarks (Nasion, Inion and Cz). A piece of black material was placed over the optodes to avoid potential crosstalk with ambient light from the room and IR light from the EyeLink illuminator. A 20-channel optode array (Figure 3.2 - NB. generated using BrainNet viewer toolbox (Xia et al., 2013)) corresponding to the links between 8 receivers and 6 transmitters, plus two proximity sensors, was used to cover the right and left PFC (4 dorsolateral

channels and 5 medial channels for each hemisphere). Long-distance channels were positioned at around 3cm, whereas the short distance channels were positioned at an inter-optode distance of around 0.8cm, as recommended (Brigadoi & Cooper, 2015). The Brodmann areas covered by the different channels were extracted via the NFRI function (Singh et al., 2005) from the MNI (Montreal Neurological Institute) coordinates of the pre-cut cap holes (see Appendix II).

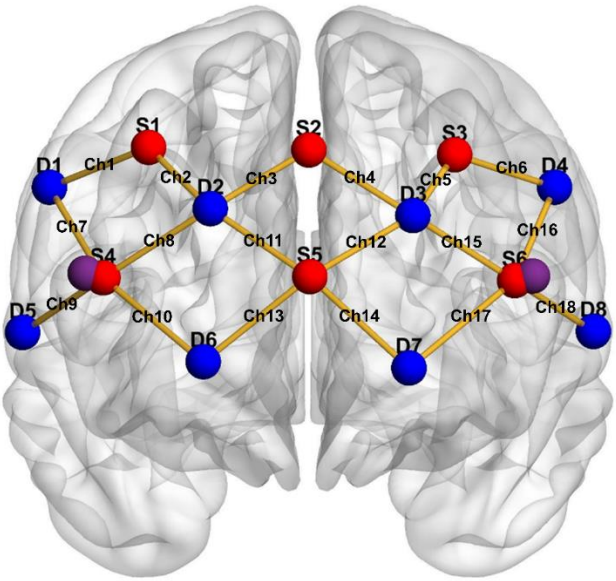

Figure 3.2: *fNIRS optode organisation. The red circles represent sources, the blue circles represent detectors, and the purple circles represent short distance detectors. The channels are represented with yellow edges.*

Although fNIRS is a relatively resistant method to motion artifacts and is commonly used for quantification of brain activity during motor tasks, the fNIRS signal may still be affected when the participant moves their head, speaks, or when there is a momentary loss of contact between the scalp and the optodes. Noisy fNIRS signals can also result from the presence of too much light, which causes signal saturation (especially in prefrontal cortex because there is no hair). To minimize any unwanted impact of noise on the

data analysis, for each participant, any channel not having a sufficient signal quality was excluded after observation of the power spectrum density of the O_2Hb signals, where the presence of a cardiac rhythm in the signal (peak around 1 Hz) indicates good contact between the scalp and optodes (Themelis et al., 2007). Following this process, 2 participants were excluded for fNIRS analysis as it was deemed that too many channels had bad quality signal. An additional participant was removed (from all analyses) because they did not perform the task as instructed. Following the signal quality verification process, 9% of channels was removed for the remaining participants. Raw data (optical intensity) extracted from the BrainSight software (V2.3) was converted to optical density (OD, light absorption variation) using the Homer2 toolbox (Huppert et al., 2009). Next, two methods were used to reduce possible head motion artifacts. First, the moving standard deviation and spline interpolation method (Scholkmann et al., 2010) was applied using parameters: SDTresh = 20, AMPTresh = 0.5, tMotion = 0.5s, tMask = 2s and p = 0.99. Second, wavelet-based signal decomposition (Molavi & Dumont, 2012) was used with parameter: iqr = 0.1, as recommended (Cooper et al., 2012). The OD time series were then converted into concentrations of O_2Hb and HHb using the modified Beer-Lambert law (Kocsis et al., 2006) corrected by a differential pathlength factor depending on the age of the participant (Duncan et al., 1996). A high (0.009Hz) followed by a low pass (0.5Hz) Butterworth zero phase digital filter (order 4) was applied to limit physiological artifacts. Finally, the short distance signal for each hemisphere was regressed to the long-distance channels located in the same hemisphere using the Matlab function *regress*. Time series of O_2Hb and HHb were extracted for each trial and baseline corrected using the mean value calculated from the 6000ms fixation time before the start of the trial. Relative changes of O_2Hb and HHb were then calculated from the mean of each time series and used in our following analysis of PFC activity.

Graphs metrics (see below) were calculated from 18-by-18 partial correlation matrices computed on the minutes 5-9 of the whole time series for each of the 6 conditions. After detrending, partial Pearson correlations, which represent the association between two channels while controlling the effect of the other

16 channels (Fornito et al., 2016; Fan et al., 2021), were calculated from the O_2Hb signal of each participant for all pairs of channels using Matlab function *partialcorr*. The resulting correlation matrices were subjected to Fisher z-transformation and all negative connections were set to zero. These weighted positive matrices were used to extract two measures of network efficiency: global efficiency, which is the average of inverse shortest path length and reflects the efficiency of information exchange in the whole network; local efficiency, which is the global efficiency computed on the neighbourhood of the node (i.e., channel) and reflects the information exchange between the immediate neighbour of a given node (Fornito et al., 2016). These efficiency metrics were calculated using functions implemented in the Brain Connectivity Toolbox (Rubinov et al., 2009).

Statistics

Judgment data from the primary and secondary tasks were analysed using generalized linear mixed modelling with a logit link function, whereas response time (secondary task), eye velocity and fNIRS data were analysed using linear mixed modelling (lme4 package v1.1-32 in RStudio 2023.03.0). Starting with the full fixed effects model in which each participant had a random intercept, an iterative, top-down process was followed in order to find the simplest model that best fit the data. Fixed effects were sequentially removed based on their statistical significance determined using Wald Chi Squared tests (CAR package v3.1-2), and those that returned p-values of 0.1 or less were provisionally retained. Model fit at each iteration was compared using conditional R^2 (MUMIn package v1.47.5 for logistic models; piecewiseSEM v2.3.0 for linear models) and AIC, with final model selection based on the outcome of a Likelihood Ratio Test (anova in R). Having determined the final reduced model, fixed effects at $p < 0.05$ were further analysed using Bonferroni-corrected pairwise comparisons (EMMEANS package v1.7.2). To provide a measure of effect magnitude, odds ratio for generalised linear mixed models, and mean differences for linear mixed models, are presented.

3.3 Results

Given the novelty of our protocol, it was first necessary to determine if participants performed the dual-task pursuit as expected. To this end, we examined the effect of Position Step (*-4, -2, +2, +4deg*), Stimulus Array (*Control, Colour, Form*) and Tracking (*OC, OM*) on behavioural measures (judgment accuracy; response time) from the prediction motion and change-detection tasks. For smooth pursuit of the moving object in the prediction motion task, we included an additional fixed effect of Time (*T1, T2, T3*) to determine the impact of removing visual feedback of the moving object during occlusion. Next, we evaluated the working memory demands of the change-detection task on PFC activity and organisation, and whether this was mediated by afferent and efferent signals from concurrent upper limb movement. Given the equivocality regarding activation of left and/or right DLPFC in pursuit tasks, and the lack of research on MPFC, our exploratory analysis for mean O_2Hb and HHb in each ROI, as well as global efficiency, investigated the effect of Tracking (*OC, OM*) and Stimulus Array (*Control, Colour, Form*). For local efficiency, we also included an additional fixed effect of Channel.

Behavioural measures

Prediction motion

For judgement accuracy the reduced model (AIC = 1014.20; marginal $R^2 = 0.61$; conditional $R^2 = 0.78$) indicated a significant main effect of Step [χ^2 (3) = 256.97; $p < 0.001$]. Consistent with our hypothesis, it can be seen in Figure 3.3a that judgments were less accurate ($p < 0.0001$) when the object reappeared with a small negative step (-2deg: 0.65) compared to all other steps (+2deg: 0.93, OR = 7.38; +4deg: 0.98, OR = 31.14; -4deg: 0.90, OR = 4.64). Judgments were also more accurate ($p < 0.0001$) when the object reappeared with a large positive step compared to small positive step (OR = 4.22) and large negative step (OR = 6.71).

For eye velocity, the reduced model (AIC = 1765.90; marginal R^2 = 0.35; conditional R^2 = 0.66) had significant main effects of Stimulus Array [χ^2 (2) = 18.57; p = 0.001], Tracking [χ^2 (1) = 14.42; p = 0.001] and Time [χ^2 (2) = 1195.85; p = 0.001], as well as a significant Stimulus Array x Tracking interaction [χ^2 (2) = 6.80; p = 0.033]. As expected, eye velocity was highest with vision of the moving object just prior to occlusion (2.76deg/s), decreased at onset of occlusion (2.21deg/s, MD = 0.55), and then decreased further as the occlusion interval progressed (1.59deg/s, MD = 0.62). Decomposition of the significant interaction effect revealed that eye velocity was significantly (p = 0.0003, MD = 0.20) higher in the *OM* (2.32deg/s) than *OC* (2.12deg/s) tracking condition for the *Form* stimulus array. There was no difference in eye velocity between the *OM* (2.14deg/s, 2.25deg/s) and *OC* (2.07deg/s, 2.22deg/s) tracking conditions for the *Colour* and *Control* stimulus arrays, respectively. In the *OC* tracking condition, eye velocity was significantly higher in the *Control* than *Colour* stimulus array (p = 0.02, MD = 0.15). In the *OM* tracking condition, eye velocity was significantly higher in the *Form* than *Colour* stimulus array (p = 0.002, MD = 0.18).

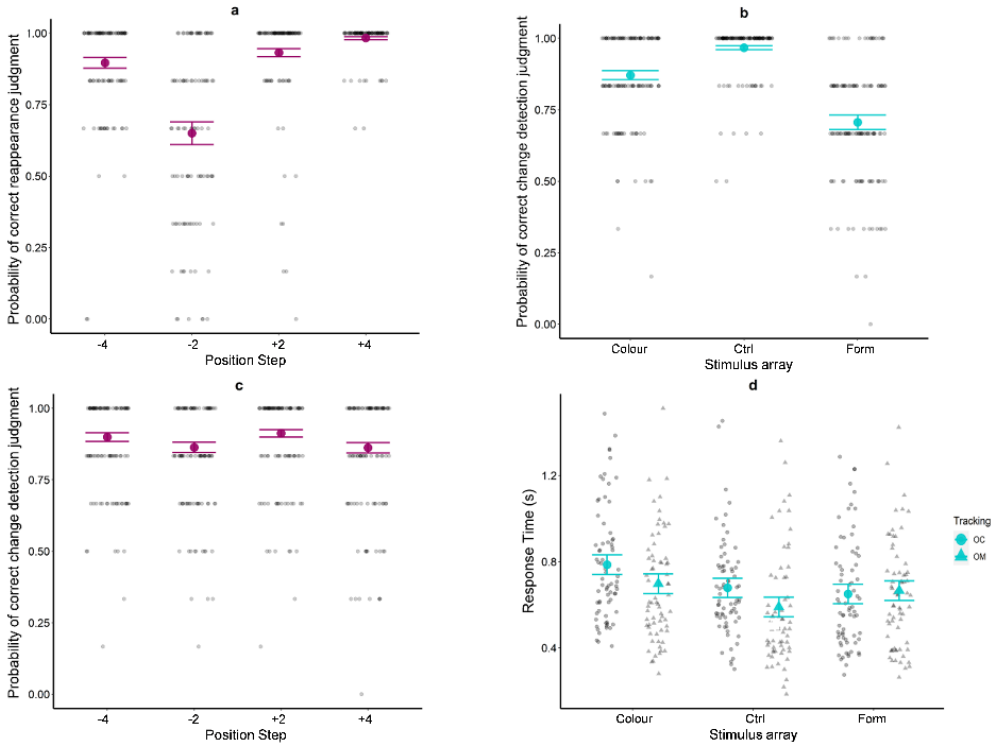

Figure 3.3: *Probability of correct judgment for each combination of Position Step (-4, -2, +2, +4deg) in the prediction motion task (panel a). Probability of correct judgment in the change-detection task for each combination of Stimulus Array (Colour, Control and Form; panel b). Probability of correct judgment for each combination of Position Step (-4, -2, +2, +4deg) in the change-detection task (panel c). Response time in the change-detection task for each combination of Stimulus Array and Tracking (panel d). Estimated marginal means (large, coloured markers) and the standard errors are shown from the accepted model. For panels a-c, individual data are represented as small, high-transparency dots and correspond to the individual probability of a correct judgement for each level of the factors not represented on the x-axis. For panel d, individual data are represented as small, high-transparency dots and correspond to the average response for each level of the factors not represented on the x-axis. For all panels, a small horizontal jitter has been introduced in order to reduce the overlap between individual data.*

Change-Detection

For judgment accuracy, the reduced model (AIC = 944.56; marginal R^2 = 0.61; conditional R^2 = 0.70) indicated a significant main effect of Stimulus Array [χ^2 (2) = 181.36; p < 0.001]. As expected, judgment accuracy for the *Control* stimulus array (0.97) was higher (p < 0.0001) than the *Form* (0.71, OR = 12.20) and *Colour* stimulus arrays (0.87, OR = 4.34). As shown in Figure 3.3c, judgment accuracy was lower for the *Form* than *Colour* stimulus array (p < 0.0001, OR = 2.81). There was also a main effect of Step [χ^2 (3) = 14.01; p = 0.003] but no interaction with Stimulus Array. As shown in Figure 3.3b, judgment accuracy on the change-detection task was higher for trials in which the primary pursuit object reappeared with a small positive position step (+2deg: 0.91) than a small negative position step (-2deg: 0.86, OR = 1.65, p = 0.017) or a large positive position step (+4deg: 0.86, OR = 1.66, p = 0.013).

For response time, the reduced model (AIC = -121.97; marginal R^2 = 0.05; conditional R^2 = 0.45) indicated a significant main effect of Stimulus Array [χ^2 (2) = 23.99; p < 0.001] and Tracking [χ^2 (1) = 7.86; p = 0.005], as well as a significant Stimulus Array x Tracking interaction [χ^2 (2) = 6.63; p = 0.04]. Response time in the *OC* tracking condition was longer for the *Colour* (0.786s) than *Control* (0.678s, MD = 0.11, p = 0.015) and *Form* (0.650s, MD = 0.14, p = 0.0005) stimulus arrays. In the *OM* tracking condition, response time was longer for the *Colour* (0.698s) than *Control* (0.590s, MD = 0.11, p = 0.02) stimulus array (Figure 3.3d).

Neuroimaging measures

Activity

For left DLPFC (Figure 3.4b), the reduced model (AIC = -141.4; marginal R^2 = 0.07; conditional R^2 = 0.23) indicated a significant main effect of Stimulus Array [χ^2 (2) = 8.85; p = 0.012]. Consistent with our expectation of an increased demand on working memory, mean O_2Hb was higher for *Colour* stimulus array (0.08µmol, MD = 0.08, p = 0.012) than the *Control* stimulus array (0.006µmol). Mean O_2Hb for the *Form* stimulus array (0.04µmol) was intermediate between the other two stimulus arrays (Figure 3.4b). However, there was no such effect for right DLPFC, with the full model

(AIC = -176.68; marginal R^2 = 0.04; conditional R^2 = 0.44) providing no better fit than the intercept-only model (AIC = -180.13; conditional R^2 = 0.41).

For left MPFC (Figure 3.4a) the reduced model (AIC = -175.74; marginal R^2 = 0.06; conditional R^2 = 0.41) indicated a significant main effect of Tracking [χ^2 (1) = 9.61; p = 0.0019]. As shown in Figure 3.4a, mean O_2Hb was greater in the *OC* (0.066µmol) than *OM* tracking condition (0.014µmol, MD = 0.05). For right MPFC, the full model (AIC = -138.77; marginal R^2 = 0.03; conditional R^2 = 0.38) indicated no significant main or interaction effects and was rejected in favour of the intercept-only model (AIC = -143.36; conditional R^2 = 0.35).

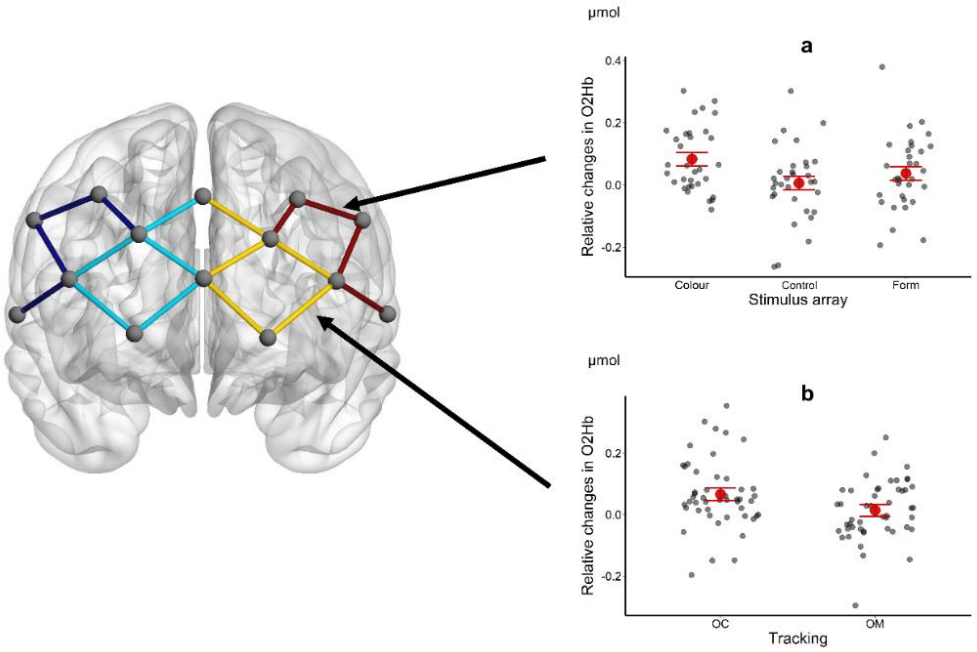

Figure 3.4: *Representation of the channels involved in each ROI (left), with the latter in different colours: dark blue = right DLPFC; light blue = right MPFC; yellow = left MPFC; red = left DLPFC. Mean O_2Hb in left DLPFC as a function of Stimulus Array (panel a) and left MPFC as a function of Tracking Condition (panel b). Estimated marginal means (large, coloured circles) and the standard errors are shown from the accepted model. Individual data are represented as small, high-transparency dots and correspond to the average response for each level of the factors not represented on the x-axis. For all panels, a small horizontal jitter has been introduced in order to reduce the overlap between individual data.*

For Mean HHb, no significant main or interaction effects were found, leaving us to accept the intercept-only model for left DLPFC (AIC = -338.75; conditional R^2 = 0.07), right DLPFC (AIC = -355.22; conditional R^2 = 0.45), left MPFC (AIC = -396.96; conditional R^2 = 0.05) and right MPFC (AIC = -344.54; conditional R^2 = 0.15).

Network organisation

The reduced model (AIC = -486.27; marginal R^2 = 0.05; conditional R^2 = 0.58) for global efficiency indicated a main effect of Tracking [χ^2 (1) = 10.79; p = 0.001]. As shown in Figure 3.5a, global efficiency was higher in the *OM* (0.19) than *OC* tracking condition (0.18, MD = 0.01).

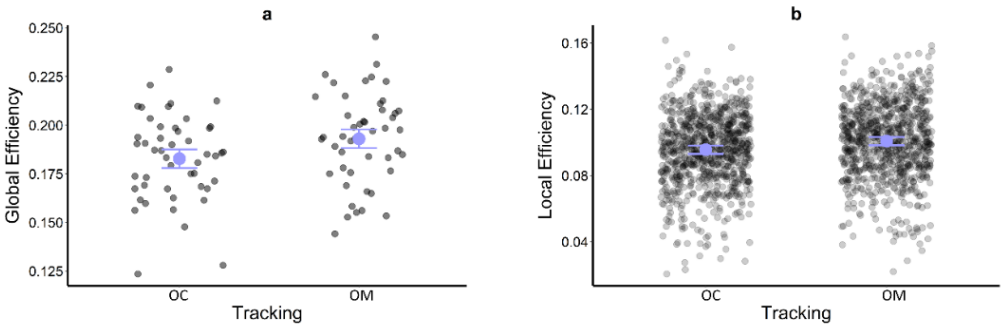

Figure 3.5: *Global efficiency (panel a) and Local efficiency (panel b) as a function of Tracking Condition, with estimated marginal means (large, coloured circles) and the standard error from the accepted model. Individual-participant data are represented by small, high-transparency dots and correspond to the average response for each level of the factors not represented on the x-axis. For all panels, a small horizontal jitter has been introduced in order to reduce the overlap between individual data.*

For local efficiency, the reduced model (AIC = -8687.3; marginal R^2 = 0.085; conditional R^2 = 0.28) had a significant main effect of Tracking [χ^2 (1) = 32.89; p < 0.001] and Channel [χ^2 (17) = 169.5, p < 0.001]. As can be seen in Figure 3.5b, local efficiency was higher in the *OM* (0.101) than the *OC* tracking condition (0.096, MD = 0.0052). Bonferroni-corrected pairwise

comparisons indicated local efficiency differed between many of the channels, but a clear pattern was for higher local efficiency in channels located with left and right MPFC (for pairwise differences see Appendix III).

3.4 Discussion

Increased demands on cognitive processes such as attention, working memory and prediction during ocular pursuit of occluded objects results in greater PFC activity (Lencer et al., 2004; Nagel et al., 2006; Ding et al., 2009). Extending these previous studies, we designed a novel dual-task pursuit protocol to determine the effects on PFC (DLPFC and MPFC) of a secondary change-detection task (visual-spatial or colour working memory), embedded within a prediction motion task. Participants performed the primary task with eyes alone or eyes and upper limb (i.e., arm), thus enabling us to determine the contribution of extra-retinal (afference and efference) signals from concurrent upper limb movement, which have been shown to enhance smooth pursuit of an occluded moving object (Gauthier & Hofferer, 1976; Bennett et al., 2012).

Consistent with previous work on spatial prediction motion (Bennett & Benguigui, 2016), judgments were less accurate when the pursuit object reappeared behind the correct location with a small negative position step (-2deg). The suggestion is that participants tend to underestimate object location along the occluded trajectory (Lyon & Waag, 1995; Tanaka et al., 2009), resulting in gaze being closely aligned with the object reappearance, and thus making judgments more difficult (Bennett & Benguigui, 2016; Wexler & Klam, 2001). In addition, there was no effect of the change-detection stimulus array on judgments of reappearance location, indicating that the allocation of attentional and working memory resource to the secondary task did not impair performance of the primary task. As expected, change-detection accuracy was highest for the control stimulus array. However, participants were less accurate at detecting a change in the form than the colour of the stimulus array. The lower accuracy was not associated

with an increased response time, which was in fact longest for the colour stimulus array. This may be indicative of a speed-accuracy relationship whereby participants achieved a high level of accuracy for the colour stimulus array by taking longer to give a response. Finally, there was no difference in judgment accuracy of the primary and secondary tasks between ocular and oculo-manual tracking conditions. The implication is that although extra-retinal signals from upper limb movement may impact upon smooth pursuit eye movements (Bennett et al., 2012), they do not necessarily affect the judgement of object reappearance (Zheng & Maraj, 2018; Wexler & Klam, 2001). Indeed, we found the expected reduction in eye velocity following the loss of visual feedback, which continued as the occlusion interval progressed (Becker & Fuchs, 1985; Bennett & Barnes, 2003), as well as evidence of a facilitatory effect from upper limb extra-retinal signals when the change-detection task involved the form stimulus array (Gauthier & Hofferer, 1976; Bennett et al., 2012).

The facilitatory effect of oculo-manual tracking on smooth eye movement was less prevalent than originally expected, even though participants were instructed to match the amplitude of object and upper limb motion, and given an opportunity to familiarise with the task. Previous work has shown that facilitation of smooth pursuit is greatest when the object motion is internally generated, cyclical with a duration of several seconds, and involves large amplitude upper limb movement (Gauthier & Hofferer, 1976). Our use of discrete, short duration, externally-generated object motion may have limited the sharing of information between ocular and motor control centres, and thus the facilitatory effect. It might also be suggested that this could also have been influenced by not having visual feedback regarding the ongoing hand movement. However, oculo-manual facilitation was found in previous work, where vision of an object attached to the moving limb was initially available and then removed for several cycles of limb motion (Gauthier & Hofferer, 1976). Importantly, oculo-manual facilitation was also observed in a condition where vision of the limb and an externally-generated object motion was not available throughout (Gauthier et al., 1988). In the latter study, there was evidence of a training effect on smooth pursuit eye movement after

several minutes in adults, which was not simply a result of improved accuracy of upper limb tracking. Whether such a training effect with the current protocol would have influenced smooth eye movement, and thus performance of the primary and/or secondary tasks remains to be seen. According to the scheme proposed in previous research (Wexler & Klam, 2001), the estimated displacement of an occluded moving object depends on a comparison between predicted and actual reappearance location (internalized), as well as current eye and actual reappearance location (externalized). Interestingly, however, the weight given to the externalized cue was reduced in oculo-manual pursuit of internally-generated object motion, implying that any training effect may depend on an improved prediction of the occluded object trajectory within the oculomotor system. If this can be trained (Madelain & Krauzlis, 2003), an improved trajectory prediction in the primary task might aid judgments of reappearance location, and potentially free-up attentional and working memory resource for detecting changes in form or colour of the stimulus array.

Our analysis of cortical activity and network organisation sought to determine if there were any changes as a function of the secondary change-detection task, and whether this differed between the ocular and oculo-manual pursuit conditions. An effect of the secondary change-detection task on mean O_2Hb was primarily found in left DLPFC. As could be expected given the role of DLPFC in working memory (Levy & Goldman-Rakic, 1999; Barbey et al., 2013), mean O_2Hb was lowest with the control stimulus array where participants knew in advance that there would be no change between cue and probe. Conversely, changes in mean O_2Hb were highest when participants were required to detect a colour change in the stimulus array. As described in the preceding section, participants were better at detecting a change in colour than form of the stimulus array, but it took them longer to give their response. As a subsidiary analysis, we investigated whether higher mean O_2Hb in left DLPFC was related to participants spending more time responding to the colour stimulus array. The model (AIC = -132.65; marginal R^2 = 0.075; conditional R^2 = 0.24) indicated a significant main effect of Stimulus Array [χ^2 (2) = 7.76; $p < 0.03$], but no significant effect of the covariate response

time [χ^2 (1) = 0.09; p > 0.05]. It would seem, therefore, that response time per se did not impact upon the change in mean O_2Hb, and instead that it was related to processing activities that occurred when faced with the colour stimulus array.

Although there was no systematic effect of the secondary change-detection task on activity in MPFC, we did find evidence of an effect for tracking condition. This was most obvious in left MPFC, with a lower mean O_2Hb in the oculo-manual than ocular tracking condition. Extending the behavioural findings discussed above, these data could indicate that extra-retinal signals from the upper limb do exert some influence on the attentional and working memory processes involved in dual-task pursuit, thereby reducing the cost for MPFC. In fact, while DLPFC is typically cited as a key area for working memory processes, such as those involved in representing an occluded object trajectory (Nagel et al., 2006; Ding et al., 2009), MPFC is involved in many cognitive processes (Braver & Bongiolatti, 2002; Ramnani & Owen, 2004), and monitors other areas of PFC (Mansouri et al., 2017). Of relevance to the current study is the role of MPFC in "cognitive branching" (Koechlin et al., 1999), which refers to situations requiring the maintenance/monitoring of a primary task goal while simultaneously allocating attention to a secondary task goal (Christoff et al., 2001). In the dual-task pursuit protocol, it is feasible that extra-retinal signals from the upper limb influenced the need for ongoing monitoring of the primary prediction motion task, and thus the associated processing demand in MPFC.

The influence of upper limb tracking in the dual-task pursuit protocol of the current study was found to extend beyond individual ROIs. At both a local and global level, network organisation in PFC was more efficient in the oculo-manual than ocular tracking conditions. This is consistent with a network organisation that supports simultaneous integration and segregation of brain function (Fornito et al., 2016), which would presumably be beneficial when there are several concurrent sources of information to process and tasks to complete. Nonetheless, this PFC organisation did not appear to be associated with increased judgment accuracy of the primary or secondary tasks, which did not differ between ocular and oculo-manual tracking conditions. That

said, oculo-manual tracking did not simply direct attention away from the primary task or act as a further task that competed for processes involved in the primary and/or secondary task. From a behavioural perspective, such an effect has recently been shown in a similar task requiring visual-spatial motion prediction (Li et al., 2023). A key difference compared to the current study is that here the upper limb was used to pursue the moving object, whereas in previous studies (Li et al., 2023) the upper limb was used to respond to a secondary interceptive timing task. The authors suggested that the condition with an upper limb movement resulted in two concurrent temporal estimations being monitored/performed, which placed an additional demand on processes occurring within the same cortical-subcortical network. Here, it should be mentioned that although we found O_2Hb in PFC changed as a function of the demands of our dual-task protocol, there was no evidence of a parallel change in HHb. We do not have a definitive answer for why this theoretical patten in the two chromophores was not observed in our fNIRS data, but it could in part be related to the fact that changes in O_2Hb are usually of higher amplitude than changes in HHb (Pinti et al., 2020). It is also important to note that we included several control measures such as a baseline comparison condition, short-distance channels, covering channels with a piece of black material to minimize cross-talk from Eyelink IR illuminator, and preprocessing steps to improve signal quality (see Tachtsidis & Scholkmann, 2016)). Therefore, we contend that our results are more likely to represent task-evoked changes in the hemodynamic response than a false positive as consequence of a confounding factor. That said, it should be recognized that a two-stage procedure was applied for the control of Type 1 errors in the current study. At the first stage, reduced models for each dependent measure ($n = 14$) were derived using an iterative, top-down process in which main and interaction effects were retained at $p < 0.05$. At the second stage, Bonferroni-corrected pairwise comparisons were performed, thus maintaining $p < 0.05$ for the decomposition of each significant main and/or interaction effect. Therefore, given that the number of statistical tests performed across the 2 stages, it is likely that at least one of the significant effects was a false positive.

3.5 Conclusion

We showed that activity and organisation of PFC was influenced by the increased demands on attentional and working-memory processes of performing a secondary change-detection task embedded within a prediction motion task. This was mediated by performing concurrent upper limb movement, and hence the availability of extra-retinal input. Future study is required to further characterise the hemodynamic (O_2Hb and HHb) response in dual-task protocols, potentially including additional dependent measures (e.g., area under curve, peak concentration, time to peak concentration, slope fitted to curve), and/or neurophysiological measurements (e.g., EEG, MEG) that provide more direct assessment of cortical activity with higher temporal resolution. This could also consider the wider brain network, such as the fronto-parietal network that controls eye-hand coordination (Battaglia-Mayer & Caminiti, 2018). Indeed, although there is some recent work on functional connectivity between visual, parietal and frontal areas during smooth pursuit (Schröder et al., 2020; 2023), the influence of higher cognitive control or the need to perform concurrent tasks remains to be determined. Tasks with competing demands are commonplace in normal daily settings, and are sensitive to changes in cognitive function associated with acute and chronic neurological conditions (Fukushima et al., 2013).

Chapter 4: Cortical activity and network organisation during oculo-manual vs ocular pursuit: The impact of task adaptation.

4.1 Introduction

Smooth pursuit eye movement (SPEM) is known to involve a wide range of cortical regions (Lencer et al., 2004; Krauzlis, 2004, 2005; Schröder et al., 2020; Nagel et al., 2006), with activity modulated by factors such as object velocity and the availability of retinal input. For example, Nagel et al., (2006) reported that activation of DLPFC (left hemisphere) was negatively correlated with object velocity, whereas LIP (right hemisphere) was negatively correlated with saccadic frequency, in conditions where the object was continuously visible or occluded (i.e., 1000ms centred to the mid-point of horizontal motion). In addition, they found in the latter condition that activation of FEF and Angular Gyrus (left hemisphere) was also negatively correlated with smooth pursuit velocity. It was concluded that regions of the frontal and parietal cortex are involved in compensatory mechanisms when there is a mismatch between eye and object velocity, and in particular when maintaining smooth pursuit in the absence of retinal input during transient occlusion. In the latter condition, participants exhibit a reduction in pursuit velocity at the onset of occlusion and the loss of retinal input (Becker & Fuchs, 1985), followed by an anticipatory (Bennett & Barnes, 2003) and predictive (Bennett & Barnes, 2004; Orban de Xivry et al., 2006) increase in pursuit velocity if the object is expected to reappear. This pattern of smooth pursuit velocity is consistent with the oculomotor control system using extra-retinal input to represent and predict the occluded object trajectory (for a behavioural model see Bennett & Barnes, 2004; Fukushima et al., 2013).

Extending upon this work, Ding et al., (2009) reported that bilateral FEF activation was evident irrespective of a moving object's visibility but was influenced by the presence of additional cues regarding the object trajectory (No Trace, Partial Trace, Full Trace). This is consistent with FEF influencing control of the eye velocity command through direct connections to the premotor nuclei of the brainstem. Conversely, bilateral DLPFC activation increased when the object was occluded, as well as when trajectory predictability decreased due to the absence of additional cues. Correlation analysis indicated a functional link (inter and intra hemispheric) between the

bilateral FEF and DLPFC when tracking a continuously visible moving object. Also, there was a significant correlation between the right anterior cingulate cortex (ACC) and FEF (left and right hemisphere), which was suggested to reflect overt attentional processing of retinal slip. However, there was a different functional organisation for trials with occlusion, with stronger interhemispheric correlations between the left and right FEF, and left and right DLPFC, and intrahemispheric correlations between right DLPFC and FEF. The authors (Ding et al., 2009) suggested that although a functional interaction exists between FEF and DLPFC whenever participants pursue a moving object, these areas of PFC make distinct contributions to oculomotor control depending on the task demands and associated requirement for higher-order cognitive processes.

As seen in the previous chapter, PFC activity (activation and network organisation) is also modified when SPEM is performed with concurrent upper limb movements. It was suggested that afference and/or efference from upper limb movements could have provided extra-retinal information on the occluded object trajectory, which thereby modulated the predictive processes operating in PFC. However, facilitation of SPEM and the influence on PFC activity by concurrent upper limb movement was less than expected, potentially due to the use of discrete, short duration externally-generated object motion. Specifically, a step ramp stimulus was used, with random occlusion duration to avoid anticipation of reappearance location that would have impacted upon the primary spatial prediction motion task. This also permitted the probe of the secondary change-detection stimulus to be presented on a blank screen after completion of the primary task. Importantly, however, most of the previous work showing facilitation of SPEM by concurrent upper limb movement (Gauthier & Hofferer, 1976), required participants to pursue cyclical object motion (i.e., triangular or sine wave) over a duration of several seconds (for facilitation in single step ramps see Bennett et al., 2012). With such stimuli, there was a training effect after several minutes in adults, which resulted in improved upper limb tracking and SPEM, as well as less correlation between these effectors (Gauthier et al., 1988). The implication is that a short period of training with concurrent upper

limb movement enables participants to better predict an upcoming object trajectory and maintain SPEM based on the exchange of information from extra-retinal signals (afference, efference), which is coordinated by a controller that permits independence between the ocular and motor systems (Vercher & Gauthier, 1988; Gauthier et al., 1988).

In the current chapter, the aim was to investigate the cortical activity and network organisation within a wider network of areas involved during occlusion in a smooth pursuit task, as well as how this is modulated by extra-retinal input provided by concurrent upper limb movement before and after a period of training. In addition to frontal regions (e.g. PFC and FEF), which are known to be involved in maintenance of SPEM, it is relevant to consider PPC, which is active during SPEM (Nagel et al., 2006; Schröder et al., 2020), and plays an important role in visuomotor integration during eye-hand coordination (Battaglia-Mayer & Caminiti, 2018). Pre-motor cortex has also been shown to be involved during pursuit of an occluded object (Lencer et al, 2004), with its activity being negatively correlated with saccade frequency, suggesting a role in saccadic suppression (Nagel et al., 2006). Pre-motor cortex associations with motor cortex are also known to be part of the network involved in control of eye-hand coordination (Battaglia-Mayer et al., 2006). For example, these regions are part of the dorsal attention network (DAN), which accounts for factors such as overt and covert spatial attention. They are also part of the fronto-parietal network (FPN) involved in cognitive processes such as working memory, which includes DLPFC, pre-motor cortex and PPC (Menon & D'Esposito, 2022). To this end, a 24 by 24 fNIRS optode array was used to image regions of MPFC, DLPFC, FEF, pre-motor and motor cortex (MC), PPC (IPL, SPL) and visual cortex (VC) while participants pursued a sinusoidal object motion that was either continuously visible or transiently occluded (predictable location and duration), with eyes alone or eyes and upper limb.

It was expected that smooth pursuit with occlusion would be improved (e.g., increased eye velocity and/or better correspondence with object velocity) by concurrent upper limb movement. Moreover, it was expected that this improvement would be influenced by a period of training in which

participants pursued a continuously visible object with eyes and upper limb. Based on findings for cortical activity and network organisation in the previous chapter, it was hypothesised that oculo-manual facilitation would be associated with a reduced change in O_2Hb compared to ocular tracking alone in more frontal regions, as well as changes in local and global efficiency. The latter measures reflect integration and segregation of a cortical network and are known to be modified as a function of task demand, with a critical role being reported in cognitive function (Sporns, 2013, Cohen & D'Esposito, 2016).

4.2 Materials and Methods

Participants

Twenty-eight participants (16 males/ 12 females) from the University staff and student population volunteered to take part in the study (mean age of 26.54 ± 5.79 years). All participants were right-handed and self-declared with normal or corrected vision and no neurological impairment. All participants provided a written informed consent to participate in the study. The study was approved by the local ethics committee (20/SPS/014) and was conducted in accordance standards of the Declaration of Helsinki, (2008).

Task and Procedure

Participants came to the laboratory on a single occasion for approximately one hour. After being given verbal and written instructions, they were invited to sit on a height-adjustable chair at a worktop with a chin rest. The cap and optodes of the NIRS neuroimaging system (NIRSport2, NIRX) was then placed on their head. To minimize potential crosstalk between the fNIRS system and ambient light from the room and LCD screen, as well as IR light from the EyeLink illuminator, a piece of black material was used to cover the optodes. Next, participants were asked to place their chin and forehead on a support, which ensured their eyes were 915 mm away from a 24-inch LCD screen (ViewPixx EEG) with 1280 x 1024 pixels resolution and 100 Hz

refresh rate. An EyeLink 1000 with remote optics was located beneath the lower edge of the LCD screen and used to record eye gaze at 250Hz. Participants gaze location was calibrated relative to the LCD screen using a nine-point grid prior to each block of trials.

Having completed the initial set-up. the experiment commenced, which comprised two testing sessions (pre and post), separated by a short training session. In each, participants were asked to pursue a red circular object (0.5 degrees diameter with a black dot at its centre), which moved horizontally against a black background on the LCD screen in accord with a sine wave (20 deg amplitude and 0.1 Hz frequency) for 3.5 cycles (35s trial duration) followed by 30s rest period. Participants were asked to pursue the object as accurately as they could with eyes alone (ocular condition – OC) or with eyes and hand (oculo-manual condition - OM). In the latter condition, hand movements were recorded as participants moved a hand-held stylus on a Wacom A3 wide digitising tablet (250 Hz sampling rate). This provided real-time input on the x and y position of the hand-held stylus, which was used to draw a grey anulus of 0.8 degrees diameter on the LCD screen (Figure 4.1). Participants were instructed to keep the anulus surrounding the moving object as accurately as they could. All trials started with 6s fixation, during which a white cross was displayed in the centre of the screen. During the last 3s second of fixation in the oculo-manual condition, the white annulus representing the hand-held stylus was displayed surrounding the fixation cross to inform participants that the next trial would involve manual tracking. Generation of the visual stimuli, recording of data from the Wacom digitising tablet and synchronisation with the EyeLink 1000 and NIRSport2 was achieved using the Cogent Toolbox in Matlab® (MATLABR2013b, The MathWorks, USA).

In the pre-test and post-test sessions, the moving object was either visible throughout the entire trial or was occluded (not during the first cycle) for 1250ms (Figure 4.1, panel 3). The occlusion was aligned to the mid-point (screen centre) of a cycle as the object moved from left to right and from right to left of the screen (i.e., 5 occlusion events per trial, see Figure 4.1). This resulted in four conditions (ocular and oculo-manual tracking with and without object occlusion), in which three trials were performed in a

randomised order, resulting in a total of 12 trials per pre-test and post-test session. In the adaptation session, participants performed 10 trials of oculo-manual tracking without occlusion.

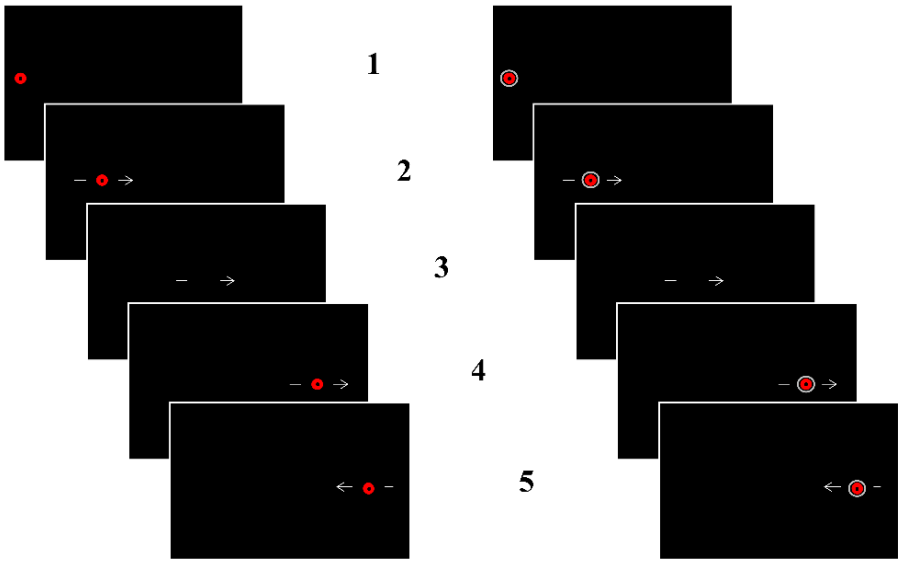

Figure 4.1: *Diagram showing the timeline of a trial for the ocular (left) and oculo-manual conditions (right). In the latter, a grey annulus line representing hand movement on the tablet was drawn on the screen. Nb. White arrow depicting direction of object motion was not visible to participants. Panel 3 represents the occlusion, during which the object and anulus were not visible to participants.*

Changes in O_2Hb and HHb were quantified with functional near infrared spectroscopy (NIRSport2), using two wavelengths (760nm and 850nm) at a sampling rate of 6.8 Hz. A 24-by-24 optode array was used, which resulted in a total of 79 long distance channels and 8 short distance channels. Optode organisation was made using NIRsite software based on the 10-5 coordinate system (Figure 4.2; Appendix IV). To define regions of interest (ROIs), Brodmann areas covered by channels were computed using the NFRI function (Singh et al., 2005), which used the MNI (Montreal Neurological Institute) coordinates of the optode array reported by the manufacturer software. This resulted in 7 ROIs, comprised from 50 long distance channels (Figure 4.2; Appendix IV).

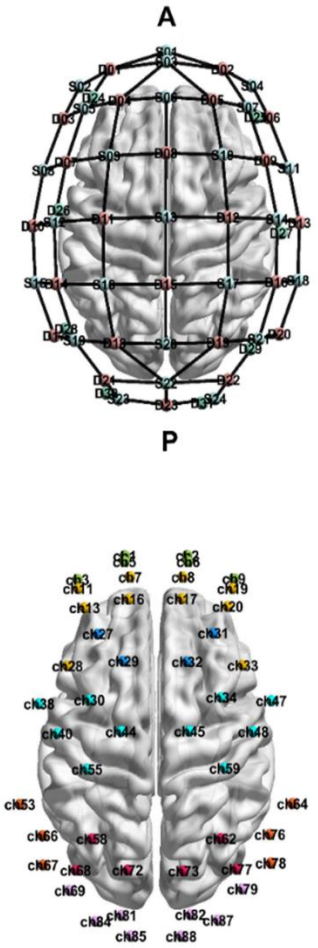

x	y	z	Brodmann area	ROI	Channel
-18.18	86.63	4.132	BA 10-11	Medial prefrontal cortex	ch1
17.831	86.686	3.61	BA 10-11	Medial prefrontal cortex	ch2
-45.39	73.735	-0.041	BA 10-11	Medial prefrontal cortex	ch3
-18.35	83.517	24.189	BA 10-11	Medial prefrontal cortex	ch5
18.291	83.473	24.403	BA 10-11	Medial prefrontal cortex	ch6
44.695	74.252	0.088	BA 10-11	Medial prefrontal cortex	ch9
-15.19	75.206	45.743	BA 9-46	Dorsolateral prefrontal cortex	ch7
15.3	75.099	45.855	BA 9-46	Dorsolateral prefrontal cortex	ch8
-44.94	68.817	26.355	BA 9-46	Dorsolateral prefrontal cortex	ch11
-41.39	58.42	48.855	BA 9-46	Dorsolateral prefrontal cortex	ch13
-15.84	63.087	62.131	BA 9-46	Dorsolateral prefrontal cortex	ch16
14.824	63.339	62.24	BA 9-46	Dorsolateral prefrontal cortex	ch17
44.019	68.912	28.114	BA 9-46	Dorsolateral prefrontal cortex	ch19
41.232	59.179	48.129	BA 9-46	Dorsolateral prefrontal cortex	ch20
-51.16	26.914	66.065	BA 9-46	Dorsolateral prefrontal cortex	ch28
49.824	27.354	67.243	BA 9-46	Dorsolateral prefrontal cortex	ch33
-33.62	44.199	68.798	BA 8	Frontal eye field	ch27
-19	29.518	84.724	BA 8	Frontal eye field	ch29
32.853	44.739	68.91	BA 8	Frontal eye field	ch31
17.84	29.239	85.234	BA 8	Frontal eye field	ch32
-38.47	8.634	84.604	BA 4-6	Motor cortex	ch30
37.492	9.942	84.648	BA 4-6	Motor cortex	ch34
-67.5	6.477	58.072	BA 4-6	Motor cortex	ch38
-57.08	-9.562	77.439	BA 4-6	Motor cortex	ch40
-20.29	-8.513	97.94	BA 4-6	Motor cortex	ch44
19.132	-8.372	98.259	BA 4-6	Motor cortex	ch45
66.337	8.158	58.736	BA 4-6	Motor cortex	ch47
55.859	-8.634	78.224	BA 4-6	Motor cortex	ch48
-39.9	-28.88	93.294	BA 4-6	Motor cortex	ch55
39.401	-28.29	93.506	BA 4-6	Motor cortex	ch59
-78.59	-47.96	46.962	BA 39-40	Inferior parietal lobule	ch53
78.473	-47.5	47.691	BA 39-40	Inferior parietal lobule	ch64
-65.59	-64.99	61.605	BA 39-40	Inferior parietal lobule	ch66
-65.27	-80.77	41.942	BA 39-40	Inferior parietal lobule	ch67
65.533	-64.26	62.278	BA 39-40	Inferior parietal lobule	ch76
66.047	-79.71	41.904	BA 39-40	Inferior parietal lobule	ch78
-37.08	-66.68	87.378	BA 7	Superior parietal lobule	ch58
37.194	-66.44	87.445	BA 7	Superior parietal lobule	ch62
-46.47	-83.65	67.196	BA 7	Superior parietal lobule	ch68
-16.52	-83.46	82.647	BA 7	Superior parietal lobule	ch72
15.737	-83.96	82.348	BA 7	Superior parietal lobule	ch73
46.356	-82.98	68.005	BA 7	Superior parietal lobule	ch77
-49.79	-94.52	46.614	BA 17-18-19	Visual cortex	ch69
49.609	-93.72	48.485	BA 17-18-19	Visual cortex	ch79
-20	-108	44.777	BA 17-18-19	Visual cortex	ch81
19.681	-107.6	45.695	BA 17-18-19	Visual cortex	ch82
-34.96	-111.3	21.892	BA 17-18-19	Visual cortex	ch84
-14.65	-119.2	10.635	BA 17-18-19	Visual cortex	ch85
35.667	-110.6	23.25	BA 17-18-19	Visual cortex	ch87
14.381	-119.3	10.575	BA 17-18-19	Visual cortex	ch88

Figure 4.2: Left top: *Representation of the 24x24 full optode organisation (emitters = light red dots; receivers = light blue dots) and channels (black edges). Left bottom: Representation of channels included in each ROI (one colour per ROI). Right: MNI coordinate for each channel included within an ROI, as well as the Brodmann area covered by the channel identified using NFRI function (Singh et al., 2005). In the right of the table, the channels included in an ROI can be identified by a colour assigned to each ROI.*

Data preprocessing

Eye Movement: Eye position (relative to display reference system) and eye velocity (relative to head reference system) signals were exported using the Eyelink parser software. In addition, the software identified and labelled saccades and blinks in the x-axis and y-axis eye position. The criterion for saccade identification was a velocity threshold of 30 deg/s, acceleration threshold of 8000 deg/s^2, and a motion threshold of 0.15 deg. Using routines written in Matlab® (MATLAB 2020b, The MathWorks, USA), the identified saccades and blinks were removed from the eye velocity trace, plus 5 additional data points at the beginning and end of the saccade/blink trajectory. The deleted data was replaced by a linear interpolation routine based on the smooth eye velocity before and after the saccade (5 data points). An additional pass was then made to identify and remove eye velocity greater than 15 deg/s. Any velocity data that was subsequently found to exceed this threshold (i.e., after the second round of linear interpolation) was replaced with NaN. The desaccaded eye velocity data were then processed with a zero-phase, low-pass filter (i.e., moving average filter with a 30 frame window semi-length: nanmoving_average by Carlos Vargas). Using synchronisation signals generated by the stimulus generation routine (i.e., TTL), smooth eye velocity for each trial was identified. Average eye velocity in each trial was then calculated during the five intervals (i.e., 1250ms) corresponding to an occlusion (e.g. five occlusions per trial). This was also calculated over the same interval in trials without occlusion.

Hand Movements: Hand position data from the tablet was processed using custom-written routines in Matlab® (MATLAB 2020b, The MathWorks, USA). Position data in the x-axis were processed with a zero-phase, low-pass filter (i.e., moving average filter with a 5 frame window semi-length: nanmoving_average) after which hand velocity was derived by applying a 3-point central difference calculation to the position data. Average hand velocity in each trial was calculated over the same intervals as smooth eye velocity. Finally, any velocity data that was subsequently found to exceed the group mean ± 3SDs was replaced with NaN. Such data were deemed to be indictive

of participants not performing the task as instructed, and thus classified as outliers and removed from subsequent analysis.

Neuroimaging: The first step of fNIRS preprocessing was to minimize the impact of signal noise on the subsequent data analysis. For this purpose, a consensus-based approach was applied to the raw data extracted from the Aurora software (2021.9). Three methods proposed in the literature to assess the signal quality were used. The first involved observation of the power spectrum density of the O_2Hb signals for each channel for each participant, where the presence of a cardiac rhythm in the signal (peak around 1 Hz) indicates good contact between the scalp and optodes (Themelis et al., 2007). The second method used the coefficient of variation on O_2Hb, with a maximal threshold of 15% used to define a channel as being of insufficient quality. The third method involved the application of QT-nirs with the following parameters: window: 3s; overlap: no; qualityThreshold = 0.75; sciThreshold = 0.7; pspThreshold = 0.1. Channels not identified as being of good quality by at least 2 from 3 of the quality control methods were excluded from the subsequent analysis. Participants classified as having more than 33% excluded channels, or more than two ROIs without any good quality channels, were excluded from the fNIRS analysis (n = 7). Two channels were automatically excluded as the source-detector distance was too long. In addition, 2 participants only had data of sufficient quality at pre-test, but these were included in subsequent processing and analysis.

Data were next processed using functions from the Homer2 toolbox (Huppert et al., 2009). Raw data extracted from the Aurora software (2021.9) was converted to optical density, after which the following two methods were applied to reduce possible head motion artifacts as recommended in Cooper et al., (2012): 1) moving standard deviation and spline interpolation (Scholkmann et al., 2010) using parameters: SDTresh = 20, AMPTresh = 0.5, tMotion = 0.5s, tMask = 2s and p = 0.99; 2) wavelet-based signal decomposition (Molavi & Dumont, 2012) with iqr = 1.5. The optical density time series were next converted into concentrations of O_2Hb and HHb using the modified Beer-Lambert law, with a differential pathlength factor depending on the age of the participant (Duncan et al., 1996). To limit the

presence of physiological artifacts in the data, a high (0.009 Hz) and low pass (0.1 Hz) Butterworth zero phase digital filter (order 4) was applied. The signal from short distance channels (n = 8) was then regressed to the long-distance channels (NB. the short distance channels were regressed to long distance channels from the closest ROI). Time series of O_2Hb and HHb were extracted for each trial using synchronisation signals generated by the stimulus generation routine (i.e., TTL), and baseline corrected using the mean value calculated on 20s of the rest period, starting 3s before the start of the next trial. The first trial of each pre-test and post-test was excluded from further analysis. Separately for O_2Hb and HHb, the respective time series from channels within each ROI were averaged (see Figure 4.2), after which the average concentration was extracted from the entire 35s trial duration. For measures of efficiency, graphs metrics (see below) per participant per trial were calculated by first detrending and then calculating partial Pearson correlations between the O_2Hb time series for all pairs of channels. The resulting 50-by-50 partial correlation matrices (channel by channel from each ROI) were next subjected to z Fisher transformation, with all negative connections then set to zero. From the weighted positive matrices, local and global efficiency were extracted using functions implemented in Brain Connectivity Toolbox (Rubinov et al., 2009).

Statistics

Intra-participant means for each dependent measure were organised in long form according to each combination of independent variables in the factorial design. For smooth eye velocity and global efficiency, these were: Tracking (OC; OM); Occlusion (with; without); and Test (pre-test; post-test). For hand velocity, Tracking could not be included, whereas for fNIRS activation and local efficiency, Hemisphere (left; right) was added. The dependent measures were analysed using linear mixed modelling (lme4 package in RStudio, v). Starting with the full model that included all main and interaction effects (fixed effects), as well as a random intercept per participant (random effect), an iterative, top-down process was followed in order to find the simplest

model that best fit the data. Fixed effects were sequentially removed based on their statistical significance determined using Wald Chi Squared tests (CAR package v3.1-2). Final model fit was reported using conditional R2 (piecewiseSEM v2.3.0) and AIC. Fixed effects at $p \leq 0.05$ were then further analysed using a set of custom contrasts including only relevant pairwise comparisons (i.e., a change in only 1 level of a single factor while keeping levels of other factors constant), which were then subject to Bonferroni pairwise correction (EMMEANS package v1.7.2). For brevity and clarity, only the significant fixed effects from the final accepted model are presented. Similarly, only pairwise comparisons at $p \leq 0.05$ are reported in the text.

4.3 Results

Eye Velocity

The reduced model (AIC = 8795; conditional R^2 = 0.786) indicated a significant main effect of *Tracking* [χ 2 (1) = 201.89; $p < 0.001$] and *Occlusion* [χ 2 (1) = 10833.97; $p < 0.001$], as well as a significant *Occlusion* x *Test* interaction [χ 2 (1) = 11.94; $p = 0.0005$] and significant *Occlusion* x *Tracking* interaction [χ 2 (1) = 11.85; $p = 0.0006$]. As can be seen in Figure 4.3, eye velocity was lower at pre-test and post-test in trials with occlusion (2.48deg/s; 2.59deg/s) than without occlusion (6.16deg/s; 6.03deg/s). Eye velocity was also lower in post-test than pre-test in trial without occlusion ($p = 0.046$). Also, eye velocity during OC and OM tracking was lower in trials with occlusion (2.23deg/s; 2.83deg/s) than without occlusion (5.91deg/s; 6.28deg/s). Finally, in trials with and without occlusion, eye velocity was lower in the OC than OM tracking condition.

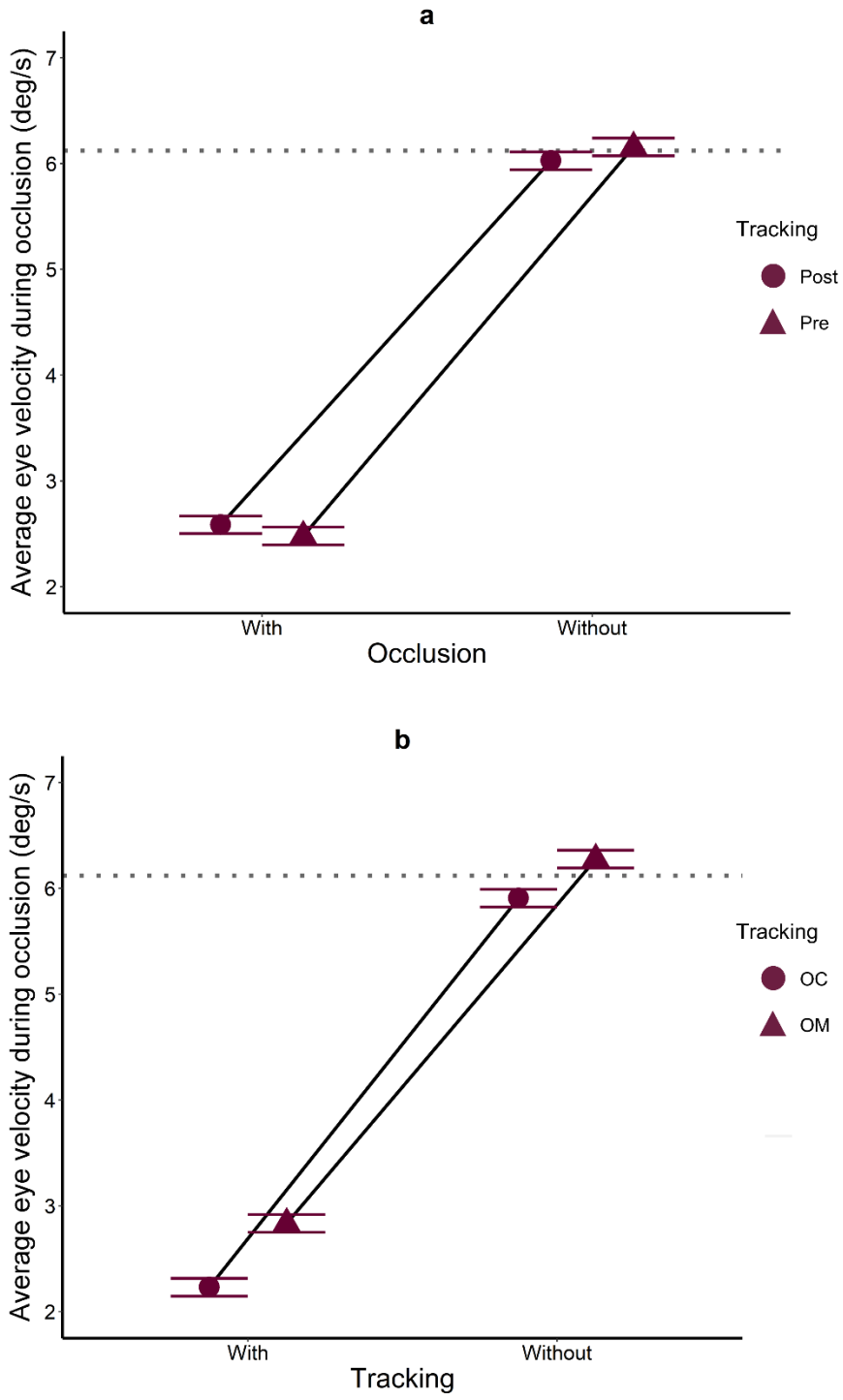

Figure 4.3: *Average eye velocity during occlusion (a: Test x Occlusion interaction; B: Tracking x Occlusion interaction). The grey dotted line corresponds to average object velocity during occlusion. Estimated marginal means (large markers) and the standard errors are shown from the accepted model.*

Hand Velocity

The final model (AIC = 344.50; conditional R^2 = 0.15) indicated a significant main effect of *Test* [χ 2 (1) = 47.40; p < 0.001] and *Occlusion* [χ 2 (1) = 43.41; p < 0.001], which was superseded by a significant *Occlusion* x *Test* interaction [χ 2 (1) = 31.36; p < 0.001]. As can be seen in Figure 4.4 hand velocity in trials with occlusion increased from pre-test (5.40deg/s) to post-test (5.56deg/s), but there was no change in trials without occlusion (5.56deg/s; 5.57deg/s). As a consequence, although hand velocity was lower at pre-test in trials with than without occlusion, there was no difference at post-test.

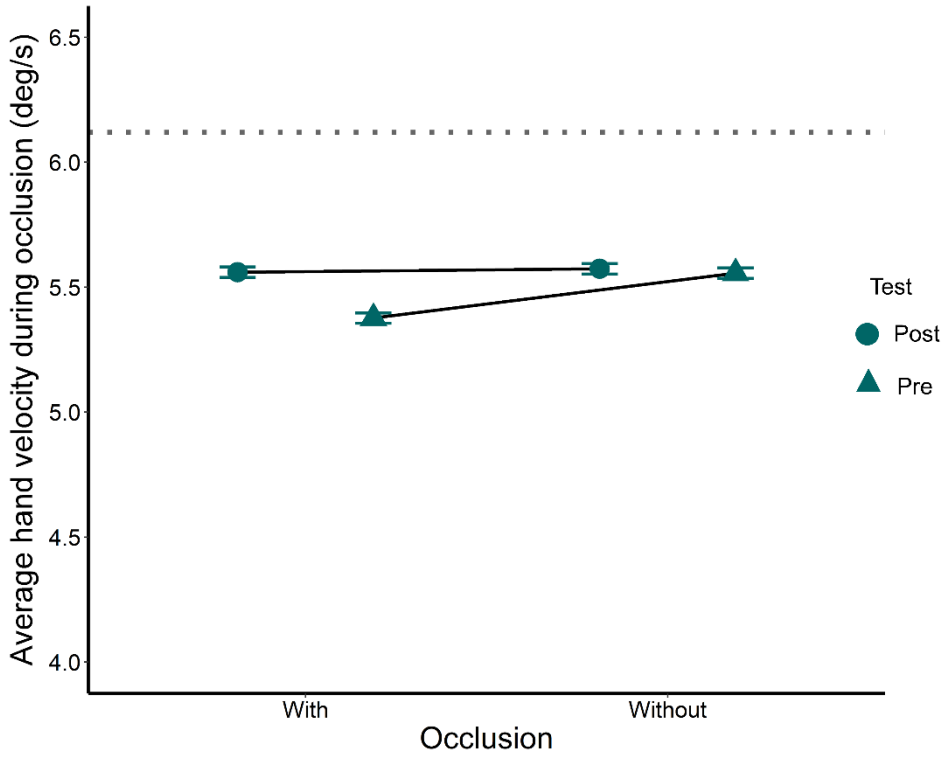

Figure 4.4: *Average hand velocity during occlusion (significant Occlusion x Test interaction). The grey dotted line corresponds to average object velocity during the period where the eye velocity was calculated. Estimated marginal means (large, filled circles) and the standard errors are shown from the accepted model.*

Neuroimaging measures

Cortical activity

MPFC - O_2Hb: The reduced model (AIC = -72227; conditional R^2 = 0.15) indicated a significant main effect of *Tracking* [χ 2 (1) = 74.28; $p < 0.001$] and *Test* [χ 2 (1) = 10.82; $p = 0.001$], as well as a significant interaction for *Tracking x Test* [χ 2 (1) = 10.94; $p = 0.001$] and *Occlusion* x *Tracking* [χ 2 (1) = 4.92; $p = 0.0266$]. Mean O_2Hb was lower at both pre-test and post-test in the OM (4.67e-09; 5.23e-09) than OC (6.35e-08; 1.35e-07) condition. Also, mean O_2Hb increased from pre-test to post-test in the OC condition but not the OM condition. Finally, for trials with and without occlusion, O_2Hb was lower in the OM (-4.59e-10; 1.04e-08) than OC (1.17e-07; 8.09e-08) condition (Figure 4.5.1).

MPFC - HHb: The reduced model (AIC = -76573; conditional R^2 = 0.14) indicated a significant main effect of *Tracking* [χ 2 (1) = 12.6; $p < 0.001$] and *Occlusion* [χ 2 (1) = 5.73; $p = 0.0166$], as well as a significant interactions for *Tracking x Test* interaction [χ 2 (1) = 13.79; $p < 0.001$], *Occlusion* x *Tracking* [χ 2 (1) = 5.66; $p = 0.017$], Figure 4.5.1. In trials with occlusion, mean HHb was lower in the OC (-4.96e-08) than OM (-2.07e-08) condition, but no significant difference was found in trials without occlusion. As a consequence, mean HHb was lower in trials with than without occlusion (-2.72e-08) in the OC condition. Finally, in the OM condition, mean HHb was higher at post-test (-1.11e-08) than pre-test (-3.03e-08). As a consequence, post-test mean HHb was higher in OM than OC (-4.62e-08).

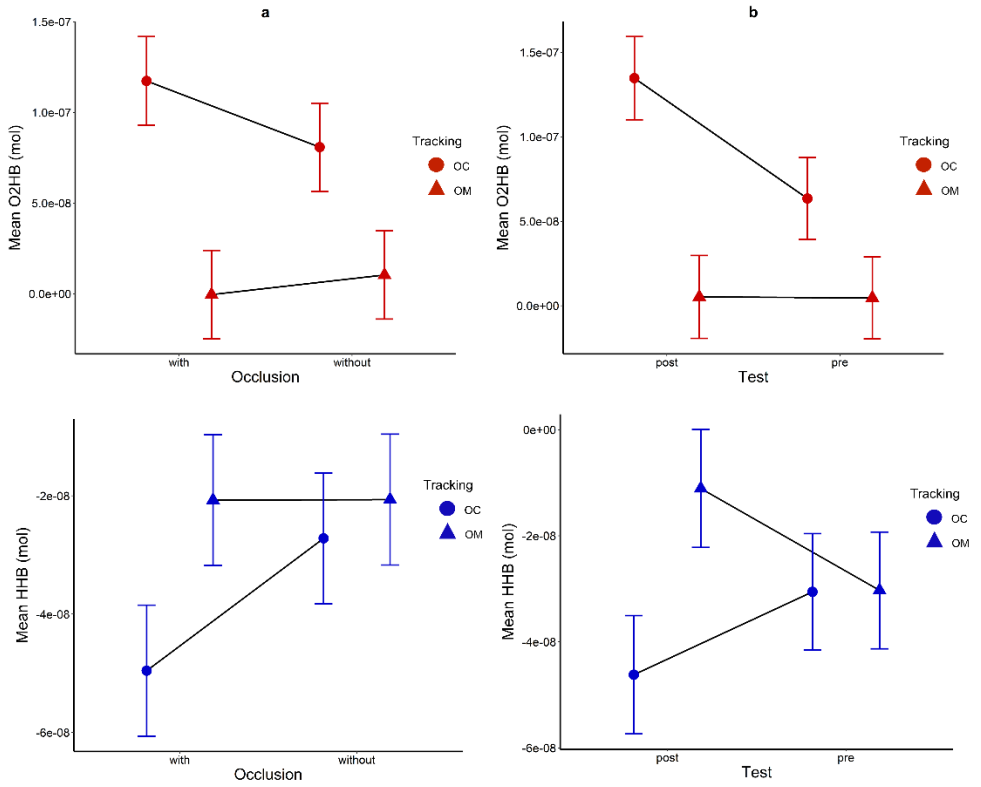

Figure 4.5.1: *Relative changes in O_2Hb (red top) and HHb (blue bottom) for MPFC (a: significant interactions Occlusion x Tracking and b: significant interactions Tracking x Test). Estimated marginal means (large, filled circles) and the standard errors are shown from the accepted models.*

DLPFC - O_2Hb: The reduced model (AIC = -116542; conditional R^2 = 0.09) indicated a significant main effect of *Tracking* [χ 2 (1) = 41.85; $p < 0.001$], *Test* [χ 2 (1) = 20.68; $p < 0.001$] and Hemisphere [χ 2 (1) = 10.12; p = 0.00146], as well as a significant interactions for *Tracking x Test* [χ 2 (1) = 13.47; $p < 0.001$], *Occlusion* x *Tracking* [χ 2 (1) = 15.98; $p < 0.001$] and *Tracking x Test x Hemisphere* [χ 2 (1) = 5.91; p = 0.015]. In the OC condition, there was an increase in mean O_2Hb from pre-test (3.62e-08) to post-test (1.14e-07) in the right hemisphere. As a result, mean O_2Hb at post-test in right hemisphere was greater in the OC condition (1.14e-07) than the OM condition (9.31e-09). It was also greater than mean O_2Hb in the left hemisphere at post-test in OC condition (5.69e-08). Finally, mean O_2Hb in trials with occlusion was lower in the OM (-2.83e-09) than OC (7.26e-08) condition, but not in

trials without occlusion. As can be seen in Figure 4.5.2, mean O_2Hb in the OC condition was higher in trials with than without (4.01e-08) occlusion.

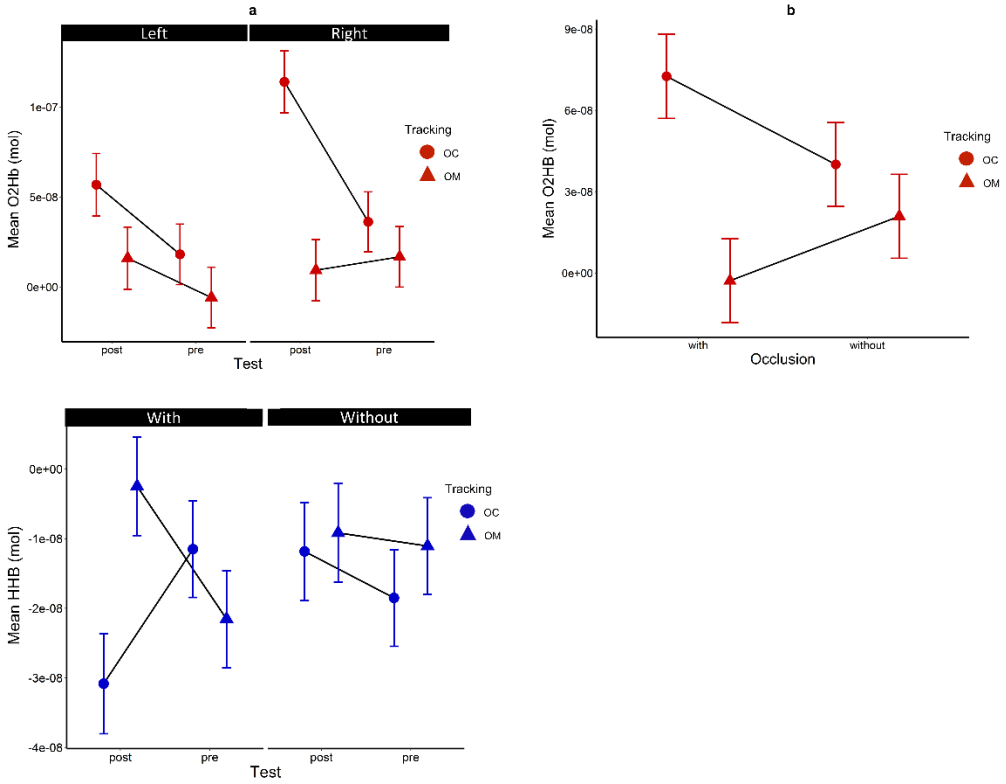

Figure 4.5.2: *Relative changes in O_2Hb (red top) and HHb (blue bottom) for DLPFC (a: significant interactions Tracking x Test x Hemisphere for O_2Hb and Tracking x Test for HHb and b: significant interactions Tracking x Occlusion for O_2Hb and bottom: Tracking x Occlusion x Test for HHb. Estimated marginal means (large, filled circles) and the standard errors are shown from the accepted models.*

DLPFC - HHb: The reduced model (AIC = -124912; conditional R^2 = 0.103) indicated a significant main effect of *Tracking* [χ 2 (1) = 6.02; p = 0.014], as well as a significant *Tracking x Test* interaction [χ 2 (1) = 9.79; p = 0.0018] and *Occlusion* x *Tracking x Test* interaction [χ 2 (1) = 17.15; p < 0.001]. Mean HHb in the OC tracking condition was lower at post-test (-3.08e-08) than pre-test (-1.15e-08) when the object was occluded. The opposite was observed in the OM condition, with higher HHb at post-test (-2.48e-09) than pre-test (-2.15e-08) when the object was occluded (Figure

4.5.2). As a consequence, mean HHb at post-test in trials with occlusion was higher in the OM than OC condition. In addition, mean HHb in the ocular condition at post-test was lower in trials with occlusion than without occlusion (-1.18e-08).

FEF - O_2Hb: The reduced model (AIC = -42435; conditional R^2 = 0.13) indicated a significant *Occlusion* x *Tracking* interaction [χ 2 (1) = 10.89; $p < 0.001$]. In the OM condition, mean O_2Hb was lower in trials with (-5.97e-09) than without (4.62e-08) occlusion. The opposite pattern was observed in the OC condition (3.65e-08; 2.01e-08) but this was not significant. As a result of these changes, mean O_2Hb in trials with occlusion was lower in the OM than OC condition (Figure 4.5.3).

FEF - HHb: The reduced model (AIC = -45372; conditional R^2 = 0.19) indicated a significant main effect of Test [χ 2 (1) = 3.96; $p = 0.046$] as well as significant *Occlusion* x *Tracking x Test* interaction [χ 2 (1) = 9.06; $p = 0.0026$]. In the OM condition, mean HHb was lower in trials with occlusion at pre-test (-3.82e-08) than post-test (-8.56e-09) (Figure 4.5.3).

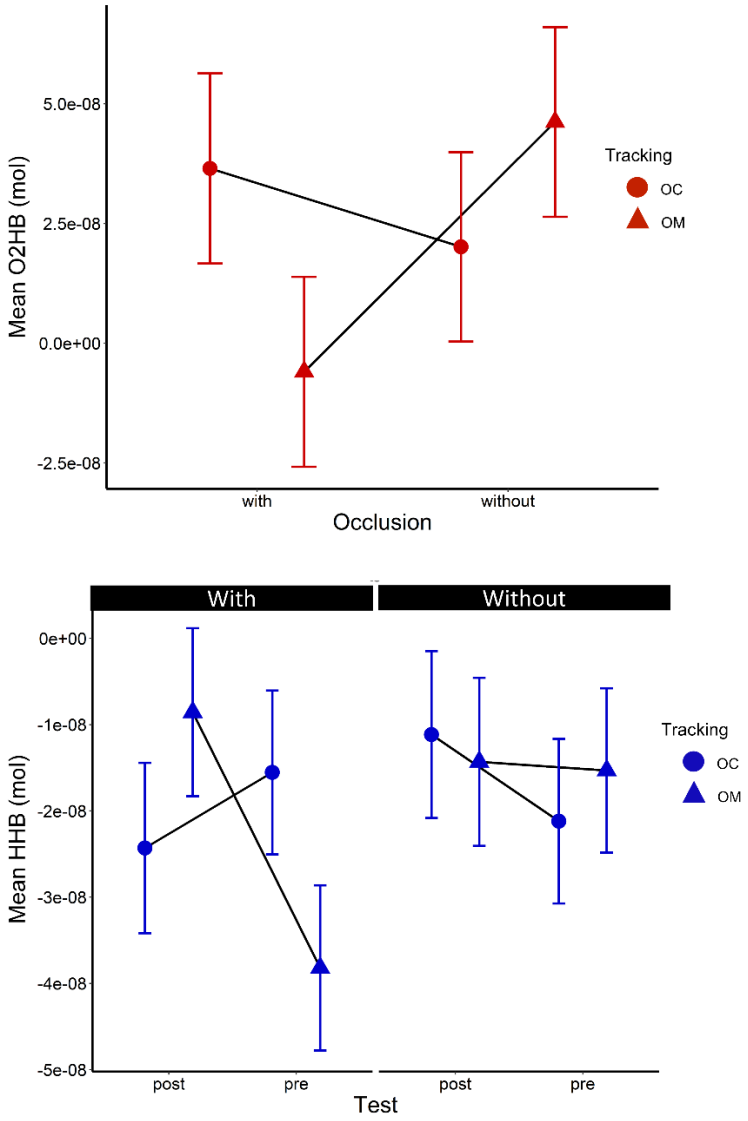

Figure 4.5.3: *Relative changes in O_2Hb (red top) and HHb (blue bottom) for FEF (Top: significant interactions Tracking x Occlusion and bottom: significant interactions Tracking x Occlusion x Test. Estimated marginal means (large, filled circles) and the standard errors are shown from the accepted models.*

MC - O_2Hb: The reduced model (AIC = -101929; conditional R^2 = 0.16) indicated a significant *Occlusion* x *Tracking* interaction [χ 2 (1) = 14.51; p < 0.001] and Tracking x Hemisphere interaction [χ 2 (1) = 8.60; p = 0.0034]. In the OM condition, mean O_2Hb was lower in trials with (2.15e-08) than without (5.27e-08) occlusion. The opposite pattern was observed in the OC condition, with higher mean O_2Hb in trials with (5.12e-08) than without (2.08e-08) occlusion. As a result of these changes, mean O_2Hb was lower in

the OC than OM condition in trials without occlusion. The opposite pattern, a higher mean O_2Hb in the OC than OM condition in trials with occlusion, only approach the significance. Finally, mean O_2Hb in the OM condition was higher for the left hemisphere (5.23e-08) than the right hemisphere (2.19e-08), Figure 4.5.4.

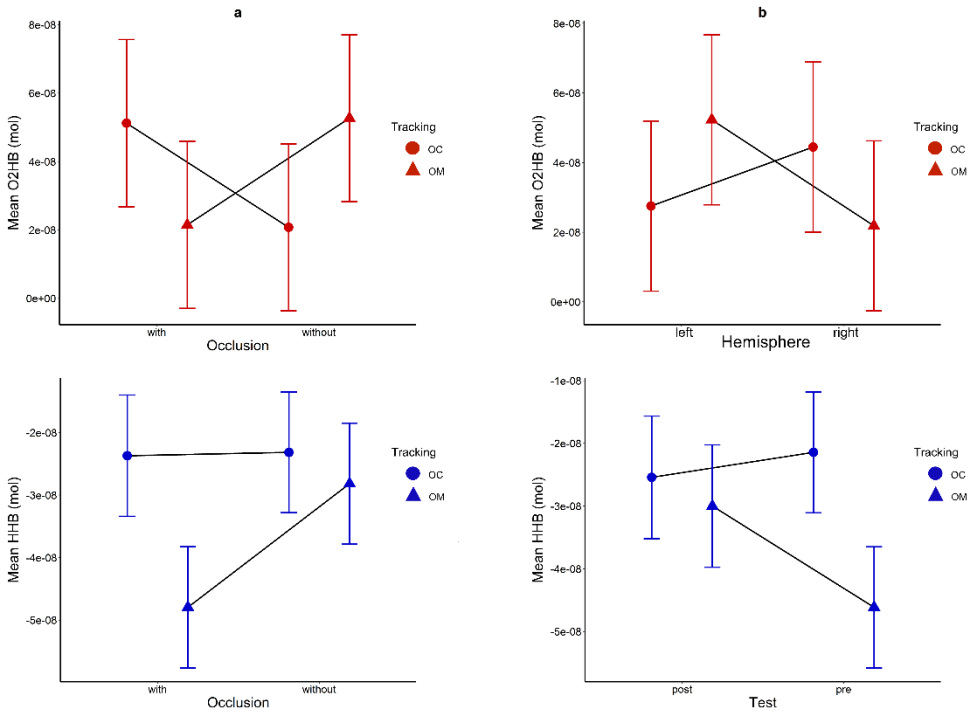

Figure 4.5.4: *Relative changes in O_2Hb (red top) and HHb (blue bottom) for MC (a: significant interactions Tracking x Occlusion and b: significant interactions Tracking x Hemisphere for O_2Hb and Tracking x Test for HHb. Estimated marginal means (large, filled circles) and the standard errors are shown from the accepted models.*

<u>*MC - HHb:*</u> The reduced model (AIC = -107558; conditional R^2 = 0.12) indicated a significant main effect of *Tracking* [χ 2 (1) = 15.87; p < 0.0001], *Occlusion* [χ 2 (1) = 7.25; p = 0.007] and *Hemisphere* [χ 2 (1) = 6.92; p = 0.0085], as well as a significant interaction for *Tracking x Test* [χ 2 (1) = 7.05; p = 0.0079] and *Occlusion* x *Tracking* [χ 2 (1) = 6.46; p = 0.011]. Mean HHb was lower in the left (-3.58e-08) than right (-2.57e-08) hemisphere. Also, it

was lower in the OM condition in trials with occlusion (-4.80e-08) than the equivalent OC condition (-2.37e-08) and compared to trials without occlusion (-2.82e-08). Finally, mean HHb in the OM condition was lower at pre-test (-4.61e-08) than post-test (-3.00e-08) and compared to the OC condition at pre-test (-2.14e-08), Figure 4.5.4.

IPL - O_2Hb: The reduced model (AIC = -66160; conditional R^2 = 0.16) indicated a significant main effect of *Hemisphere* [χ 2 (1) = 15.78; $p < 0.001$], with a lower mean O_2Hb in the right (3.94e-08) than left (8.71e-08; $p = 0.0001$) hemisphere. There were also significant interactions for *Tracking x Test* [χ 2 (1) = 13.20; $p < 0.001$], *Occlusion* x *Tracking* [χ 2 (1) = 3.85; $p < 0.05$] and *Occlusion x Test* [χ 2 (1) = 4.53; $p = 0.033$]. At pre-test, mean O_2Hb was higher in the OM (8.02e-08) than OC (3.46e-08) condition. In the OC condition, mean O_2Hb increased from pre-test to post-test (8.97e-08). The opposite pattern was observed in the OM condition, but this was not significant. As a result, there was no difference at post-test between the OM and OC conditions (Figure 4.5.5). No other pairwise comparisons for the remaining interactions were significant after correction.

IPL - HHb: The reduced model (AIC = -71954; conditional R^2 = 0.10) indicated a significant *Occlusion x Test* interaction [χ 2 (1) = 13.87; $p < 0.001$]. In trials without occlusion, mean HHb was lower at pre-test (-5.13e-09) than post-test (1.09e-08). At pre-test mean HHb was lower in trial without (-5.13e-09) than with occlusion (1.02e-08), Figure 4.5.5.

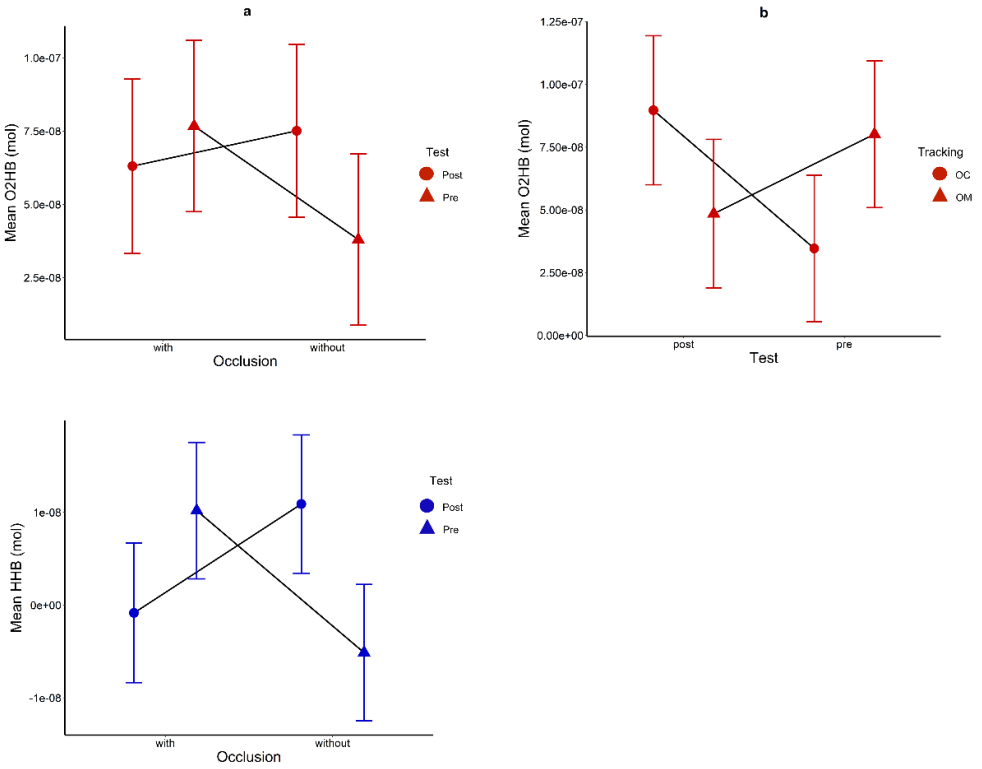

Figure 4.5.5: *Relative changes in O_2Hb (red top) and HHb (blue bottom) for IPL (a: significant interactions Occlusion x Test and b: significant interactions Tracking x Test for O_2Hb. Estimated marginal means (large, filled circles) and the standard errors are shown from the accepted models.*

SPL - O_2Hb: The reduced model (AIC = -68522; conditional R^2 = 0.15) indicated a significant main effect of *Tracking* [χ 2 (1) = 5.81; p = 0.016] and *Hemisphere* [χ 2 (1) = 17.28; p < 0.001], as well as a significant interaction for *Tracking x Test* [χ 2 (1) = 5.22; p = 0.022] and *Occlusion* x *Test* [χ 2 (1) = 6.45; p = 0.011]. Mean O_2Hb was lower in left (4.83e-08) than right (9.46e-08; p < 0.0001) hemisphere. Also, mean O_2Hb in the pre-test was higher in the OM (1.00e-07) than OC (4.93e-08) condition (Figure 4.5.6). None of the pairwise comparisons were significant after correction.

SPL - HHb: The reduced model (AIC = -73786; conditional R^2 = 0.021) indicated a significant main effect of *Tracking* [χ 2 (1) = 17.14; p < 0.001], as well as a significant *Tracking x Test* interaction [χ 2 (1) = 9.55; p = 0.002]. Mean HHb in post-test was higher in OM (1.52e-08) condition than OC (-1.39e-08), Figure 4.5.6.

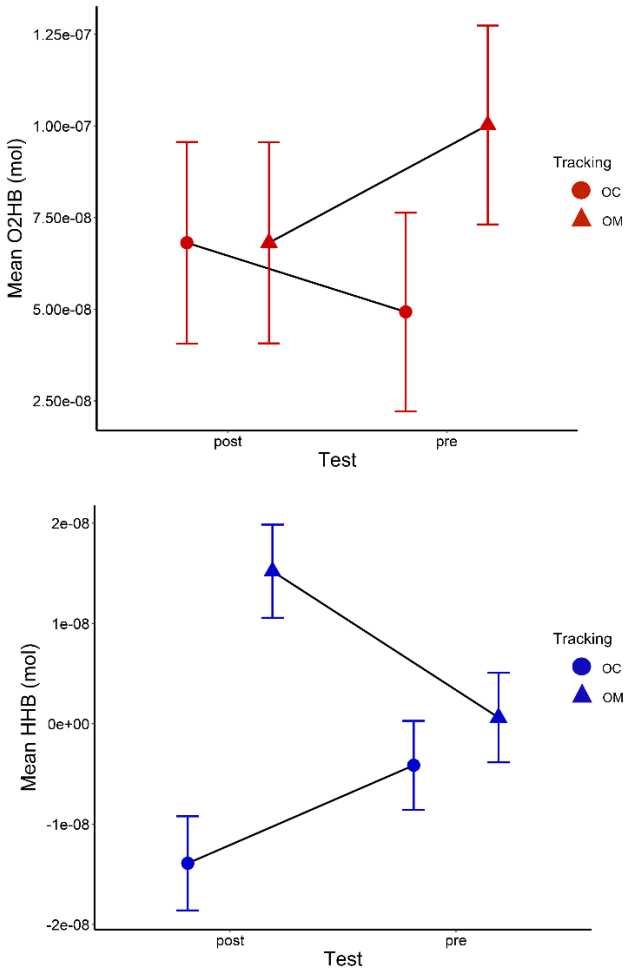

Figure 4.5.6: *Relative changes in O_2Hb (red top) and HHb (blue bottom) for SPL (significant interactions Tracking x Test). Estimated marginal means (large, filled circles) and the standard errors are shown from the accepted models.*

VC - O_2Hb: The full model (AIC = -72455; conditional R^2 = 0.13) indicated a significant main effect of *Tracking* [χ 2 (1) = 18.3; $p < 0.001$], as well as a significant interactions for *Tracking x Test* [χ 2 (1) = 10.80; p = 0.001], *Tracking x Test x Hemisphere* [χ 2 (1) = 7.33; p = 0.007] and *Tracking x Occlusion x Test x Hemisphere* [χ 2 (1) = 5.27; p = 0.022]. The only significant change in mean O_2Hb between pre-test and post-test was in right hemisphere in trials with occlusion in the OC condition (-1.15e-08; 1.53e-07). Again, in the right hemisphere, mean O_2Hb was lower in the OM than OC condition at post-test for trials with occlusion (-4.17e-08; 1.53e-07), Figure 4.5.7.

VC - HHb: The reduced model (AIC = -78248; conditional R^2 = 0.1) indicated a significant main effect of *Hemisphere* [χ 2 (1) = 7.17; p = 0.0075], with higher mean HHb in the left (3.59e-09) than right hemisphere (-9.62e-09).

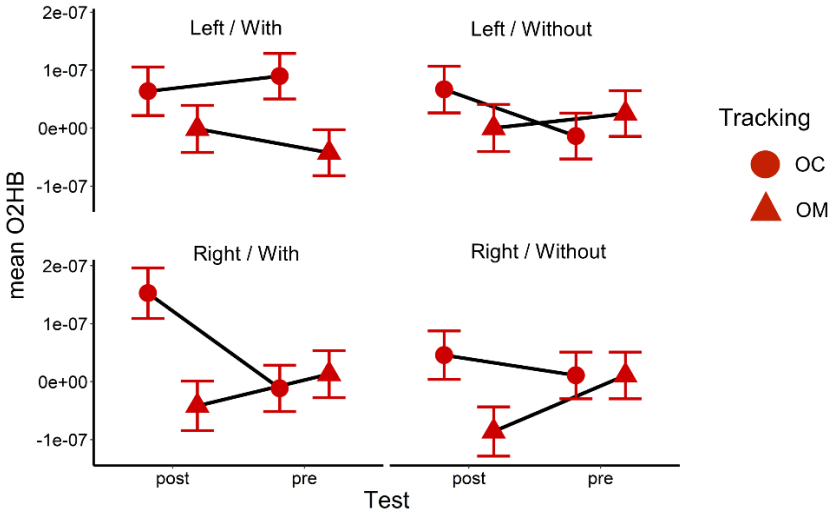

Figure 4.5.7: *Relative changes in O_2Hb for VC (significant interactions four-way interaction). Estimated marginal means (large, filled circles) and the standard errors are shown from the accepted models.*

Network organisation – Local efficiency:

The full model (AIC = -30716; conditional R^2 = 0.055) indicated a significant *main effect of Test* [χ 2 (1) = 12.75; p < 0.001], a significant *Tracking x Test interaction* [χ 2 (1) = 34.19; p < 0.001] and a significant *Tracking x Test x Occlusion interaction* [χ 2 (1) = 5.58; p = 0.018]. When the object was occluded, local efficiency was higher at pre-test (0.516) than post-test (0.494) in the OC condition, but not the OM condition (Figure 4.6). Also, when the object was occluded, local efficiency was higher in the OC (0.516) than OM (0.503) condition at pre-test, but lower in the OC (0.494) than OM (0.508) condition at post-test. A similar pattern was evident in the data when the object was visible throughout, but this was not significant.

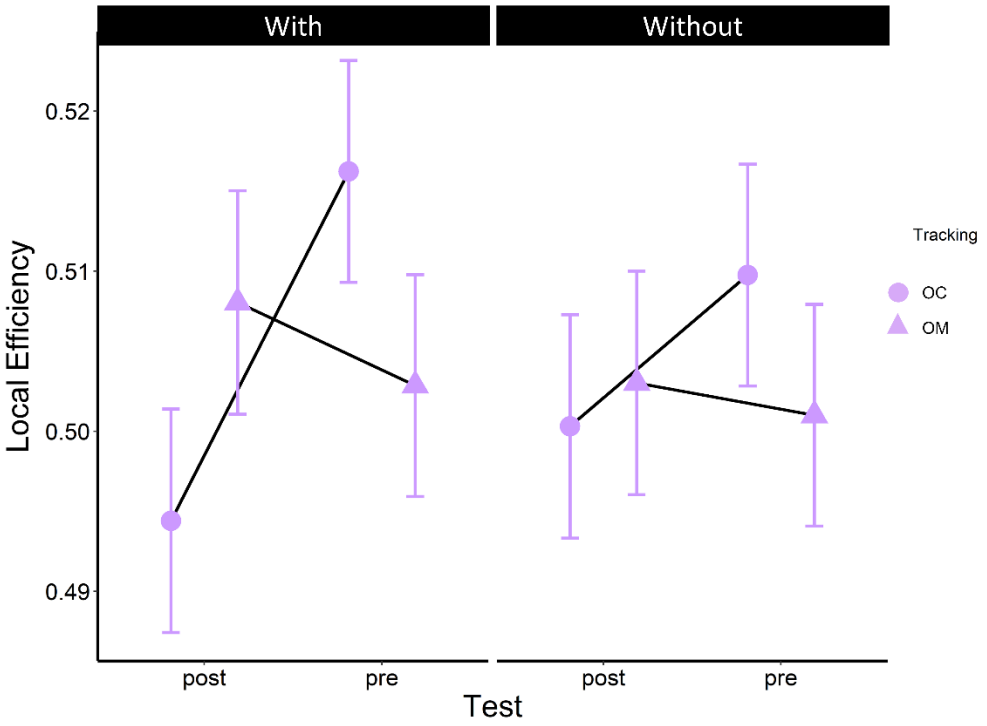

Figure 4.6*: Local Efficiency (significant Tracking x Test x Occlusion interaction). Estimated marginal means (large, filled circles) and the standard errors are shown from the accepted models.*

Network organisation – Global efficiency:

The full model (AIC = -1079.2; conditional R^2 = 0.14) indicated no significant effect and was not significantly different from the intercept only model (AIC = -1087.2; conditional R^2 = 0.13).

4.4 Discussion

Studies of human adults pursuing a moving object with eyes alone have shown involvement of a number of cortical regions, with activation and functional connectivity (interhemispheric and intrahemispheric) modulated by object velocity, motion predictability and the availability of retinal input (Lencer et al., 2004; Nagel et al., 2006; Ding et al., 2009; Schröder et al., 2020). Here, it was considered how the availability of extra-retinal input from concurrent upper limb movement (i.e., afference and efference) influences

cortical activity and organisation when pursuing sinusoidal object motion that was either continuously visible or had intervals of predictable (i.e., timing and duration) transient occlusion. However, it was first relevant to consider if there was indeed evidence of oculo-manual facilitation of SPEM when tracking an externally-generated sinusoidal object motion.

Eye and hand movement:

Average eye velocity was lower in trials with occlusion than without occlusion, even after a short period of training. Pursuing the occluded object with the eyes and upper limb did not eliminate this difference, but there was clear evidence of oculo-manual facilitation. Irrespective of whether the moving object was occluded or not, average eye velocity was greater in the OM than OC tracking condition. This is consistent with previous work that has shown oculo-manual facilitation of SPEM when participants pursue internally-generated (Gauthier & Hofferer, 1976) or externally-generated (Gauthier et al., 1988) sinusoidal object motion over several cycles. It has been proposed that this facilitation is based on an exchange of information from extra-retinal signals (limb afference and/or efference), which is thought to be co-ordinated by a controller that enables the ocular and motor systems to act independently or interdependently depending on the task demands (Vercher & Gauthier, 1988; Gauthier et al., 1988). For average hand velocity, the effect of occlusion was moderated by the short period of training. In trials with occlusion, there was a small but significant increase in hand velocity between pre-test and post-test. There was no change between pre-test and post-test in trials without occlusion. Overall, though, the difference between hand and object velocity was much less than the difference between eye and object velocity, which is consistent with the fact that the hand can be moved voluntarily in the absence of retinal input. Subsidiary analysis indicated that the average intra-participant correlation between eye and hand velocity was 0.144 ± 0.164, with a range from -0.105 to 0.397, thus confirming the interdependence between eye and hand control.

Cortical activity and network organisation:

Across all regions measured in the current study, but particularly in PFC through to MC, cortical activity differed as a function of the availability of retinal input and/or the effectors used to track the moving object. More specifically, consistent with Chapter 3, there was a difference in activity (e.g. increased mean O_2Hb and decreased mean HHb) in MPFC in trials with occlusion when tracking the object in the OC compared to OM condition. The increase in O_2Hb was also present in trials without occlusion. It would seem, therefore, that irrespective of whether the moving object is occluded or not, extra-retinal inputs from hand tracking may help to reduce the demand in MPFC for monitoring other cortical areas involved the task (Mansouri et al., 2017; Koechlin et al., 1999). For DLPFC, there was a similar pattern of effects, with the largest difference in O_2Hb between the OC and OM tracking condition in trials with occlusion (only at post-test for HHb). There was also increased O_2Hb in trials with object occlusion compared to trials without occlusion, in the OC condition. This latter result is consistent with those of Nagel et al., (2006) and Ding et al., (2009), who suggested that DLPFC is part of the extra-retinal mechanism that attempts to maintain SPEM in absence of retinal input. Interestingly, however, there was no significant difference (e.g. non-significant trend to the opposite pattern) in trials with compared to without occlusion in the OM condition. This could indicate that limb afference/efference provides extra-retinal information that reduces the attentional and working memory demand on DLPFC to extrapolate an occluded object trajectory. In FEF, O_2Hb did not differ between trials with and without occlusion in the OC tracking condition. A similar finding was reported by Ding et al., (2009), who showed that while activity in FEF is moderated by additional (external) cues that influence predictability of object motion, this involvement was not dependant on visibility of moving object per se. However, O_2Hb in FEF was lower in trials with than without occlusion in the OM tracking condition. Again, our results in OM condition, seem to suggest that having access to limb afference/efference reduced the demand on FEF to extrapolate an occluded object trajectory.

In MC, which here also included pre-motor cortex, there was increased O_2Hb in trials with compared to without occlusion in the OC tracking condition. Lencer et al., (2004) also reported an increased activity in pre-motor cortex during pursuit of an occluded object compared to a non-occluded object. They suggested that this higher activity in pre-motor cortex was related to coordination of extra-retinal information. Extending upon this, the findings of the current study for the OM tracking condition indicated a reduced mean O_2Hb in MC in trials with compared to without occlusion. The reduced mean O_2Hb in trials with occlusion may be the result of participants exhibiting fewer corrective hand movements associated with keeping the annulus surrounding the moving object (Miall et al., 1993; Bennett et al., 2012). Interestingly, however, there was little evidence that cortical activity in SPL and IPL was influenced by the availability of retinal input. This differs from the results of Lencer et al., (2004), who showed that while parietal cortex was activated during pursuit with and without object occlusion, activation was higher in the latter condition. Here, observation of the group mean data from the significant Tracking x Occlusion interaction in IPL did indicate a tendency in the OC tracking condition for higher mean O_2Hb in trials without (4.38e-08) than with occlusion (8.05e-08), but this was not significant after Bonferroni correction. For HHb, the only effect was at pre-test, with a lower mean HHb in trials without than with occlusion, but this was not moderated by tracking condition. However, extending upon Lencer et al., (2004), work, our results also show a significant effect of Tracking on parietal cortex activity. More specifically, mean O_2Hb at pre-test was higher in the OM tracking compared to OC tracking in both IPL and SPL.

Another consistent pattern observed in MPFC, DLPFC and IPL was that activation increased from pre-test to post-test in the OC condition but tended to decrease or remain the same in the OM condition. As a consequence, mean O_2Hb at post-test was lower in the OM compared to OC tracking condition for MPFC and DLPFC. This was accompanied by changes in mean HHb, which was higher in the OM than OC tracking condition at post-test in the right hemisphere of MPFC, and higher in the OM than OC tracking condition in trials with occlusion at post-test in DLPFC. Additionally, at pre-test there

was a higher mean O_2Hb in parietal cortex (IPL and SPL) in OM condition than OC. This effect was present in VC but only reached significance in the right hemisphere when tracking the object in trials with occlusion. Battaglia-Mayer & Caminiti, (2018) suggested that some cortical areas (e.g. distributed parieto-frontal network) play an important role in eye-hand coordination, and moreover that this coordination emerges from parietal operations interacting with more frontal regions. The results of the current study could be indicative of a better oculo-manual coupling after a short period of oculo-manual training, reflected by a lower activity in frontal and parietal regions at post-test.

The influence of a short period of training in the OM condition was also evident in network organisation. While no changes were found in global efficiency (e.g. measure of network integration), local efficiency (measure of network segregation) in trials with occlusion changed as a function of tracking condition between pre-test and post-test. Specifically, in trials with occlusion, there was a decrease in local efficiency from pre-test to post-test in the OC condition. As a consequence, while local efficiency at pre-test was higher in the OC than OM tracking condition, the opposite was found at post-test. However, this effect was not present in trials without occlusion. In combination, then, the findings indicate that a short period of training in the OM condition resulted in a more costly (increased mean O_2Hb) and less segregated network organisation when transferring back to trials with occlusion in the OC condition. This could be because training reinforced the coupling between eye and upper limb movement, which resulted in more reliance on limb afference/efference, and thus a somewhat reduced ability to predict the sinusoidal object trajectory during occlusion in the OC condition at post-test. This is partially consistent with the results found in the previous chapter in which the moving object always underwent a transient occlusion. That is, PFC had an increased mean O_2Hb, as well as a less integrated and segregated (e.g. decreased local and global efficiency) network organisation, in the OC than OM tracking conditions.

Finally, it should be mentioned that although there were significant changes in O_2Hb and HHb for all ROIs, these were not always consistent with the

expected inverse pattern between both chromophores (e.g. increase in O_2Hb and decrease in HHb), especially for the MC, IPL and VC (e.g., changes in only one chromophore, or concomitant increase/decrease). It is not obvious why this theoretical pattern was not consistently found in the data, but as described in Chapter 3, it could be a consequence of noisier data in ROIs where participants tend to have a greater quantity of hair on the scalp. That said, it is important to note that several methods were included to check the signal quality of the data, as well as control measures such as a baseline correction, short-distance channels, and preprocessing steps to improve signal quality (Tachtsidis & Scholkmann, 2016). In addition, the protocol indirectly included a control comparison in the sense that a clear pattern of cortical activity should have been present in MC when tracking the moving object with eye alone or eye and upper limb. This was clearly evident, with an increased mean O_2Hb in left hemisphere (contralateral to the moved limb) compared to the right hemisphere (ipsilateral to the moved limb) in the OM condition only. Mean HHb was also globally lower in the left than right hemisphere. Therefore, while a strict inverse pattern between O_2Hb and HHb was not found, there was evidence of stronger contralateral neural activity in motor cortex in the oculo-manual tracking condition. Together, the combination of various control measures helps provide confidence in the results, which for O_2Hb are more likely to represent task-evoked changes in the haemodynamic response than a false positive as consequence of a confounding factor.

Taken in combination, the results of the current study indicate that the availability of extra-retinal input (i.e., afference and efference) in the OM tracking condition impacted, although in slightly different ways, upon SPEM, cortical activity and network organisation. For SPEM, OM facilitation was present irrespective of whether the moving object was occluded or not. For cortical activity, the effect of OM tracking was most evident when the object was occluded, resulting in a lower cost (e.g. reduced mean O_2Hb) in PFC through to MC. Cortical activity in the OM tracking condition was stable across pre-test and post-test, as was local efficiency. However, cortical activity increased in some regions of PFC in the OC tracking condition

following a short a period of training (in the OM tracking condition), which was mirrored by a decrease in local efficiency. In sum, then, it would seem that extra-retinal input from concurrent upper-limb movement enabled participants to maintain a reduced cortical cost and more segregated network organisation when faced with greater attentional and working-memory demands to predict an occluded object trajectory. These findings from neurotypical adults provide an important first step in subsequently understanding of how brain organisation during oculo-manual tracking is affected by normal aging or acute and chronic neurological conditions.

Chapter 5: General Discussion

5.1 Overview of studies

The aim of this PhD was to investigate the impact of concurrent upper limb movements on brain activity and cortical network organisation during smooth pursuit tasks of varying complexity, which have greater fidelity with tasks performed in daily life. Indeed, while smooth pursuit eye movements are known to involve a wide range of cortical areas, the functional coupling between them remains unclear, and specifically when facilitation from concurrent upper limb movement occurs. Across all studies in this PhD, the main finding was that oculo-manual pursuit resulted in facilitation of eye movement, especially when the pursued object was momentarily occluded (less prevalent in Chapter 3). Oculo-manual pursuit also resulted in changes in cortical activity and network organisation compared to eye movements alone. More specifically there was a reduced activity in the more frontal regions, as well as changes in network local and global efficiency. These results represent an important step forward to understand cortical activity and network organisation during smooth pursuit eye movements, as well as the cortical mechanism of oculo-manual facilitation. In the following paragraphs a more exhaustive overview of the results obtained in this work will be given.

During this PhD a series of four studies was performed. The first study (Chapter 2) aimed to develop a dual-task pursuit protocol, which placed specific demands on visual-spatial working memory. For this purpose, a series of four online experiments was conducted in which participants performed a primary prediction motion task in combination with secondary change detection task in ocular (OC) and oculo-manual (OM) conditions. The effect of difficulty of the primary (i.e., magnitude of reappearance step) and secondary (i.e., number of colour or form items) tasks, as well as task sequencing (i.e., primary and secondary task presented concurrently or consecutively) were examined. In accord with previous findings, it was expected that judgement accuracy of object reappearance after transient occlusion would be lower when the object reappeared with a small negative position step compared to other steps. For change detection, a higher judgment accuracy was expected with the control compared to form and colour stimulus array. As afferent and efferent signals

from performing concurrent upper limb (i.e., arm) movement are shared with the ocular control system, thereby facilitating the predictive mechanisms involved in extrapolating an occluded moving object (Gauthier & Hofferer, 1976; Bennett et al., 2012), it was expected that their presence in the oculo-manual condition could influence performance of the primary task, and/or secondary task, via a possible contribution to the internal model of the object trajectory (Wexler & Klam, 2001).

Following this, a lab-based experiment was reported in Chapter 3, which built upon the methods and findings of earlier chapters for the purpose of concurrent neuroimaging (fNIRS) and video-oculography. The overall aim was to determine whether smooth pursuit eye movement and PFC activity during dual-task pursuit was influenced by the presence of concurrent upper limb movements. The first hypothesis was that smooth pursuit would benefit from concurrent upper limb movement. The second hypothesis was that PFC activity would be affected by the increased attentional and working memory demand of the secondary task, as well as by the presence of concurrent upper limb movement. In terms of the latter, if oculo-manual tracking facilitates the extrapolation of a moving object, and particularly during occlusion, it could be expected that this will result in decreased activity in PFC compared to a condition of ocular pursuit.

Finally, a second lab-based study using a single task protocol was conducted to examine the wider cortical network involved in oculo-manual facilitation during pursuit of a continuously presented object compared to pursuit of an object that undergoes a predictable, momentary occlusion (Chapter 4). The main hypothesis was that smooth pursuit in both occluded and non-occluded condition will be improved in the oculo-manual condition. It was also expected that this improvement would be influenced by a short period of training. The final hypothesis was that there would be reduced cortical activity in oculo-manual tracking compared to ocular tracking alone, as well as changes in network efficiency.

5.2 Chapters 2 and 3

A consistent finding obtained in both the online (Chapter 2) and lab-based (Chapter 3) dual-task pursuit was a lower judgement accuracy in the primary task when the pursuit object reappeared behind the correct location with a small negative position step. This replicates previous findings (Bennett & Benguigui, 2016) and can be explained by an underestimation of the object location during the occluded trajectory (Lyon & Waag, 1995; Tanaka et al., 2009). Accordingly, when the object suddenly reappears with a small negative step, this tends to coincide with the participants' extrapolation of the object along its occluded trajectory, thus making the judgement more difficult. Here, it is important to note that while pursuit of the occluded object results in better judgment accuracy compared to fixation (Bennett et al., 2010), participants do not simply use the difference between eye and object position as the basis for their judgment. Although this does make a contribution, a more important source of information is the difference between the expected and actual object reappearance position (Wexler & Klam, 2001). The implication, therefore, is that by maintaining pursuit in the vicinity of the occluded object, participants are better able to perceive the actual object reappearance position, as well as form a more accurate dynamic prediction of the expected object reappearance position based on the available extra-retinal input.

A second consistency across all dual-task pursuit studies was a lower judgment accuracy for the form than colour stimulus array of the secondary change-detection task, both of which tended to have lower judgment accuracy than the control stimulus array. The findings for control stimulus array were not surprising given that this condition was included in order to provide a baseline for the impact of the primary spatial-prediction motion task. That is, participants still had to extrapolate the occluded object trajectory and judge its reappearance location, as well as perform the secondary task, but without an increased working memory demand due to there being no change between the cue and probe stimuli. However, the lower judgement accuracy for the form than colour stimulus array condition would appear to indicate that participants found it more

difficult to encode, store and compare in working memory the spatial configuration of multiple elements compared to their colour (Jiang et al., 2000).

Here, it is important to note that the use of the term working memory as it relates to both the primary and secondary task in the current thesis is consistent with the definition given by Oberauer, (2019), who stated that: "there is a broad consensus on what the term working memory refers to: The mechanisms and processes that hold the mental representations currently most needed for an ongoing cognitive task available for processing". Since the seminal work of Baddeley & Hitch, (1974), it is also recognized that working memory is closely linked with attention, and has a limited capacity to store, manipulate, and retrieve information. Accordingly, a failure to attend to the elements of the form stimulus array could have impacted upon the subsequent encoding and storage of those elements in working memory. As there were an equal number of elements in the form and colour stimulus arrays, a failure of attention due to a limited capacity would not seem to be a reasonable explanation. Alternatively, it is possible that colour elements were more salient and thus grabbed attention, which facilitated encoding and storage into working memory. It is not possible to conclude if and how attention was involved in the secondary change-detection task, but this could be an interesting issue to consider in future work. What is clear, however, is that the secondary change-detection task required participants to make a judgment based on a comparison between a cue and probe stimulus, which were presented at different times, and thus required encoding, storage and retrieval processes in working memory.

Interestingly, higher accuracy in change detection for the colour compared to form stimulus array was accompanied by a longer response time, which was suggested in Chapter 3 to potentially be a result of a speed-accuracy relationship where participants took longer to give a more accurate response. A subsidiary analysis indicated that response time per se did not impact upon the change in mean O_2Hb, thus leading to the suggestion that the increased mean O_2Hb in DLPFC was related to processing activities involved in detecting a change in the colour compared to form stimulus arrays. According to Jiang et al., (2000), the spatial configuration of elements in a stimulus array act as an important source of relational information encoded in working memory, which then facilitates

identification of a change in spatial location, colour or shape. The implication is that the spatial configuration and colour of elements in the colour stimulus array would have been processed in working memory, thus requiring increased contribution from DLPFC (Curtis, & D'Esposito, 2003) compared to the form stimulus array, where only the spatial configuration was relevant.

Another common finding in these two studies is that there was no consistent effect of oculo-manual tracking on performance of the primary or secondary task. In terms of the primary task, this would seem at odds with the study of Wexler & Klam, (2001), who reported that spatial prediction motion was influenced by oculo-manual tracking in a condition where the limb and object motion were congruent in gain and direction (i.e., both rotary). The authors explained this effect by saying that limb afference and/or efference provides input to the predictive mechanism that perpetuates SPEM during an occlusion, and that this could involve population coding of limb motion in motor cortex, combined with continuous updating of the predictive mechanism through PPC. Closer inspection of their findings shows that there was in fact no difference in spatial prediction motion between an oculo-manual tracking condition in which the limb motion was rotary and the object motion was linear, compared to an ocular condition when the exact same linear object motion was presented. The impact of extra-retinal input was also shown to vary as a function of object/limb motion and the object displacement during occlusion. Finally, although they compared oculo-manual pursuit to fixation, there was no control condition in which the object was pursued with eye alone. Given that actual object reappearance position can be accurately perceived without the need for highly precise eye movements, an interesting avenue for further work could be to consider the conditions under which oculo-manual tracking can improve a participant's expectation regarding object reappearance (Wexler & Klam, 2001).

In Chapter 3, where it was possible to record eye movements, there was some evidence of oculo-manual facilitation of smooth pursuit, but this was less than originally expected. As discussed before, this could be due to the use of a discrete, short duration, externally-generated object motion as the pursuit stimulus. Indeed, previous work has suggested that the greatest facilitation of smooth pursuit occurs when the pursued object moves sinusoidally over a large

amplitude for several cycles and is the result of internally generated (i.e., active) motion commands (Gauthier & Hofferer, 1976). Still, even with a potentially less than optimal object motion, the fNIRS results suggest that oculo-manual tracking did impact on PFC activity. More specifically, the reduced mean O_2Hb in MPFC with oculo-manual compared to ocular tracking is suggestive of a lower metabolic demand (Logothetis et al., 2001) for the same outcome performance. Given the role of MPFC in "cognitive branching" in situations that require the monitoring of a primary task while allocating attention to a secondary task goal (Mansouri et al., 2017; Koechlin et al., 1999), it seemed reasonable to suggest that the presence extra-retinal signals from the upper limb could have influenced the predictive mechanism involved when pursuing an occluded object trajectory, and thus the need for monitoring of the primary task. In addition, there was evidence from Graph analysis on the PFC network of increased local and global efficiency in oculo-manual compared to ocular tracking. As developed in Chapter 1, in terms of network organisation, an increased global efficiency (integration) could reflect a more efficient information transfer in the network, but this is also suggested to increase the cost in supporting connection (Achard & Bullmore, 2007). The results of Chapter 3 suggest that oculo-manual tracking results in a more integrated and segregated PFC network organisation, supporting a more efficient information sharing than ocular tracking. A possibility is that oculo-manual tracking may require both systems to share a common input (i.e., interdependence), but not necessarily a common command (i.e., dependence), and thus may require more information sharing, which is supported by a more segregated and integrated organisation compared to ocular tracking alone.

Here, it should be reiterated that cortical imaging in Chapter 3 was limited to the PFC, whereas a wider brain network is known to be involved in SPEM and working memory, comprising areas such as the pre-motor cortex and PPC (e.g. FPN). Therefore, a follow-up study could investigate the impact of oculo-manual tracking in the current dual-task pursuit protocol on a wider cortical network. Given the suggested role of PPC in updating an internal prediction of an occluded object trajectory (Wexler & Klam, 2001), it could be expected that PPC activity will be impacted by oculo-manual tracking. Whether and how this is

reflected in measures of network organisation, and hence integration and segregation within the fronto-parietal network, will also be relevant to determine. To this end, it will potentially be necessary to change the experimental protocol, for example by embedding the secondary task after several cycles of sinusoidal object motion. As well as providing more opportunity for facilitation of SPEM by concurrent upper limb movement (Gauthier & Hofferer, 1976), this would presumably result in an improved prediction of the occluded object motion, which according to Wexler & Klam, (2001) is the most important source of information underlying prediction of spatial prediction motion. Based on the results obtained in Chapter 3, it could be expected that the opportunity for short-term adaptation to the sinusoidal motion during oculo-manual tracking would result in a lower activity in MPFC (i.e., task switching), as well as FEF (i.e., SPEM control). In addition, it could be relevant to investigate the impact of active vs passive oculo-manual pursuit. While SPEM is improved when motion of the pursuit object is a result of participants' actively moving their hand, a smaller but significant facilitation is observed when the object motion is a result of passive hand movement (i.e., moved by an external source such as an experimenter) compared to pursuit with the eyes alone (Vercher et al., 1996). The suggestion is that manual pursuit of a passively moved object still provides access to limb afference, which is important for the maintenance of SPEM. By removing access to, and processing of limb efference, it should be possible to determine if limb afference is sufficient to improve prediction of the occluded object trajectory, and hence judgment accuracy of spatial prediction motion. It could also be expected that a passive oculo-manual condition could reduce the cost of PFC network organisation, while still enabling a similar outcome. Although the work here is limited to neurotypical participants, the contribution of limb afference and efference to oculo-manual tracking could have implications for research with specific populations. For example, it could be interesting to determine if patients with peripheral neuropathy, who have no or impaired afference, exhibit different outcome performance and cortical activity compared to neurotypical participants of the current thesis. In addition, it could be interesting to study high-functioning autistic individuals, who have been suggested to rely more on limb afference than visual afference when performing visual tracking tasks.

Dual task pursuit interference

In both Chapter 2 and 3, there was no consistent interaction between the primary and secondary tasks. There was some evidence that judgment accuracy of the secondary task was influenced by the reappearance step of the primary task, but this was not consistent with a difficulty effect (i.e., -2deg different from all other steps) or direction effect (i.e., -2deg and -4deg different from +2deg and +4deg). Together these results indicate that the working memory demands of the primary task to predict and extrapolate the trajectory of the occluded moving object did not directly affect performance of the secondary task, and vice versa. This finding differs from those obtained by Jonikaitis et al., (2009), who found that performing a pro-saccade to an eccentric location disrupted performance of a spatial prediction motion task. Specifically, the reappearance judgment was delayed by approximatively the same duration as that required by the shift in attention when performing the pro-saccade, suggesting that this disrupted the processes involved in the primary task. Kerzel & Ziegler, (2005) also found interference between a pursuit task and performance of a secondary task that required participants to determine changes in spatial layout of eccentrically located elements. No interference was present when the secondary task stimulus array was artificially stabilised on the fovea, or when it moved across a stationary eye in a fixation condition. The authors suggested that the effect of secondary target eccentricity during smooth pursuit indicates that attention may be closely focussed on the moving object, thus allowing elements of the stabilised image to be correctly identified without demanding additional working memory processes. The absence of interference was also found when the secondary task involved detecting changes in colour. The authors suggested that this latter result could be because covert attention for processing colour elements is unrelated to attention directed to a pursued object. A follow-up study could include a pursuit only condition where no secondary task stimulus would be presented, thus avoiding the potential shift of attention that could have occurred with the Control stimulus array. It could also be relevant to investigate the impact of secondary task difficulty, for example by changing the colour of only one of the four squares or presenting the colour stimulus array in a different spatial configuration between the cue and probe presentation. This would provide better

understanding on how colour change and spatial organisation of the stimulus array in the change-detection task influence relational information encoded in working memory. Further study of how the interaction between prediction motion and change detection, and the associated cortical activity, are impacted by task difficulty, as well as how this is mediated by concurrent upper limb movement, could also represent a step forward in our understanding of more complex cognitive processes involved in many daily activities such driving or cycling in a busy street. In these situations, it is necessary to make prediction motion judgements (e.g. when will I arrive at a junction) while processing information about the spatial layout and motion of other objects in the surrounds (e.g. static and moving cars, bicycles and/or pedestrians). How this is influenced by ageing, for example, remains to be determined (see below for related discussion). Similarly, performing such tasks without a contribution from limb afference/efference, such as during the Hazard perception test, may misrepresent the processing and cortical demands of real-world settings.

In addition, it will be relevant to consider why in the current thesis there was some limited impact of the secondary task on SPEM. For example, eye velocity in Chapter 3 was higher in the oculo-manual than ocular tracking conditions when judging the Form stimulus array. This was the secondary task stimulus array that resulted in the lowest judgement accuracy, although this was not different between the oculo-manual and ocular tracking conditions. A follow-up study could also aim to investigate the impact of the object motion. Indeed, instead of the discrete, short duration, object motion used in Chapter 3, the use of a sinusoidal object motion lasting several cycles could have an impact on judgment accuracy of the primary and secondary task. Better understanding of the impact of the object motion could be of major interest for interventions in rehabilitation using smooth pursuit eye movement such with population experiencing stroke and spatial neglect (Hill et al., 2015).

Smooth pursuit, cognition and normal aging

Sprenger et al., (2011) studied the effect of aging on SPEM and showed that motor parameters seem to be impacted by normal aging, whereas predictive

and anticipatory parameters are unaffected. The authors suggested that the maintenance of predictive and anticipatory processes in smooth pursuit can compensate for an age-related decline in sensorimotor processes. These results are in line with those obtained by Fukushima et al., (2014), who studied the effect of aging on a simple ramp task and memory-based smooth pursuit tasks. Their results highlighted that movement parameters like initial pursuit latency, acceleration and velocity, as well as peak pursuit velocity, were impaired with aging. However, they showed that the error rate was the same for elderly and young adults in a memory-based pursuit task (go no-go), where participants had to remember a pattern colour and the movement direction. Together, the results obtained by Sprenger et al., (2011) and Fukushima et al., (2014) suggest that extra-retinal mechanisms involved in smooth pursuit, such as anticipation, prediction and working memory, remain functional with normal aging, while oculomotor parameters seem to be impaired.

Some authors have also suggested that eye-hand coordination is also impacted by normal aging (O'Rielly & Ma-Wyatt, 2018; Burke et al., 2015). In a study of a double-step reaching task realised under time pressure, O'Rielly & Ma-Wyatt, (2018) showed that some aspects of oculo-manual coordination are modified with aging. Specifically, they showed that aging resulted in a shorter eye-hand latency (i.e., interval between saccade initiation and reach initiation), which they suggested was indicative of older participants spending less time extracting relevant visual information about the target location, as well as less time planning the reach response. As a result, the authors suggested that older participants were generally slower in their reach movement, presumably because they required more online processing of information in order to maintain a similar final touch accuracy as the younger participants. It was also reported that older participants exhibited a larger eye-hand distance (distance between the final eye position and the touch location) than younger participants, which would normally be indicative of a worse outcome performance. However, the two movements were correlated to a similar extent in the older and younger participants, presumably providing sufficient alignment between the eye and hand at the end of the movements to maintain a high level of final touch accuracy.

Burke et al., (2015) also studied the impact of normal aging on eye-hand coordination, and how this could be impacted by increased cognitive demand (memory and attention). For this purpose, they used a task comprising four main conditions in which participants had to remember a change in colour or shape in a specific temporal order or just remember the location of changes. The authors also studied the effect of the to-be-remembered target set size (e.g. 2, 3, 4, or 5 targets) and the delay (0, 5, or 10s between the stimulus presentation and the recall screen). The results seem to suggest that the coupling between eye and hand is impacted by aging. Specifically, the lag between the eye and hand movement (mean difference between the eye movement onset and the touch movement onset) increased as a function of task difficulty (e.g. during conditions with a specific temporal order to remember) during the 10s delay condition, with the effect principally a result of a delayed onset of the hand in the older group only. Older adults were also less accurate in their response to the task compared to younger adults, and this decrease in accuracy increased with the set size. The authors suggested that this could be due to a problem of competing recourses between the cognitive task and the motor demand. Together, these results suggest that normal aging has an impact on oculo-manual behaviour, which is associated with poorer performance in cognitive aspects of the task.

In considering the work of O'Rielly & Ma-Wyatt, (2018) and Burke et al., (2015), it is possible that with the dual-pursuit task of the current thesis, normal aging could have a negative impact on SPEM if there is impaired concurrent upper limb movement. In addition, while Chapter 2 and 3 found no consistent evidence of oculo-manual facilitation on the primary and secondary task performance with young adults, the same effects may not be expected with an elderly group of participants. Indeed, while the predictive mechanism involved in the primary task seems to be maintained with aging, elderly participants may have difficulty dealing with the competing cognitive and motor resources. How they allocate those resources to the different aspects of the dual-task remains to be seen.

It has been argued that aging is associated with a global decline (e.g., lower possessing speed) in cognitive functions, including attention and working memory. However, in their review, Dexter & Ossmy, (2023) argued that some

recent advances challenge this point of view. Their first argument is that there is a heterogeneity in findings regarding the decline in cognitive function with normal aging. This is coherent with the results obtained by Fukushima et al., (2014), and Sprenger et al., (2011), who showed that extra-retinal mechanisms such as working memory, prediction and anticipation during smooth pursuit are maintained in normal aging. At a brain level, normal aging is associated with changes in network organisation. In a study of brain network organisation during resting state across the healthy adult lifespan sample (20–89 years), Chan et al., (2014) reported that an increase in age was associated with a decrease in segregation in different subnetworks, such as the associative system (e.g. fronto-parietal network) and sensory-motor system (e.g. visual network, motor network). However, the age-related decrease in segregation was greater in associative subnetworks, which the authors also showed (independently of age) was associated with performance in a memory task. This is consistent with the suggestion that subnetwork segregation could be a biomarker of differences in cognition (Chan et al., 2014), as well responses to intervention (e.g. cognitive training, exercise (Gallen & D'Esposito, 2019). In Chapter 3 of the current thesis, competing cognitive demands of the primary and secondary tasks resulted in higher local (measure of segregation) and global efficiency (measure of integration) of the PFC network in young adults when performing oculo-manual pursuit. Future research could investigate how cognitive processes of performing a dual-task pursuit are impacted by normal aging, how this is reflected in brain network organisation, whether this is mediated by extra-retinal input provided by concurrent upper limb movements. The use of this dual-task pursuit paradigm could be an interesting way to investigate the impact of aging on extra-retinal mechanisms involved in smooth pursuit, prediction and working memory. A possible hypothesis is that aging would be reflected in a modified brain functional organisation (less segregated network organisation compared to younger), which could be associated with a longer response time. It can also be expected that predictive mechanisms involved in the primary task, and working memory performance in the secondary task, will be maintained. However, as suggested previously, the addition of concurrent upper limb movement could have a detrimental impact in an elderly population.

5.3 Oculo-manual adaptation

Activation of several cortical areas such DLPFC, FEF, premotor cortex, PPC, and V5 has been reported previously by authors who have studied brain activity during SPEM of continuously visible or temporarily occluded moving objects (Lencer et al., 2004; Nagel et al., 2006). Other authors have studied how functional connectivity between cortical areas during SPEM is impacted by object frequency (Schröder et al., 2020), and predictability (i.e., occlusion and/or stationary cues) of object trajectory (Ding et al., 2009). The importance of the network comprising frontal and parietal cortex in oculo-manual coordination has also been reported (Battaglia-Mayer & Caminiti, 2018). Extending on these studies, Chapter 4 examined the impact of oculo-manual tracking on cortical activity and network organisation (using Graph metrics) in conditions where the object was continuously visible or temporarily occluded. In addition, there was an opportunity for participants to adapt their oculo-manual coordination between pre-test and post-test. The short amount of training was performed in the oculo-manual condition without occlusion (see Vercher & Gauthier, 1988; Gauthier et al., 1988), thus allowing an examination of the impact of specific and general adaptation on brain organisation. Unlike the dual task protocol studied in Chapter 2 and 3, which involved discrete, short duration ramps of constant velocity object motion, in Chapter 4 participants pursued externally-generated, large amplitude sinusoidal motion over several cycles. This choice of stimulus was made to encourage oculo-manual facilitation, and as expected resulted in increased eye velocity in the oculo-manual than ocular condition.

Consistent with the results of Chapter 3, where the moving object was always occluded, it was found in Chapter 4 that there was increased activity (e.g. increased mean O_2Hb and decreased mean HHb) in MPFC in the OC condition compared to OM condition. This effect was also observed when the object was continuously visible (only for O_2Hb). However, unlike the results obtained in Chapter 3, where there was an effect of stimulus array but no effect of tracking mode, in Chapter 4 there was a reduced mean O_2Hb in DPLFC in the OM condition when the object was occluded compared to OC. This effect was not

present when the object remained visible. A possible explanation for this difference in results between Chapters 3 and 4 could be that in Chapter 3 the increased working memory demand, and thus involvement of DLPFC, outweighed the relatively small oculo-manual effect. Still, in Chapter 4 there was increased O_2Hb in DLPFC in trials with compared to without occlusion in the OC condition. This is consistent with results obtained by Nagel et al., (2006) and Ding et al., (2009), who both showed an increased activity in DLPFC during smooth pursuit with occlusion compared to a non-occluded condition. Extending upon the results of Chapter 3, mean O_2Hb in the OM condition was also lower in FEF, and VC at post-test and approach the significance for MC in Chapter 4 in trials with occlusion.

Interestingly, however, for IPL and SPL there was an increased mean O_2Hb in OM condition compared to OC condition, but this effect was only present at pre-test. The only change between pre and post-test in parietal areas occurred in IPL during the OC condition, and was reflected in an increase in O_2Hb. After a short period of training, the effect in frontal areas remained or became significant (DLPFC), but the effect in parietal areas was no longer evident. The parietal cortex is known to play a major role in oculo-manual coordination (Battaglia-Mayer & Caminiti, 2018), and here it would seem that the involvement of parietal cortex was reduced by a short period of specific training, suggesting a more optimal oculo-manual coordination that was less demanding for the parietal cortex. Together, the reduced mean O_2Hb during occlusion trials and the higher eye velocity in the oculo-manual condition compared to ocular alone condition, could indicate that access to extra-retinal information from upper limb movements facilitated smooth pursuit eye movements, with a lower metabolic cost (Logothetis et al., 2001).

As evoked in Chapter 1, brain network organisation can be understood in terms of integration and segregation. Both of these properties are thought to be critical for cognitive function (Sporns, 2013, Cohen & D'Esposito, 2016). The balance between integration and segregation is modified as a function of task demand, with the modification related to performance (Cohen & D'Esposito, 2016). It has been suggested that increased cognitive demand would lead to a more integrated network organisation, while a return to low cognitive task demand would be

associated with a more segregated network organisation (Fornito et al., 2016). Cohen & D'Esposito, (2016) studied the organisation of networks in terms of integration and segregation during different tasks, such as sequence tapping (motor) and n-back (working memory). Their results highlighted that more segregated network organisation was associated with the motor task, while more integrated network organisation was associated with the working memory task. The suggestion is that more integrated network organisation would lead to efficient transfer of information to meet task demand but would be less economical in terms of network organisation. Conversely, more segregated network organisation would be associated with less efficient transfer of information but greater economy (Achard & Bullmore, 2007). This is also supported by results obtained of Bassett et al., (2015), who showed an increased autonomy of motor and visual modules in a motor task after learning. The suggestion is that this organisation after learning is reflective of greater task automaticity, which would require less processing resource, and thus more economical network organisation.

In Chapter 4, there was no change in global efficiency (measure of integration), but local efficiency (measure of segregation) was reduced at post-test compared to pre-test in the OC tracking condition when the pursued object was occluded. There was also increased mean O_2Hb in the OC tracking condition from pre-test to post-test in prefrontal areas. Although these effects for local efficiency and mean O_2Hb were not identical, these findings could be indicative of a brain reorganisation following a short period of training in the oculo-manual condition. Still, it should be noted that this did eliminate the difference in eye velocity between the OC and OM tracking conditions. Why this reorganisation was not evident in global efficiency (network integration) remains to be determined. Indeed, it was shown in Chapter 3 that OM tracking was associated with increased global efficiency than OC tracking, although it should be remembered the dual pursuit task likely involved higher demand in working memory, which is thought to be associated with increased network integration (Cohen & D'Esposito, 2016). It is possible that imaging a wider network in Chapter 4 may have impacted upon the global efficiency metric. For example, it could be the case that global efficiency is more likely to change within different

subnetworks, such as the associative system (e.g. fronto-parietal network) and sensory-motor system (e.g. visual network, motor network), rather than across the entire network formed by 50 pairs of NIRS channels. As discussed below, it could also be relevant to consider other approaches to analysing NIRS data from large networks.

5.4 Methodological issues and considerations

This section attention will initially be directed to some potential limitations of the experimental work presented in this thesis, with a specific focus on the fNIRS studies. This will then be followed by a brief overview of the potential benefits of other neuroimaging analysis for future work.

Potential limitations in the fNIRS studies

As described previously in Chapter 3, O_2Hb changed as a function of demands in the dual-task protocol. However, there was no evidence of task related changes in HHb. In Chapter 4, while some significant results were found in HHb, as well as some evidence of the expected theorical pattern (see below), for example in MPFC, this was not consistently found. This is relevant because theoretically, the principle of neurovascular coupling would predict that an increase in neuronal activity should lead to a near symmetrical increase in O_2Hb and decrease in HHb (Tachtsidis & Scholkmann, 2016; Pinti et al., 2020). Indeed, this ability to assess changes in these two chromophores is suggested to be one of the main advantages of fNIRS. Importantly, however, changes in O_2Hb are usually of higher amplitude than changes in HHb (Pinti et al., 2020), which could lead to a lower statistical power and often a lack of significant changes in HHb. This could account for the recent suggestion that O_2Hb is more sensitive to task manipulations than HHb regardless of brain region (Luke et al., 2021).

An important concern for fNIRS research is that the signal is well known to be influenced by cerebral metabolic activity unrelated to task evoked neural activity, or by extracerebral metabolic activity, with both potentially resulting in

false positive and negative results (Tachtsidis & Scholkmann, 2016). Indeed, change in systemic activity like heart rate, blood pressure, and respiration can have a major impact on fNIRS measurement. While HHb is suggested to be less influenced by extracerebral activity, the influence of systemic noise is considered to be a major confounding factor for both O_2Hb and HHb. Considering the absence of this theorical pattern (e.g. increased O_2Hb and decreased HHb) in Chapter 3, it could be argued that the results may be due to the influence of non-neural metabolic activity. It has been suggested that the presence of this noise could be related to the experimental protocol used (Tachtsidis & Scholkmann, 2016). For example, the use of an active task involving large muscle groups could lead to larger task-evoked changes in cardiac rhythm, respiration, or blood pressure. This is unlikely to have had an impact on the results presented in this thesis as participants were seated during the whole study and made small amplitude upper arm movements in the oculo-manual tracking condition. Consistent with this suggestion is the finding that mean O_2Hb was lower in oculo-manual than ocular condition, suggesting that the results were simply not impacted by the larger task-evoked changes due to larger muscle group involved in this condition. Another important point against a significant influence of non-neural metabolic noise is that both fNIRS experiments in the current thesis used an optode array that included short distance channels. This allowed the signals from extracerebral layers to be regressed from the signals recorded by long distance channels. In addition, the signals from long distance channels were baseline corrected to subtract haemodynamic activity not evoked by the task (Tachtsidis & Scholkmann, 2016). It is therefore reasonable to suggest that the cortical imaging results presented in Chapters 3 and 4 are due to changes in neuronal activity even in absence of significant results in HHb.

Features analysis and multimodal approach for fNIRS neuroimaging

In the two studies involving fNIRS, the mean of O_2Hb and HHb signals was computed and used as a dependent variable to determine the influence of the task factors. While this approach revealed significant differences in line with the

expectations, it may not be optimally suited to analysing the lower sensitivity of HHb to task manipulation, as well as the lower amplitude changes in this signal (Pinti et al., 2020; Luke et al., 2021). To better understand the potential of fNIRS for brain computer interface, some authors have studied the use of different combinations of features in fNIRS data to discriminate between different tasks. For example, Naseer et al., (2016) used different combinations of features (mean, slope, variance, peak, skewness and kurtosis) from the HHb and O_2Hb signal to classify a mental arithmetic task from rest using linear discriminant analysis (LDA). Their results showed a higher accuracy in the combination of features including the peak and the mean of both O_2Hb (93% of accuracy) and HHb (89% of accuracy). Using the similar features associated with different measures of functional connectivity to the classify different states engagement of pilots during landing (manual vs. automated), Verdière et al., (2018) showed a better classification accuracy was obtained by combining wavelet coherence (e.g. functional connectivity feature) and area under curve (rounded average accuracy: 67% and 62% O_2Hb and HHb respectively). Taken together these results suggest that combining features of the fNIRS signal could be an interesting avenue for future work.

Another potential way to expand understanding of brain activity related to SPEM, and oculo-manual facilitation of SPEM, is to use a multimodal approach. Indeed, using the same approach as evoked previously for fNIRS features, some authors have studied the potential of multimodal imaging comprising EEG combined with fNIRS as a way to add complimentary information to discriminate between tasks. Indeed, EEG has previously been used to study SPEM (Jeong et al., 2019; Chen et al., 2017), and the two methods offers some complementary advantages. For example, EEG offers a high temporal resolution compared to fNIRS, and is a direct measurement of neuronal activity. fNIRS is an indirect measurement of neuronal activity via the quantification of changes in O_2Hb and HHb, and offers a good spatial resolution compared to EEG, as well as a relatively good tolerance to motion artifacts (Mehta & Parasuraman, 2013; Perrey, 2008). In a recent review, Li et al., (2022) highlighted that a main rational for combining both neuroimaging techniques is that, beside their complementarity in term of properties, they can be linked by the neurovascular

coupling principle. Indeed, according to this theory, an increase in neuronal activity (quantified by EEG) will lead to an increase in blood flow in this region, which lead to fluctuation of O_2Hb and HHb. In consideration of the strengths and weaknesses of EEG and fNIRS, the use of a multimodal approach combining these imaging techniques could offer a promising advance for future investigation of oculo-manual facilitation in SPEM.

Graph edge-centric approach

As detailed in the Chapter 1, two different approaches have previously been used to study the pattern of brain activity during SPEM (Lancer et al., 2004; Nagel et al., 2006; Schröder et al., (2020); Ding et al., 2009). The first aims to summarise the properties of a discrete and demarcated brain area (e.g. region-based analysis), whereas the second aims to measure the interactions between brain areas (e.g. connection-based analysis; Horien et al., 2020). These two approaches are complementary and were used in the current thesis to understand different aspects of brain functioning. In Chapter 3 and 4, each channel was considered as a node, such that the statistical dependency between time series from each pair of nodes (computed using partial correlation) represented an edge. The resulting correlation matrices were then used to compute Graph metrics. In other words, nodes are the neural elements, and edges reflect the functional coupling between these neural elements.

Although highly informative, region-based analyses focussed on nodes, and connections-based analyses focussed on edges (Horien et al., 2020), omit a potentially important aspect in that they do not consider the possible interactions between edges and their topology (Betzel et al., 2023, Faskowitz et al., 2022). This limitation can in part be overcome by creating an edge-centric network (see Figure 5.1). For this purpose, an edge time series can be created by calculating the time-by-time magnitude of the two node co-fluctuations, providing a time-varying estimation of the intensity of link between nodes (Sun et al., 2023). Then, a higher-order brain network can be created, which is richer in information and represents the interaction between intensity of the link between nodes. In this network, each edge becomes a “node” and the interaction between edges becomes an “edge”. The edge-by-edge matrix can be then reanalysed using

Graph theory metrics, such as a modularity analysis to determine the nodes involved in multiple communities (Betzel et al., 2023). Modularity is a measure of segregation between modules or communities (i.e., groups of nodes), which are densely connected to each other but less so with other groups of nodes within the entire network (Fornito et al., 2016) This approach has already been reported in several domains. For example, Sun et al., (2023) highlighted the advantage of using edge-centric measurements in autism spectrum disorder diagnosis. It has also been used to study brain activity of patients with early mild cognitive impairment (Wang et al., 2023). Focussing on the information provided by the edges within fNIRS time series data could be a promising way the better understand functional network organisation during cognitively demanding pursuit tasks, as well as the impact of oculo-manual facilitation. However, for now, this approach has been mainly used in task-free protocols like resting state, with the impact of task related activity remaining an important point to investigate (Betzel et al., 2023).

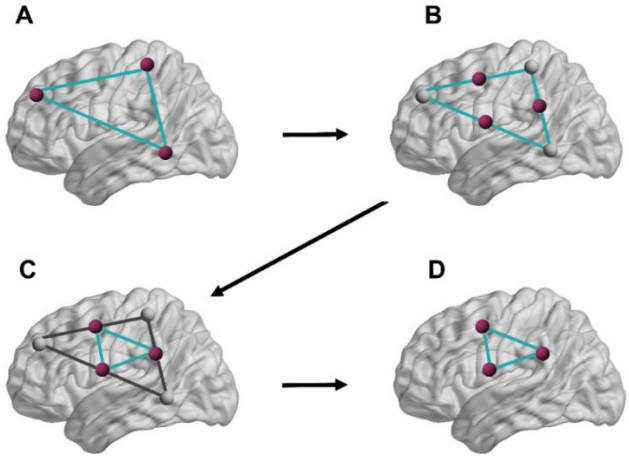

Figure 5.1: *A) representation of a network when each node (purple dots) corresponds to a to a measurement recoded on a brain region (e.g. channel in fNIRS) and each edge (blue line) corresponds to the statistical dependency between two nodes time series B) Each edge (blue line) is now represented as a node (purple dot), C) the interactions between edges are now represented as an edge (blue line), D) Representation of an edge centric network.*

5.5 Conclusion

Oculo-manual facilitation of smooth pursuit eye moment has been reported in several lab-based studies, and is likely to occur in daily activities. While previous research has identified several cortical areas involved in control of smooth pursuit eye movement, the impact of concurrent upper-limb movement on their activity and network organisation remains poorly understood. In order to extend understanding on oculo-manual facilitation of smooth pursuit eye movement, a series of multi-method and multi-measure studies were conducted that varied in complexity and cognitive demand. Across the studies, the most compelling finding was that oculo-manual pursuit led to changes in measures of brain function. More specifically, a reduced activity in prefrontal areas, as well as changes in efficiency of network organisation, was observed in oculo-manual compared to ocular tracking. The implication is that extra-retinal information from concurrent upper limb movement influences the predictive processes that operate during smooth pursuit eye movement. These findings provide an important step forward in understanding brain function during oculo-manual pursuit in neurotypical adults. They also provide the basis for future study of populations like older people who exhibit changes in ocular and cognitive function, as well as brain network organisation, patients with peripheral neuropathy who have no or impaired afference, or autistic people who place a greater emphasis on limb afference than visual efference during visual tracking tasks.

References

Abdalmalak, A., Milej, D., Cohen, D. J., Anazodo, U., Ssali, T., Diop, M., ... & Lawrence, K. S. (2020). Using fMRI to investigate the potential cause of inverse oxygenation reported in fNIRS studies of motor imagery. *Neuroscience letters*, *714*, 134607.

Achard, S., & Bullmore, E. (2007). Efficiency and cost of economical brain functional networks. *PLoS computational biology*, *3*(2), e17.

Anwar, A. R., Muthalib, M., Perrey, S., Galka, A., Granert, O., Wolff, S., ... & Muthuraman, M. (2016). Effective connectivity of cortical sensorimotor networks during finger movement tasks: a simultaneous fNIRS, fMRI, EEG study. *Brain topography*, *29*, 645-660.

Anwyl-Irvine, A., Dalmaijer, E. S., Hodges, N., & Evershed, J. K. (2021). Realistic precision and accuracy of online experiment platforms, web browsers, and devices. *Behavior research methods*, *53*(4), 1407-1425.

Baddeley, A. D., & Hitch, G. J. (1974). Working memory. *New York: GA Bower (ed), Recent advances in learning and motivation*, vol.8, 47-89

Barbey, A. K., Koenigs, M., & Grafman, J. (2013). Dorsolateral prefrontal contributions to human working memory. *cortex*, *49*(5), 1195-1205.

Barnes, G. R. (2008). Cognitive processes involved in smooth pursuit eye movements. *Brain and cognition*, *68*(3), 309-326.

Barton, J. J., Simpson, T., Kiriakopoulos, E., Stewart, C., Crawley, A., Guthrie, B., ... & Mikulis, D. (1996). Functional MRI of lateral occipitotemporal cortex during pursuit and motion perception. *Annals of Neurology: Official Journal of the American Neurological Association and the Child Neurology Society*, *40*(3), 387-398.

Bassett, D. S., Yang, M., Wymbs, N. F., & Grafton, S. T. (2015). Learning-induced autonomy of sensorimotor systems. *Nature neuroscience*, *18*(5), 744-751.

Bastos, A. M., & Schoffelen, J. M. (2016). A tutorial review of functional connectivity analysis methods and their interpretational pitfalls. *Frontiers in systems neuroscience*, *9*, 175.

Battaglia-Mayer, A., Archambault, P. S., & Caminiti, R. (2006). The cortical network for eye–hand coordination and its relevance to understanding motor disorders of parietal patients. *Neuropsychologia*, *44*(13), 2607-2620.

Battaglia-Mayer, A., & Caminiti, R. (2018). Parieto-frontal networks for eye–hand coordination and movements. *Handbook of clinical neurology*, *151*, 499-524.

Becker, W., & Fuchs, A. F. (1985). Prediction in the oculomotor system: smooth pursuit during transient disappearance of a visual target. *Experimental brain research*, *57*(3), 562-575.

Bennett, S. J., & Barnes, G. R. (2003). Human ocular pursuit during the transient disappearance of a visual target. *Journal of Neurophysiology*, *90*(4), 2504-2520.

Bennett, S. J., & Barnes, G. R. (2004). Predictive smooth ocular pursuit during the transient disappearance of a visual target. *Journal of neurophysiology*, *92*(1), 578-590.

Bennett, S. J., Baures, R., Hecht, H., & Benguigui, N. (2010). Eye movements influence estimation of time-to-contact in prediction motion. *Experimental brain research*, *206*, 399-407.

Bennett, S. J., O'Donnell, D., Hansen, S., & Barnes, G. R. (2012). Facilitation of ocular pursuit during transient occlusion of externally-generated target motion by concurrent upper limb movement. *Journal of vision*, *12*(13), 17-17.

Bennett, S. J., & Benguigui, N. (2016). Spatial estimation of accelerated stimuli is based on a linear extrapolation of first-order information. *Experimental psychology*.

Betzel, R. F., Faskowitz, J., & Sporns, O. (2023). Living on the edge: network neuroscience beyond nodes. *Trends in cognitive sciences*.

Biswal, B., Zerrin Yetkin, F., Haughton, V. M., & Hyde, J. S. (1995). Functional connectivity in the motor cortex of resting human brain using echo-planar MRI. *Magnetic resonance in medicine*, *34*(4), 537-541.

Braver, T. S., & Bongiolatti, S. R. (2002). The role of frontopolar cortex in subgoal processing during working memory. *Neuroimage*, *15*(3), 523-536.

Brigadoi, S., & Cooper, R. J. (2015). How short is short? Optimum source–detector distance for short-separation channels in functional near-infrared spectroscopy. *Neurophotonics*, *2*(2), 025005-025005.

Bullmore, E., & Sporns, O. (2012). The economy of brain network organization. *Nature reviews neuroscience*, *13*(5), 336-349.

Burke, M. R., & Barnes, G. R. (2008). Brain and behavior: a task-dependent eye movement study. *Cerebral Cortex*, *18*(1), 126-135.

Burke, M. R., Poyser, C., & Schiessl, I. (2015). Age-related deficits in visuospatial memory are due to changes in preparatory set and eye–hand coordination. Journals of Gerontology Series B: Psychological Sciences and Social Sciences, 70(5), 682-690.

Chan, M. Y., Park, D. C., Savalia, N. K., Petersen, S. E., & Wig, G. S. (2014). Decreased segregation of brain systems across the healthy adult lifespan. *Proceedings of the National Academy of Sciences*, *111*(46), E4997-E5006.

Chen, J., Valsecchi, M., & Gegenfurtner, K. R. (2017). Attention is allocated closely ahead of the target during smooth pursuit eye movements: Evidence from EEG frequency tagging. *Neuropsychologia*, *102*, 206-216.

Christoff, K., Prabhakaran, V., Dorfman, J., Zhao, Z., Kroger, J. K., Holyoak, K. J., & Gabrieli, J. D. (2001). Rostrolateral prefrontal cortex involvement in relational integration during reasoning. *Neuroimage*, *14*(5), 1136-1149.

Churchland, M. M., Chou, I. H., & Lisberger, S. G. (2003). Evidence for object permanence in the smooth-pursuit eye movements of monkeys. *Journal of neurophysiology*, *90*(4), 2205-2218.

Cohen, J. R., & D'Esposito, M. (2016). The segregation and integration of distinct brain networks and their relationship to cognition. *Journal of Neuroscience*, *36*(48), 12083-12094.

Cooper, R. J., Selb, J., Gagnon, L., Phillip, D., Schytz, H. W., Iversen, H. K., ... & Boas, D. A. (2012). A systematic comparison of motion artifact correction techniques for functional near-infrared spectroscopy. *Frontiers in neuroscience*, *6*, 147.

Cui, X., Bray, S., Bryant, D. M., Glover, G. H., & Reiss, A. L. (2011). A quantitative comparison of NIRS and fMRI across multiple cognitive tasks. *Neuroimage*, *54*(4), 2808-2821.

Curtis, C. E., & D'Esposito, M. (2003). Persistent activity in the prefrontal cortex during working memory. *Trends in cognitive sciences*, *7*(9), 415-423.

Dallos, P. J., & Jones, R. (1963). Learning behavior of the eye fixation control system. *IEEE Transactions on automatic control*, *8*(3), 218-227.

De Brouwer, S., Yuksel, D., Blohm, G., Missal, M., & Lefèvre, P. (2002). What triggers catch-up saccades during visual tracking?. *Journal of neurophysiology*, *87*(3), 1646-1650.

Decat, N., Walter, J., Koh, Z. H., Sribanditmongkol, P., Fulcher, B. D., Windt, J. M., ... & Tsuchiya, N. (2022). Beyond traditional sleep scoring: Massive feature extraction and data-driven clustering of sleep time series. *Sleep Medicine*, *98*, 39-52.

Dexter, M., & Ossmy, O. (2023). The effects of typical ageing on cognitive control: recent advances and future directions. *Frontiers in Aging Neuroscience*, *15*.

Ding, J., Powell, D., & Jiang, Y. (2009). Dissociable frontal controls during visible and memory-guided eye-tracking of moving targets. *Human brain mapping*, *30*(11), 3541-3552.

Duncan, A., Meek, J. H., Clemence, M., Elwell, C. E., Fallon, P., Tyszczuk, L., ... & Delpy, D. T. (1996). Measurement of cranial optical path length as a function of age using phase resolved near infrared spectroscopy. *Pediatric research*, *39*(5), 889-894.

Fan, S., Blanco-Davis, E., Zhang, J., Bury, A., Warren, J., Yang, Z., ... & Fairclough, S. (2021). The role of the prefrontal cortex and functional connectivity during maritime operations: an fNIRS study. *Brain and Behavior*, *11*(1), e01910.

Faskowitz, J., Betzel, R. F., & Sporns, O. (2022). Edges in brain networks: Contributions to models of structure and function. *Network Neuroscience*, *6*(1), 1-28.

Ferrari, M., & Quaresima, V. (2012). A brief review on the history of human functional near-infrared spectroscopy (fNIRS) development and fields of application. Neuroimage, 63(2), 921-935.

Ferrera, V. P., & Lisberger, S. G. (1995). Attention and target selection for smooth pursuit eye movements. *Journal of Neuroscience*, *15*(11), 7472-7484.

Fornito, A., Zalesky, A., & Bullmore, E. (2016). *Fundamentals of brain network analysis*. Academic press.

Fukushima, K., Yamanobe, T., Shinmei, Y., & Fukushima, J. (2002). Predictive responses of periarcuate pursuit neurons to visual target motion. *Experimental brain research*, *145*, 104-120.

Fukushima, K., Fukushima, J., Warabi, T., & Barnes, G. R. (2013). Cognitive processes involved in smooth pursuit eye movements: behavioral evidence, neural substrate and clinical correlation. *Frontiers in systems neuroscience*, *7*, 4.

Fukushima, K., Barnes, G. R., Ito, N., Olley, P. M., & Warabi, T. (2014). Normal aging affects movement execution but not visual motion working memory and decision-making delay during cue-dependent memory-based smooth-pursuit. *Experimental brain research*, *232*, 2369-2379.

Fulcher, B. D., Little, M. A., & Jones, N. S. (2013). Highly comparative time-series analysis: the empirical structure of time series and their methods. *Journal of the Royal Society Interface*, *10*(83), 20130048.

Fulcher, B. D., & Jones, N. S. (2017). hctsa: A computational framework for automated time-series phenotyping using massive feature extraction. *Cell systems*, *5*(5), 527-531.

Gallen, C. L., & D'Esposito, M. (2019). Brain modularity: a biomarker of intervention-related plasticity. *Trends in cognitive sciences*, *23*(4), 293-304.

Gauthier, G. M., & Hofferer, J. M. (1976). Eye tracking of self-moved targets in the absence of vision. *Experimental brain research*, *26*, 121-139.

Gauthier, G. M., Vercher, J. L., Mussa Ivaldi, F., & Marchetti, E. (1988). Oculo-manual tracking of visual targets: control learning, coordination control and coordination model. *Experimental Brain Research*, *73*, 127-137.

Gauthier, G. M., & Mussa Ivaldi, F. (1988). Oculo-manual tracking of visual targets in monkey: role of the arm afferent information in the control of arm and eye movements. *Experimental Brain Research*, *73*(1), 138-154.

Heide, W., Kurzidim, K., & Kömpf, D. (1996). Deficits of smooth pursuit eye movements after frontal and parietal lesions. *Brain*, *119*(6), 1951-1969.

Heinen, S. J. (1995). Single neuron activity in the dorsomedial frontal cortex during smooth pursuit eye movements. *Experimental Brain Research*, *104*, 357-361.

Heinen, S. J., Jin, Z., & Watamaniuk, S. N. (2011). Flexibility of foveal attention during ocular pursuit. *Journal of Vision*, *11*(2), 9-9.

Hill, D., Coats, R. O., Halstead, A., & Burke, M. R. (2015). A systematic research review assessing the effectiveness of pursuit interventions in spatial neglect following stroke. *Translational stroke research*, *6*, 410-420.

Holper, L., Shalóm, D. E., Wolf, M., & Sigman, M. (2011). Understanding inverse oxygenation responses during motor imagery: A functional near-infrared spectroscopy study. *European Journal of Neuroscience*, *33*(12), 2318-2328.

Horien, C., Greene, A. S., Constable, R. T., & Scheinost, D. (2020). Regions and connections: complementary approaches to characterize brain organization and function. *The Neuroscientist*, *26*(2), 117-133.

Huppert, T. J., Diamond, S. G., Franceschini, M. A., & Boas, D. A. (2009). HomER: a review of time-series analysis methods for near-infrared spectroscopy of the brain. *Applied optics*, *48*(10), D280-D298.

Ilg, U. J., & Thier, P. (2003). Visual tracking neurons in primate area MST are activated by smooth-pursuit eye movements of an "imaginary" target. *Journal of neurophysiology*, *90*(3), 1489-1502.

Ilg, U. J., & Thier, P. (2008). The neural basis of smooth pursuit eye movements in the rhesus monkey brain. *Brain and cognition*, *68*(3), 229-240.

Ito, T., Hearne, L. J., & Cole, M. W. (2020). A cortical hierarchy of localized and distributed processes revealed via dissociation of task activations, connectivity changes, and intrinsic timescales. *NeuroImage*, *221*, 117141.

Jarrett, C., & Barnes, G. (2005). The use of non-motion-based cues to pre-programme the timing of predictive velocity reversal in human smooth pursuit. *Experimental brain research*, *164*, 423-430.

Jeong, W., Kim, S., Kim, Y. J., & Lee, J. (2019). Motion direction representation in multivariate electroencephalography activity for smooth pursuit eye movements. *NeuroImage*, *202*, 116160.

Jiang, Y., Olson, I. R., & Chun, M. M. (2000). Organization of visual short-term memory. *Journal of Experimental Psychology: Learning, memory, and cognition*, *26*(3), 683.

Jin, Z., Reeves, A., Watamaniuk, S. N., & Heinen, S. J. (2013). Shared attention for smooth pursuit and saccades. *Journal of vision*, *13*(4), 7-7.

Jin, Z., Watamaniuk, S. N., Khan, A. Z., Potapchuk, E., & Heinen, S. J. (2014). Motion integration for ocular pursuit does not hinder perceptual segregation of moving objects. *Journal of Neuroscience, 34*(17), 5835-5841.

Jonikaitis, D., Deubel, H., & de'Sperati, C. (2009). Time gaps in mental imagery introduced by competing saccadic tasks. *Vision Research*, *49*(17), 2164-2175.

Kerzel, D., & Ziegler, N. E. (2005). Visual short-term memory during smooth pursuit eye movements. *Journal of Experimental Psychology: Human Perception and Performance*, *31*(2), 354.

Khurana, B., & Kowler, E. (1987). Shared attentional control of smooth eye movement and perception. *Vision research*, *27*(9), 1603-1618.

Kocsis, L., Herman, P., & Eke, A. (2006). The modified Beer–Lambert law revisited. *Physics in Medicine & Biology*, *51*(5), N91.

Koechlin, E., Basso, G., Pietrini, P., Panzer, S., & Grafman, J. (1999). The role of the anterior prefrontal cortex in human cognition. *Nature*, *399*(6732), 148-151.

Kohl-Bareis, M. (2012). NIRS: Theoretical background and practical aspects. In *Functional Neuroimaging in Exercise and Sport Sciences* (pp. 213-235). New York, NY: Springer New York.

Koken, P. W., & Erkelens, C. J. (1992). Influences of hand movements on eye movements in tracking tasks in man. *Experimental Brain Research*, *88*, 657-664.

Konen, C. S., & Kastner, S. (2008). Representation of eye movements and stimulus motion in topographically organized areas of human posterior parietal cortex. *Journal of Neuroscience*, *28*(33), 8361-8375.

Kowler, E. (1989). Cognitive expectations, not habits, control anticipatory smooth oculomotor pursuit. *Vision research*, *29*(9), 1049-1057.

Krauzlis, R. J., & Lisberger, S. G. (1989). A control systems model of smooth pursuit eye movements with realistic emergent properties. *Neural Computation*, *1*(1), 116-122.

Krauzlis, R. J. (2004). Recasting the smooth pursuit eye movement system. *Journal of neurophysiology*, *91*(2), 591-603.

Lencer, R., Nagel, M., Sprenger, A., Zapf, S., Erdmann, C., Heide, W., & Binkofski, F. (2004). Cortical mechanisms of smooth pursuit eye movements with target blanking. An fMRI study. *European Journal of Neuroscience*, *19*(5), 1430-1436.

Lencer, R., & Trillenberg, P. (2008). Neurophysiology and neuroanatomy of smooth pursuit in humans. *Brain and cognition*, *68*(3), 219-228.

Lencer, R., Sprenger, A., & Trillenberg, P. (2019). Smooth eye movements in humans: smooth pursuit, optokinetic nystagmus and vestibular ocular reflex. *Eye movement research: An introduction to its scientific foundations and applications*, 117-163.

Levy, R., & Goldman-Rakic, P. S. (1999). Association of storage and processing functions in the dorsolateral prefrontal cortex of the nonhuman primate. *Journal of Neuroscience*, *19*(12), 5149-5158.

Li, R., Yang, D., Fang, F., Hong, K. S., Reiss, A. L., & Zhang, Y. (2022). Concurrent fNIRS and EEG for brain function investigation: a systematic, methodology-focused review. *Sensors*, *22*(15), 5865.

Li, X., Baurès, R., & Cremoux, S. (2023). Hand movements influence the perception of time in a prediction motion task. *Attention, Perception, & Psychophysics*, *85*(4), 1276-1286.

Liu, H., Kaneko, Y., Ouyang, X., Li, L., Hao, Y., Chen, E. Y., ... & Liu, Z. (2012). Schizophrenic patients and their unaffected siblings share increased resting-state connectivity in the task-negative network but not its anticorrelated task-positive network. *Schizophrenia bulletin*, *38*(2), 285-294.

Logothetis, N. K., Pauls, J., Augath, M., Trinath, T., & Oeltermann, A. (2001). Neurophysiological investigation of the basis of the fMRI signal. *nature*, *412*(6843), 150-157.

Lord, L. D., Stevner, A. B., Deco, G., & Kringelbach, M. L. (2017). Understanding principles of integration and segregation using whole-brain computational connectomics: implications for neuropsychiatric disorders. *Philosophical Transactions of the Royal Society A: Mathematical, Physical and Engineering Sciences*, *375*(2096), 20160283.

Lovejoy, L. P., Fowler, G. A., & Krauzlis, R. J. (2009). Spatial allocation of attention during smooth pursuit eye movements. *Vision research*, *49*(10), 1275-1285.

Lowe, M. J. (2010). A historical perspective on the evolution of resting-state functional connectivity with MRI. *Magnetic Resonance Materials in Physics, Biology and Medicine*, *23*, 279-288.

Luke, R., Shader, M. J., Gramfort, A., Larson, E., Lee, A. K., & McAlpine, D. (2021). Oxygenated hemoglobin signal provides greater predictive performance of experimental condition than de-oxygenated. *BioRxiv*, 2021-11.

Lyon, D. R., & Waag, W. L. (1995). Time course of visual extrapolation accuracy. *Acta psychologica*, *89*(3), 239-260.

Madelain, L., & Krauzlis, R. J. (2003). Effects of learning on smooth pursuit during transient disappearance of a visual target. *Journal of neurophysiology*, *90*(2), 972-982.

Maioli, C., Falciati, L., & Gianesini, T. (2007). Pursuit eye movements involve a covert motor plan for manual tracking. *Journal of Neuroscience*, *27*(27), 7168-7173.

Makovski, T., & Jiang, Y. V. (2009). The role of visual working memory in attentive tracking of unique objects. *Journal of Experimental Psychology: Human Perception and Performance*, *35*(6), 1687.

Mandrick, K. (2013). *Application de la spectroscopie proche infrarouge dans la discrimination de la charge de travail* (Doctoral dissertation, Université Montpellier I).

Mansouri, F. A., Koechlin, E., Rosa, M. G., & Buckley, M. J. (2017). Managing competing goals—a key role for the frontopolar cortex. *Nature Reviews Neuroscience*, *18*(11), 645-657.

Mehta, R. K., & Parasuraman, R. (2013). Neuroergonomics: a review of applications to physical and cognitive work. *Frontiers in human neuroscience*, *7*, 889.

Menon, V., & D'Esposito, M. (2022). The role of PFC networks in cognitive control and executive function. *Neuropsychopharmacology*, *47*(1), 90-103.

Merigan, W. H., Katz, L. M., & Maunsell, J. H. (1991). The effects of parvocellular lateral geniculate lesions on the acuity and contrast sensitivity of macaque monkeys. *Journal of Neuroscience*, *11*(4), 994-1001.

Miall, R. C., Weir, D. J., & Stein, J. F. (1993). Intermittency in human manual tracking tasks. *Journal of motor behavior*, *25*(1), 53-63.

Miall, R. C., Reckess, G. Z., & Imamizu, H. (2001). The cerebellum coordinates eye and hand tracking movements. *Nature neuroscience*, *4*(6), 638-644.

Miller, J. (2023). Outlier exclusion procedures for reaction time analysis: The cures are generally worse than the disease. *Journal of Experimental Psychology: General*.

Mills, B. D., Miranda-Dominguez, O., Mills, K. L., Earl, E., Cordova, M., Painter, J., ... & Fair, D. A. (2018). ADHD and attentional control: Impaired segregation of task positive and task negative brain networks. *Network Neuroscience*, *2*(02), 200-217.

Molavi, B., & Dumont, G. A. (2012). Wavelet-based motion artifact removal for functional near-infrared spectroscopy. *Physiological measurement*, *33*(2), 259.

Nagel, M., Sprenger, A., Zapf, S., Erdmann, C., Kömpf, D., Heide, W., ... & Lencer, R. (2006). Parametric modulation of cortical activation during smooth pursuit with and without target blanking. An fMRI study. *Neuroimage*, *29*(4), 1319-1325.

Naseer, N., Noori, F. M., Qureshi, N. K., & Hong, K. S. (2016). Determining optimal feature-combination for LDA classification of functional near-infrared spectroscopy signals in brain-computer interface application. *Frontiers in human neuroscience*, *10*, 237.

Nasios, G., Dardiotis, E., & Messinis, L. (2019). From Broca and Wernicke to the neuromodulation era: insights of brain language networks for neurorehabilitation. *Behavioural neurology*, *2019*.

Oberauer, K. (2019). Working memory and attention–A conceptual analysis and review. *Journal of cognition*, *2*(1).

Orban de Xivry, J. J., Bennett, S. J., Lefèvre, P., & Barnes, G. R. (2006). Evidence for synergy between saccades and smooth pursuit during transient target disappearance. *Journal of neurophysiology*, *95*(1), 418-427.

O'Rielly, J. L., & Ma-Wyatt, A. (2018). Changes to online control and eye-hand coordination with healthy ageing. *Human Movement Science*, *59*, 244-257.

Perrey, S. (2008). Non-invasive NIR spectroscopy of human brain function during exercise. *Methods*, *45*(4), 289-299.

Pierrot-Deseilligny, C., Müri, R. M., Ploner, C. J., Gaymard, B., Demeret, S., & Rivaud-Pechoux, S. (2003). Decisional role of the dorsolateral prefrontal cortex in ocular motor behaviour. *Brain*, *126*(6), 1460-1473.

Pinti, P., Tachtsidis, I., Hamilton, A., Hirsch, J., Aichelburg, C., Gilbert, S., & Burgess, P. W. (2020). The present and future use of functional near-infrared spectroscopy (fNIRS) for cognitive neuroscience. *Annals of the new York Academy of Sciences*, *1464*(1), 5-29.

Pola, J., & Wyatt, H. J. (1997). Offset dynamics of human smooth pursuit eye movements: effects of target presence and subject attention. *Vision research*, *37*(18), 2579-2595.

Pollonini, L., Bortfeld, H., & Oghalai, J. S. (2016). PHOEBE: a method for real time mapping of optodes-scalp coupling in functional near-infrared spectroscopy. *Biomedical optics express*, *7*(12), 5104-5119.

Pouget, P. (2019). Introduction to the study of eye movements. *Eye movement research: an introduction to its scientific foundations and applications*, 3-10.

Ramnani, N., & Owen, A. M. (2004). Anterior prefrontal cortex: insights into function from anatomy and neuroimaging. *Nature reviews neuroscience*, *5*(3), 184-194.

Reijneveld, J. C., Ponten, S. C., Berendse, H. W., & Stam, C. J. (2007). The application of graph theoretical analysis to complex networks in the brain. *Clinical neurophysiology*, *118*(11), 2317-2331.

Rizzo, J. R., Beheshti, M., Naeimi, T., Feiz, F., Fatterpekar, G., Balcer, L. J., ... & Hudson, T. E. (2020). The complexity of eye-hand coordination: a perspective on cortico-cerebellar cooperation. *Cerebellum & Ataxias*, *7*, 1-9.

Robinson, D. A., Gordon, J. L., & Gordon, S. E. (1986). A model of the smooth pursuit eye movement system. *Biological cybernetics*, *55*, 43-57.

Rubinov, M., Kötter, R., Hagmann, P., & Sporns, O. (2009). Brain connectivity toolbox: a collection of complex network measurements and brain connectivity datasets. *NeuroImage*, *47*, S169.

Rubinov, M., & Sporns, O. (2010). Complex network measures of brain connectivity: uses and interpretations. *Neuroimage*, *52*(3), 1059-1069.

Sato, H., Yahata, N., Funane, T., Takizawa, R., Katura, T., Atsumori, H., ... & Kasai, K. (2013). A NIRS–fMRI investigation of prefrontal cortex activity during a working memory task. *Neuroimage*, *83*, 158-173.

Schmid, A., Rees, G., Frith, C., & Barnes, G. (2001). An fMRI study of anticipation and learning of smooth pursuit eye movements in humans. *Neuroreport*, *12*(7), 1409-1414.

Scholkmann, F., Spichtig, S., Muehlemann, T., & Wolf, M. (2010). How to detect and reduce movement artifacts in near-infrared imaging using moving standard deviation and spline interpolation. *Physiological measurement*, *31*(5), 649.

Schröder, R., Kasparbauer, A. M., Meyhöfer, I., Steffens, M., Trautner, P., & Ettinger, U. (2020). Functional connectivity during smooth pursuit eye movements. *Journal of Neurophysiology*, *124*(6), 1839-1856.

Schröder, R., Keidel, K., Trautner, P., Radbruch, A., & Ettinger, U. (2023). Neural mechanisms of background and velocity effects in smooth pursuit eye movements. *Human brain mapping*, *44*(3), 1002-1018.

Seitzman, B. A., Snyder, A. Z., Leuthardt, E. C., & Shimony, J. S. (2019). The state of resting state networks. *Topics in Magnetic Resonance Imaging*, *28*(4), 189-196.

Shi, Y., Zhu, Y., Mehta, R. K., & Du, J. (2020). A neurophysiological approach to assess training outcome under stress: A virtual reality experiment of industrial shutdown maintenance using Functional Near-Infrared Spectroscopy (fNIRS). *Advanced Engineering Informatics*, *46*, 101153.

Shichinohe, N., Akao, T., Kurkin, S., Fukushima, J., Kaneko, C. R., & Fukushima, K. (2009). Memory and decision making in the frontal cortex during visual motion processing for smooth pursuit eye movements. *Neuron*, *62*(5), 717-732.

Singh, A. K., Okamoto, M., Dan, H., Jurcak, V., & Dan, I. (2005). Spatial registration of multichannel multi-subject fNIRS data to MNI space without MRI. *Neuroimage*, *27*(4), 842-851.

Sporns, O., Chialvo, D. R., Kaiser, M., & Hilgetag, C. C. (2004). Organization, development and function of complex brain networks. *Trends in cognitive sciences*, *8*(9), 418-425.

Sporns, O. (2013). Network attributes for segregation and integration in the human brain. *Current opinion in neurobiology*, *23*(2), 162-171.

Sporns, O. (2016). *Networks of the Brain*. MIT press.

Sprenger, A., Trillenberg, P., Pohlmann, J., Herold, K., Lencer, R., & Helmchen, C. (2011). The role of prediction and anticipation on age-related effects on smooth pursuit eye movements. *Annals of the New York Academy of Sciences*, *1233*(1), 168-176.

Strangman, G. E., Li, Z., & Zhang, Q. (2013). Depth sensitivity and source-detector separations for near infrared spectroscopy based on the Colin27 brain template. *PloS one*, *8*(8), e66319.

St-Onge, F., Javanray, M., Pichet Binette, A., Strikwerda-Brown, C., Remz, J., Spreng, R. N., ... & Villeneuve, S. (2023). Functional connectome fingerprinting across the lifespan. *Network Neuroscience*, *7*(3), 1206-1227.

Sun, A., Wang, J., & Zhang, J. (2023). Identifying autism spectrum disorder using edge-centric functional connectivity. *Cerebral Cortex*, *33*(13), 8122-8130.

Tachtsidis, I., & Scholkmann, F. (2016). False positives and false negatives in functional near-infrared spectroscopy: issues, challenges, and the way forward. *Neurophotonics*, *3*(3), 031405-031405.

Tanaka, M., Yoshida, T., & Fukushima, K. (1998). Latency of saccades during smooth-pursuit eye movement in man Directional asymmetries: Directional asymmetries. *Experimental Brain Research*, *121*, 92-98.

Tanaka, H., Worringham, C., & Kerr, G. (2009). Contributions of vision–proprioception interactions to the estimation of time-varying hand and target locations. *Experimental brain research*, *195*, 371-382.

Themelis, G., D'Arceuil, H., Diamond, S. G., Thaker, S., Huppert, T. J., Boas, D. A., & Franceschini, M. A. (2007). Near-infrared spectroscopy measurement of the pulsatile component of cerebral blood flow and volume from arterial oscillations. *Journal of biomedical optics*, *12*(1), 014033-014033.

Thériault, R., Ben-Shachar, M. S., Patil, I., Lüdecke, D., Wiernik, B. M., & Makowski, D. (2023). Check your outliers! An introduction to identifying statistical outliers in R with easystats. PsyArXiv. October, 20.

Tian, J. R., & Lynch, J. C. (1996). Corticocortical input to the smooth and saccadic eye movement subregions of the frontal eye field in Cebus monkeys. *Journal of Neurophysiology*, *76*(4), 2754-2771.

Urakawa, S., Takamoto, K., Ishikawa, A., Ono, T., & Nishijo, H. (2015). Selective medial prefrontal cortex responses during live mutual gaze interactions in human infants: an fNIRS study. *Brain topography*, *28*, 691-701.

Van Den Heuvel, M. P., & Pol, H. E. H. (2010). Exploring the brain network: a review on resting-state fMRI functional connectivity. *European neuropsychopharmacology*, *20*(8), 519-534.

Van Donkelaar, P., & Drew, A. S. (2002). The allocation of attention during smooth pursuit eye movements. *Progress in brain research*, *140*, 267-277.

Vercher, J. L., Gauthier, G. M., Guedon, O., Blouin, J., Cole, J., & Lamarre, Y. V. E. S. (1996). Self-moved target eye tracking in control and deafferented subjects: roles of arm motor command and proprioception in arm-eye coordination. *Journal of Neurophysiology*, *76*(2), 1133-1144.

Vercher, J. L., Lazzari, S., & Gauthier, G. (1997). Manuo-ocular coordination in target tracking. II. Comparing the model with human behavior. *Biological cybernetics*, *77*(4), 267-275.

Vercher, J. L., & Gauthier, G. M. (1988). Cerebellar involvement in the coordination control of the oculo-manual tracking system: effects of cerebellar dentate nucleus lesion. *Experimental Brain Research*, *73*, 155-166.

Verdière, K. J., Roy, R. N., & Dehais, F. (2018). Detecting pilot's engagement using fNIRS connectivity features in an automated vs. manual landing scenario. *Frontiers in human neuroscience*, *12*, 6.

Wang, R., Liu, M., Cheng, X., Wu, Y., Hildebrandt, A., & Zhou, C. (2021). Segregation, integration, and balance of large-scale resting brain networks configure different cognitive abilities. *Proceedings of the National Academy of Sciences*, *118*(23), e2022288118.

Wang, W., Du, R., Wang, Z., Luo, X., Zhao, H., Luan, P., ... & Liu, S. (2023). Edge-centric functional network reveals new spatiotemporal biomarkers of early mild cognitive impairment. *Brain-X*, *1*(3), e35.

Watamaniuk, S. N., & Heinen, S. J. (2015). Allocation of attention during pursuit of large objects is no different than during fixation. *Journal of Vision*, *15*(9), 9-9.

Wexler, M., & Klam, F. (2001). Movement prediction and movement production. *Journal of experimental psychology: Human perception and performance*, *27*(1), 48.

Xia, M., Wang, J., & He, Y. (2013). BrainNet Viewer: a network visualization tool for human brain connectomics. *PloS one*, *8*(7), e68910.

Yue, S., Jin, Z., Chenggui, F., Qian, Z., & Li, L. (2017). Interference between smooth pursuit and color working memory. *Journal of eye movement research*, *10*(3).

Zheng, R., & Maraj, B. K. (2018). The effect of concurrent hand movement on estimated time to contact in a prediction motion task. *Experimental Brain Research*, *236*, 1953-1962. https://doi.org/10.1007/s00221-018-5276-5

Appendix I: Methodological Considerations

I.1 Introduction

The aim of this chapter is to provide a brief introduction to neuroimaging via functional Near-Infrared Spectroscopy (fNIRS) and to highlight two main methodological considerations that informed the data collection methods used in subsequent experimental testing (Chapters 3 and 4). Following a summary of key concepts underpinning the development and application of fNIRS, details will be given on the way the measurement points locations (e.g. channels) were chosen for the experimental studies involving fNIRS. Next, the potential for crosstalk between fNIRS and eye tracking using video-oculography, both of which use near-infrared light, will be described. This will be followed by an analysis of data collected with two fNIRS devices (i.e., Brainsight and NIRSport2) in conditions that ranged from minimum to maximum potential for crosstalk.

I.2 Overview of fNIRS neuroimaging

Near Infrared Spectroscopy (fNIRS) is a non-invasive functional neuroimaging technique based on neurovascular coupling allowing the quantification of haemodynamic flow variations, which enable an indirect estimation of neuronal activity. According to the principle of neurovascular coupling, an increase in the activity of neurons (electrical and metabolic) leads to an increase in blood volume and flow to compensate for the metabolic demand. This increase leads to changes in concentrations of oxy-haemoglobin (O_2Hb) and deoxy-haemoglobin (HHb), which can then be quantified by fNIRS. Theoretically, this increase in neuronal activity is expected to lead to a near symmetric (in timing but not amplitude; Pinti et al., 2020) increase in [O_2Hb] and decrease in [HHb]. Although this theorical pattern is well accepted, inverse patterns (e.g., decrease in [O_2Hb] and increase [HHb]) are sometimes found in experimental data, and have been described in motor imagery task (Holper et al., 2011; Abdalmalak et al., 2020). The causes of this inverse pattern are, at the moment, not well understood but some methodological explanations have been proposed in the literature. For

example, this could be caused by a poor localisation of the brain region of interest or unwanted subject movement during baseline periods. As a consequence, the quantified response amplitude would be underestimated due to poor baseline quantification or poor coverage of the targeted cortical areas by the fNIRS channels (measurement zone a source and a detector), leading to signal contamination due to changes in haemoglobin concentration in the undesired area (Abdalmalak et al., 2020).

It is also a possibility that the fNIRS signals recorded on a channel associated with a cerebral area may not be due to the effect of neurovascular coupling, but instead could be due to changes in intracerebral or extra-cerebral systemic activity evoked or not by the task (heart rate, respiration, Mayer wave etc). This could mask the haemodynamic response, leading to false negatives or, on the contrary, mimicking the haemodynamic response and leading to false positives (Tachtsidis & Scholkmann, 2016). The presence of this systemic noise could depend largely on the experimental protocol used (e.g., passive versus active tasks, involving large or small muscle groups) and on the individual participant studied (e.g., two participants could react differently to the same stressor) (Tachtsidis & Scholkmann, 2016).

Although several factors can affect the fNIRS signal, it has shown a strong correlation with the BOLD signal recorded in fMRI. Indeed, several authors have carried out studies to compare the task-related responses (e.g., activation) measured with fNIRS and fMRI in the frontal and parietal areas during a set of different cognitive tasks (Cui et al., 2011), and in the prefrontal cortex during a working memory task or sensorimotor areas during a finger tapping task (Sato et al., 2013). In Cui et al., (2011), it was reported that r = 0.26 for BOLD vs O_2Hb, and r = 0.23 for BOLD vs HHb. In Sato et al., (2013), the block averaged fNIRS signal was correlated in time with the BOLD signal from grey matter in PFC during a working memory task (r value was 0.69 ± 0.26 and −0.50 ± 0.35 for O_2Hb and HHb respectively) and sensorimotor cortex for a tapping task (r value was 0.69 0.60 ± 0.33 −0.56 ± 0.33 for O_2Hb and HHb respectively). Their results also show significant correlation in amplitude (i.e., a discrete measure extracted from the signal time series) between the signals from both devices during working memory

task (O_2Hb: r = 0.65, HHb: r = −0.76) but this was lower (O_2Hb: r = 0.52; HHb: r = −0.53) during tapping task. Similar results on connectivity metrics were also found for fNIRS, fMRI and EEG during simple and complex finger movement tasks (Anwar et al., 2016). All of these results suggest that the fNIRS signal is sufficiently reliable to quantify cortical activity. However, while fMRI remain the gold standard for neuroimaging, fNIRS has several advantages over fMRI, such as the quantification of changes in both O_2Hb and HHb concentration, a higher temporal resolution, low cost, relatively robust to motion artefacts and greater possibilities for experimentation in tasks involving motor skills. Nevertheless, although less restrictive than other tools such as fMRI, fNIRS has significantly lower spatial resolution, lower SNR and is limited to brain regions close to the scalp.

Indeed, to quantify the concentration of the two chromophores (O_2Hb and HHb), fNIRS uses near-infrared light of two different wavelengths that propagate through the human head, which is a scattering medium made up of heterogeneous elements (skin, bone, meninges, etc.). When light penetrates the head, part of this incident light is reflected, a part is absorbed, and a part is transmitted. Human biological tissues are relatively transparent for near infrared wavelength (650 to 1,000 nm), this allows a deeper penetration through the layers of the human head (Mandrick, 2013; Kohl-Bareis, 2012, Ferrari & Quaresima, 2012). The absorption of a chromophore, and hence their concentration in non-scattering homogeneous medium, can be quantified using the Beer Lambert law. Importantly, to be applied to an environment like the human head, it is necessary to include a correction term. This term is called the differential pathlength factor (DPF) and is a distance correction factor can be calculated based on subject's age (see Duncan et al., 1996).

The sensitivity of fNIRS to brain and extra-cerebral tissue (which tissues are probed by a given measurement: brain tissues, skull, scalp etc…) depends on the source-detector separation (e.g. inter-optode distance). This source-detector separation is a compromise between light penetration, which increases with separation length, signal-to-noise ratio, which also increases with separation length, and spatial resolution, which decreases with

separation length. The typical inter-optode distance in fNIRS is between 25–35 mm, resulting in a sensitivity to brain tissue of approximatively 8–13%, but it has been shown that there is 6% of total sensitivity to brain tissue for a 20 mm separation and that this sensitivity increases to 22% for a 65 mm separation (Strangman et al., 2013). The sensitivity of fNIRS to brain tissue is also dependant on the location of the optodes on the head (Strangman et al., 2013).

As previously mentioned, fNIRS measurements are also highly sensitive to the physiological aspects of extra-cerebral components. To reduce the impact of these extracerebral components on fNIRS measurements, based on the principle that light penetration depends on source-detector separation, it has been proposed to use short-distance channels with a separation of around 8.4 mm (Brigadoi & Cooper, 2015). The extra-cerebral components can then be removed from the fNIRS signal measured from long-distance channels, thus providing local concentrations of O_2Hb and HHb in cortical tissue.

While recommendations and methods exist to maximize sensitivity of fNIRS for measuring cortical activity, another point to bear in mind is that the fNIRS method is potentially sensitive to ambient light sources with wavelengths close to those of the fNIRS device (up to 750 nm). Of particular importance in the current thesis is the potential for crosstalk from the near-infrared light used during video-oculography. The following paragraphs will explain the various steps involved in creating a suitable optode array for the experimental work in Chapters 3 and 4, and how the problem of potential crosstalk between fNIRS and the EyeLink 1000 was addressed.

I.3 Optode array

During this PhD, two different fNIRS device were used with different constraints regarding the number of sources and detectors available, and thus the possible optode organisation (e.g. 6 sources, 8 detectors for the Brainsight device; 24 sources and 24 detectors for the NIRSsport2 device). The greater number of optodes available with the NIRSsport2 made it possible to use an

optode organisation based on the EEG 10-5 system, which is adopted in the pre-cut optode locations of the proprietary caps (i.e., EasyCap). Given the fewer optodes available with the Brainsight device, and the intention to examine the impact of a secondary working memory task in Chapter 3, it was decided to focus on prefrontal cortex. Using the proprietary cap, which uses pre-cut optode locations intended to maintain a 30mm inter-optode distance rather than alignment with specific cortical areas, it was necessary to decide based on simulations in Matlab where to locate the optodes to best cover prefrontal cortex. To this end, the first part of the process determined all possible links between the different pre-cut holes. Then, given that an optimal distance of approximately 30 mm between a NIRS source and detector to obtain an optimal ratio between penetration of light into tissues and spatial resolution, the next step involved the selection of all possible links with a distance between 25 and 35 mm, resulting in 466 possible channels (Figure I.1). Using the provided MNI (Montreal Neurological Institute) coordinates of each pre-cut hole, the three-dimensional coordinates for each channel were then obtained by calculating the midway point of the vector norm corresponding to the link between the pre-cut holes. Then, the Brodmann areas covered by the different channels were extracted via the NFRI function (Singh et al., 2005) from the MNI coordinates of the source-detector distance mid-point. The spatial organization of optodes and their location were then selected according to channels that best covered the key areas of interest in prefrontal cortex. Two channels out of the range (between 20mm and 25mm) were also included to maximise the coverage of prefrontal cortex. It has been shown that although not optimal, cerebral activity still detected up to 20 mm inter-optode distance (Strangman et al., 2013).

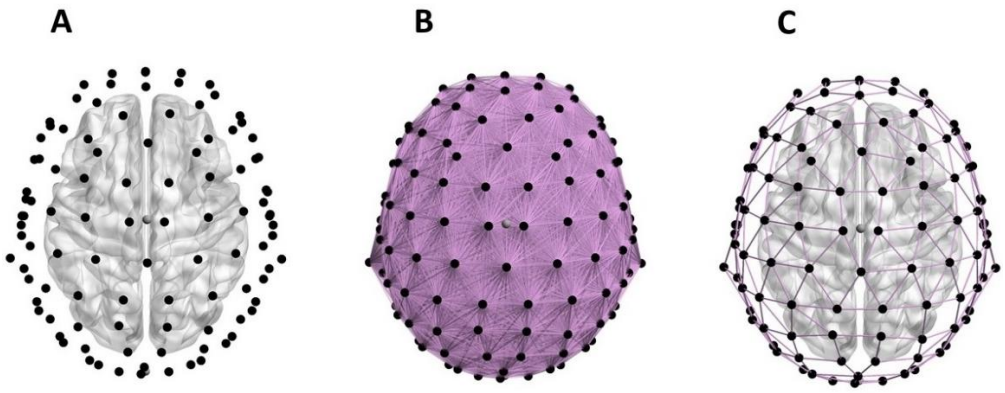

Figure I.1: *A) Spatial organisation of different Brainsight cap holes (Black dot) and Cz (Gray dot). B) Pink edge represents all possibilities of channels between. C) Pink edge represents all the possibilities of channels spaces from 2.5 to 3.5 cm. The figure was made using BrainNet viewer toolbox (Xia et al., 2013).*

I.4 Crosstalk analysis

Since the IR wavelengths of the video-oculography device used for eye-tracking (850 to 910nm) and fNIRS (705 and 830nm for Brainsight; 760 and 850nm for NIRSsport2) are close, a series of tests were conducted to determine the presence and impact of crosstalk on the fNIRS signal. It is common for manufacturers of fNIRS devices to advise covering the optode array with a piece of material or over-cap in order to minimise the impact of ambient light or other near-infrared light sources on the fNIRS signal. The same approach has been reported when combining fNIRS and eye tracking measurements (e.g. Urakawa et al., 2015; Shi et al., 2020). Here, then, an analysis was performed on fNIRS data collected with the two devices (i.e., Brainsight and NIRSport2) in order to determine the impact of crosstalk from the IR illuminator of the EyeLInk1000.

Data acquisition:

The testing session involved a series of resting state acquisitions, on a single male participant (35 years old with no known neurological conditions), in three conditions: 1) fNIRS recording without eye tracker and black material

(Rest condition), 2) fNIRS recording with eye tracker and black material *(Black condition)* and 3) fNIRS recording with eye tracker and without black material *(Eye condition)*. Each acquisition lasted for five minutes and was conducted with 2 different fNIRS devices (NIRSsport2 and Brainsight) and a single video-oculography device (EyeLink 1000). Each of the three conditions (e.g. Rest, Black, Eye) was repeated three times for both fNIRS devices, resulting in 18 recordings made on different days at different times.

Testing took place in a dark room, with the participant seated in front of the EyeLink on a height-adjustable chair, in front of the EyeLink IR illuminator, which was placed on a large table. The head was supported by a chin rest in order to minimize head movement, and the arms were resting comfortably on the table. The EyeLink IR illuminator power was set at 75% during the Black and Eye conditions. A calibration was also made to ensure the recording was as close as possible to a typical experimental testing condition. All the computer screens for Eyelink data acquisition and stimulus generation were turned off during testing, except the fNIRS recording screen. fNIRS data was recorded using a laptop placed behind the participant with the screen facing the opposite side of participant's head (i.e., to avoid light of the screen reaching the fNIRS optodes). These precautions were taken to avoid confounding factors.

The fNIRS signal was recorded using one channel located on right PFC. To ensure the tests were made in the same conditions for the Brainsight and NIRSsport2, a head band was made specifically for this study with pre-cut holes of 3.5cm distance. The head band was placed on participant's head before each acquisition by the same experimenter to ensure the source and detector was 2cm beneath the right eyebrow and at 2cm from Fpz.

Analysis:

Step 1: Analyses were performed on fNIRS signals that were not subjected to pre-processing (e.g., no artifact removal, no filtering) to limit any potential confounding effect of these steps. First, signal quality was checked using Quality Testing of Near Infrared Scans (QT-nirs) matlab toolbox (https://github.com/lpollonini/qt-nirs; Pollonini et al., 2016). The QT-nirs

method for signal quality is based on two different metrics. The first is the Scalp Coupling Index (SCI), which aims to quantify the prominence of the photoplethysmographic cardiac waveform in the fNIRS signal (see Figure I.2). For that, the fNIRS signal was band-pass filtered ([0.5 2.5Hz]) in order to extract the frequency corresponding to the cardiac rhythms. The signal was then normalized to its standard deviation to minimize the difference between the two chromophores. The zero-lag cross-correlation between the band-pass filtered Optical Density signals over a sliding window (param: 5 sec, non-overlap) was then computed and the median of these values was extracted. A threshold of 0.7 was then applied, such that only channels with an SCI higher or equal to the threshold is considered as good quality. The SCI value is dependent on the IR wavelength of the fNIRS system used for data collection. Indeed, the lower value of the wavelengths used by Brainsight (705nm; the more sensitive to HHb) is closer to the visible light spectra than the wavelength used by NIRSPort2 (760nm) and can lead to a noisier cardiac signal in the HHb signal and hence a lower SCI (Pollonini et al., 2016). To improve upon the SCI method, the second metric, Peak Power of the photoplethysmographic cardiac signal, was applied. This metric corresponds to the spectral peak power of the normalized cross-correlation signals (see Figure I.2). A threshold equal to or greater than 0.1 has been empirically proposed by Pollonini et al., (2016) to indicate a good quality signal.

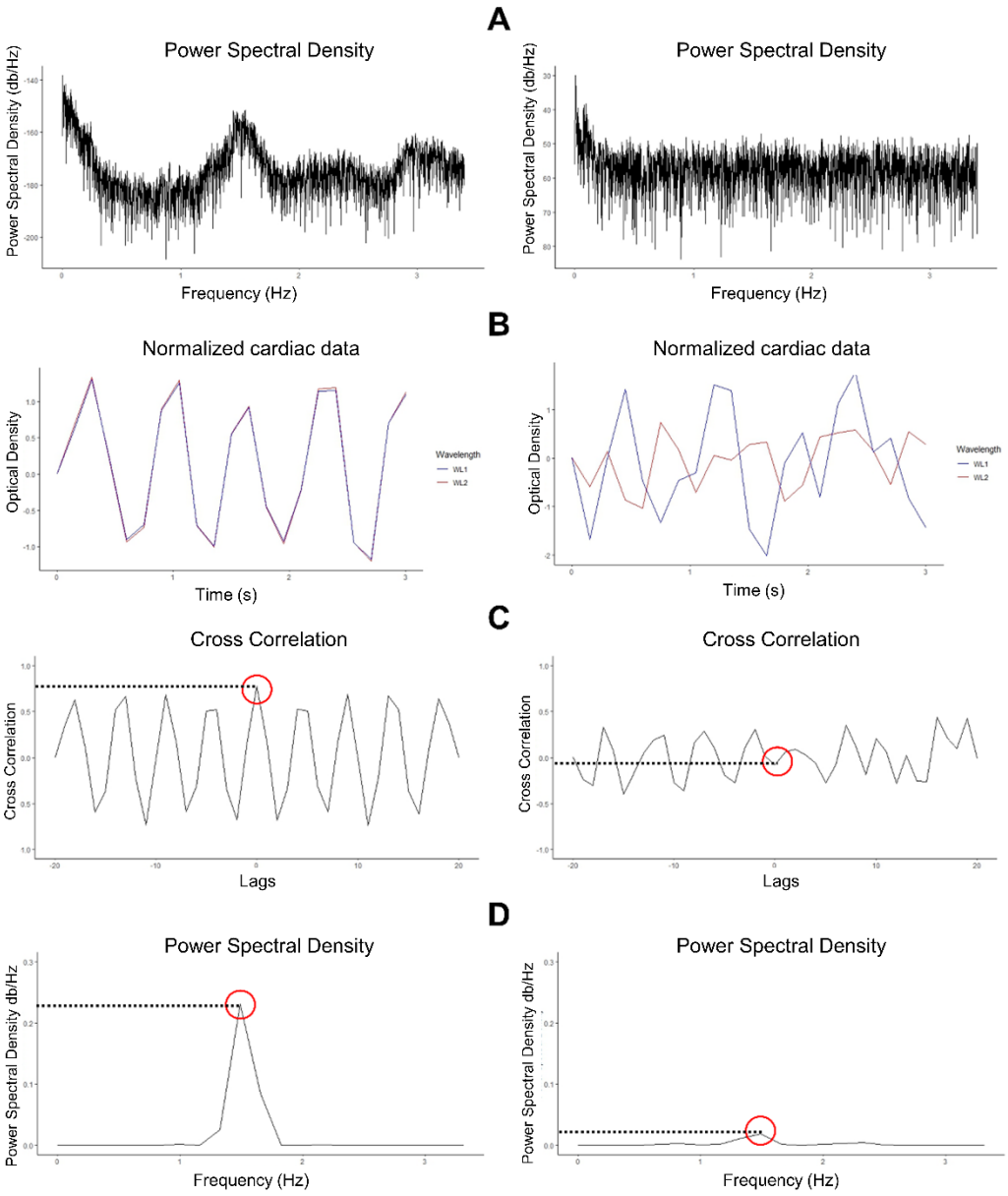

Figure I.2: *A) Power spectrum density obtained from a real fNIRS signal (O_2Hb). B) Real data from 3s fNIRS signal filtered using a band-pass ([0.5 2.5Hz]) and normalised to its standard deviation (O_2Hb in red and HHb in blue). C) Cross-correlation between the band-passed and normalised O_2Hb and HHb signals. The red circle shows the cross-correlation value at zero-lag (e.g. SCI value). D) Representation of the spectral peak power of the cross-correlation signals, red circle indicates the value of this peak (e.g. Peak Power value). Finally, the left panels show the values obtained for a signal considered as good, and the right panels show the values obtained for a signal considered as bad.*

For the crosstalk analysis, SCI and Peak Power were calculated from the single channel for each combination of condition and NIRS system. As can be seen in the left panel of Figure I.3 (red dashed line represents a threshold of 0.7 for SCI and 0.1 for Peak Power), the SCI was very close to 1 except for three acquisitions corresponding to the three repetitions of the Eye condition (EyeLink on and no black material to cover the optode) acquired with NIRSPort2. A similar but less pronounced pattern was evident for Peak Power. Still, it should be noted that the SCI and Peak Power for the Eye condition with NIRSPort2system were still above threshold, and thus the signal can be considered to be good.

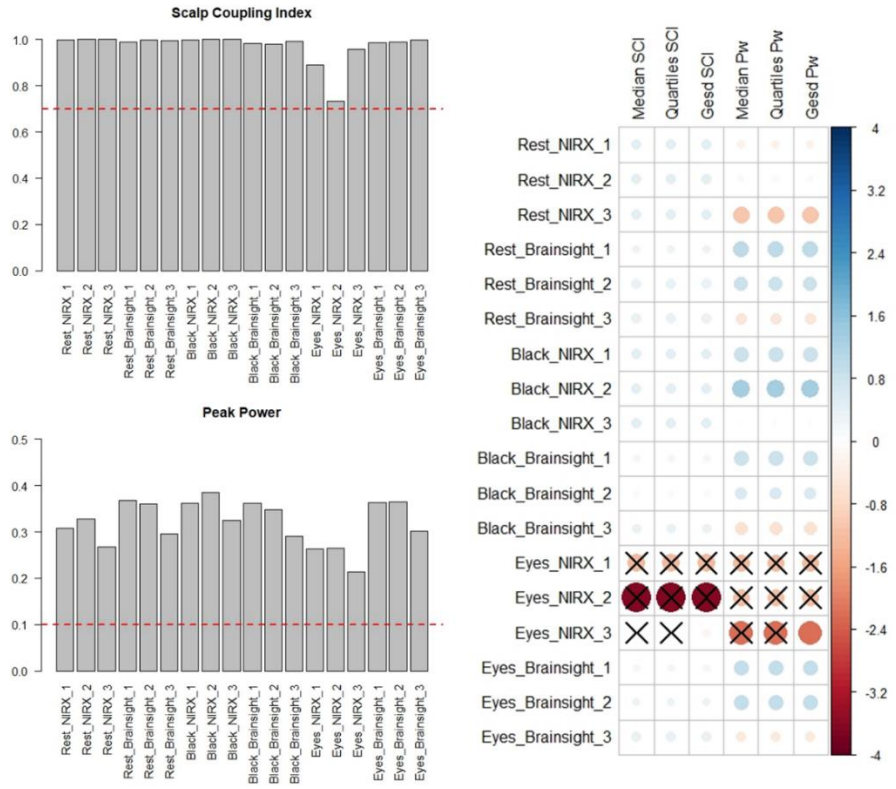

Figure I.3: *Left) Bar plot representing SCI value for each recording (top left panel) and Peak Power (bottom left panel). Right panel shows a heatmap representing the Z-score (colour and circle size). Each column corresponds to an outlier detection method. A black cross indicates value detected as an outlier.*

Step 2: In light of those results, a complementary step was performed in order detect if there were outliers that influenced the analysis. To this end, the Matlab function *isoutlier* was performed on normalised data (Z-scored SCI and Peak Power values) with three different methods available (median, quartiles and Generalised Extreme Studentised Deviate test (GESD)). The choice of using three different methods was made with the aim of finding consistency as the results of those methods has been shown to be variable, for example with response time data (Miller, 2023). A similar consensus-based approach for outlier detection has been proposed in Thériault et al., (2023) for R. The results presented in the right panel of Figure I.3 show that the signal recorded in the Eye condition by the NIRSPort2 was identified as an outlier by each method except for GESD.

Step 3: Threshold and outlier detection methods are forms of univariate analysis, which can result in a consensus between SCI and Peak Power not being reached. To examine this further, an unsupervised clustering method (Fuzzy C-Mean) was used with both metrics as input (Z-scored). This analysis was computed using the R library e1071, with parameters set at k = 2, iter-max = 500 and m = 2. The results from this bivariate analysis indicated that SCI and Peak Power from the Eye condition with NIRSport2 were not part of the same cluster as the other conditions (Figure I.4).

Step 4: Although the data from the Eye condition with NIRSport2 differ from the other conditions (Rest and Black), which may be a consequence of crosstalk from the EyeLink IR illuminator, it would still be considered as good quality by the QT-nirs method. It was therefore, decided to perform further analyses in an effort to understand if other features could be sensitive to a signal impacted by crosstalk and whether this effect is wavelength specific (e.g., only the higher NIRS wavelength that is closer to the wavelength of the EyeLink IR illuminator). To this end, the intensity data from each 5 minutes fNIRS acquisition were extracted and converted to Optical Density using the Homer2 function *hmr_Intensity2OD* (Huppert et al., 2009). Mass univariate features were then calculated and extracted using the Highly Comparative Time Series Analysis toolbox for Matlab (HCTSA v.1.9; Fulcher & Jones, 2017; Fulcher et al., 2013). This version includes 7729

features derived from multiple scientific fields (https://hctsa-users.gitbook.io/) and has been successfully applied in multiple research domains on time series data such as bold fMRI (St-Onge et al., 2023), EEG (Decat et al., 2022). Among all the features, variables were excluded when at least one special value was returned (not a number, no real value, or fatal errors). The final matrix resulted in a 36 by 6633 two-dimension dataset (3 repetitions of 3 conditions for each wavelength of the 2 NIRS devices; 1106 features were removed). The Z-score normalised matrix is shown in Figure I.5.

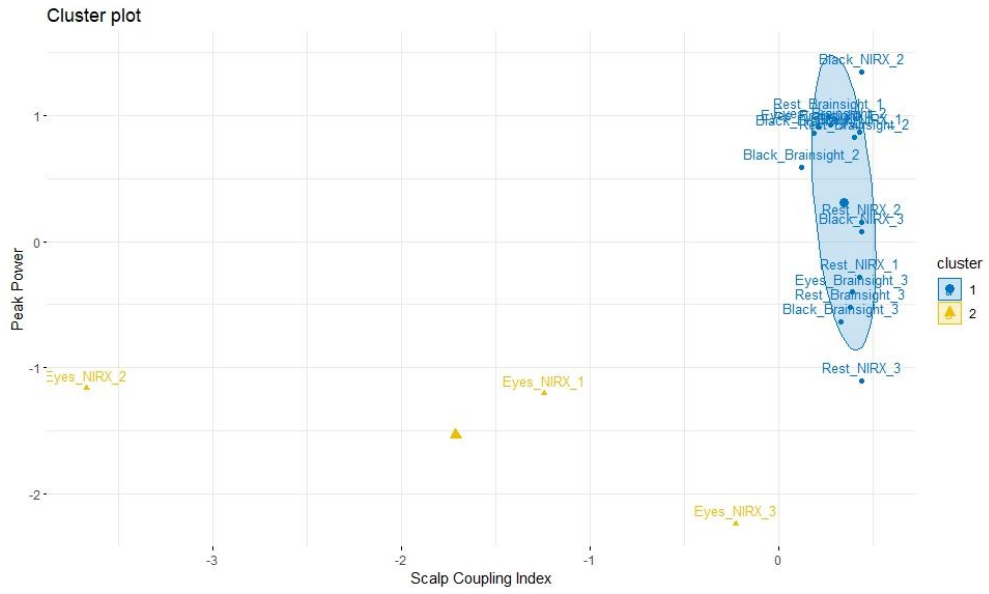

Figure I.4: *Representation of clusters obtained using Fuzzy C-Mean on the Z-scored SCI (x axis) and Peak Power (y axis). Colours reflect the principal membership to cluster 1 (blue) and 2 (yellow).*

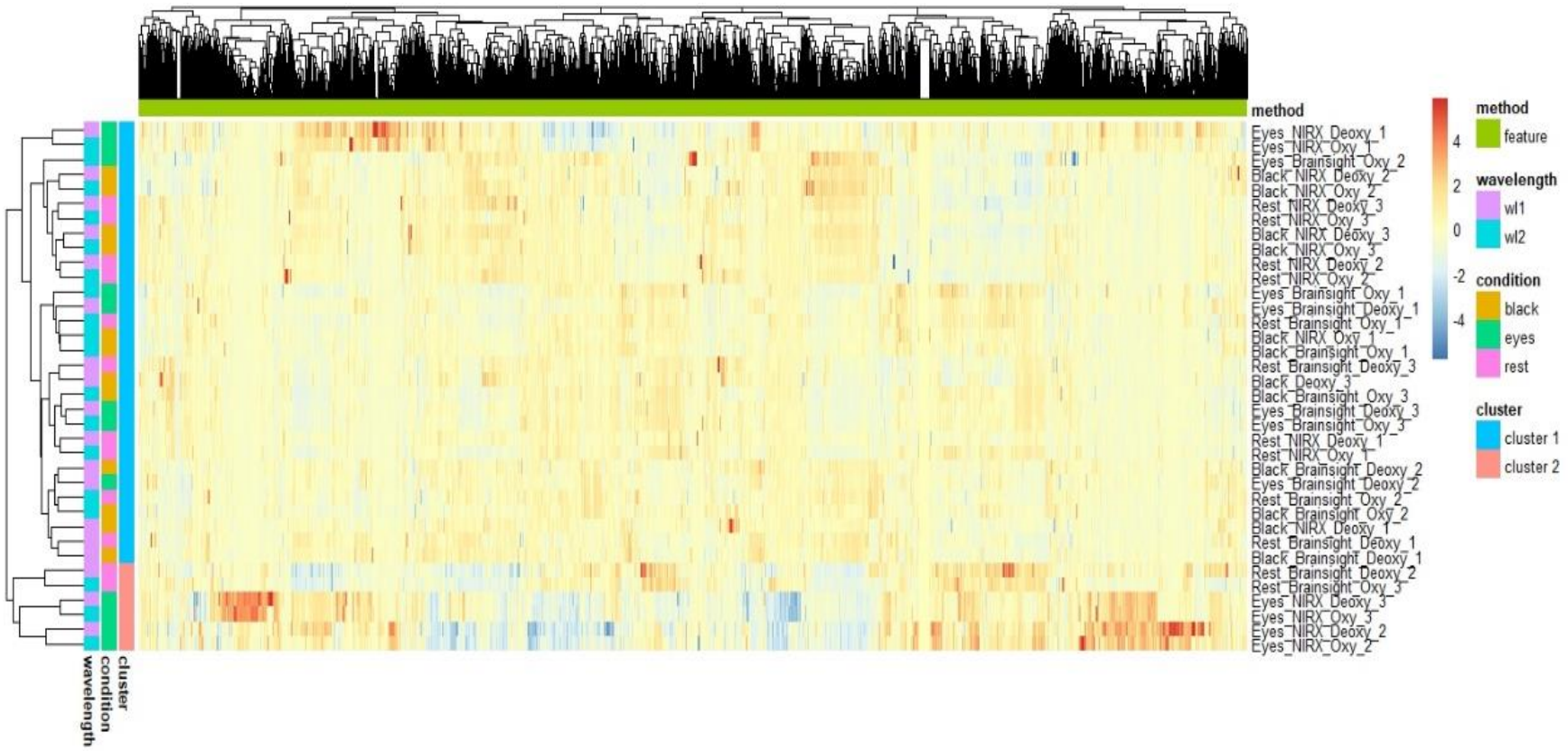

Figure I.5: *Heatmap of the 6633 Z-scored features. Each row corresponds to a condition (e.g. 36 rows corresponding to 3 repetitions of 3 conditions for each wavelength of the 2 NIRs devices) and column corresponds to the features (n= 6633). Tree on the bottom axis reflects the Euclidian distances between each time series. Tree on the left axis reflects the Euclidian distance between features. Clusters 1 and 2 (represented by a blue and salmon bar) are based on the time series tree. On the left, we can see that six conditions were identified as part of a different cluster including four conditions responding to two of the 3 trials recorded for the NIRx Eye condition (O_2Hb and HHb).*

Step 5: While it is interesting to extract numerous features that characterize time series data, one drawback of this approach is that it is not obvious from such a large matrix what meaningful information can be extracted. One of simplest approaches is to count the number of times in the 6633 features a time series is considered as an outlier compared to the other time series. For that, the same three outlier detection methods were computed for each feature extracted above from each of the 36 datasets. Figure I.6 shows radar plots based on the percentage of outliers detected. Again, a higher number of outliers were identified in the features for the NIRPort2 in the Eye condition (approximatively 20% depending on the methods used) compared to Black and Rest conditions for the two IR wavelengths (globally below 10%).

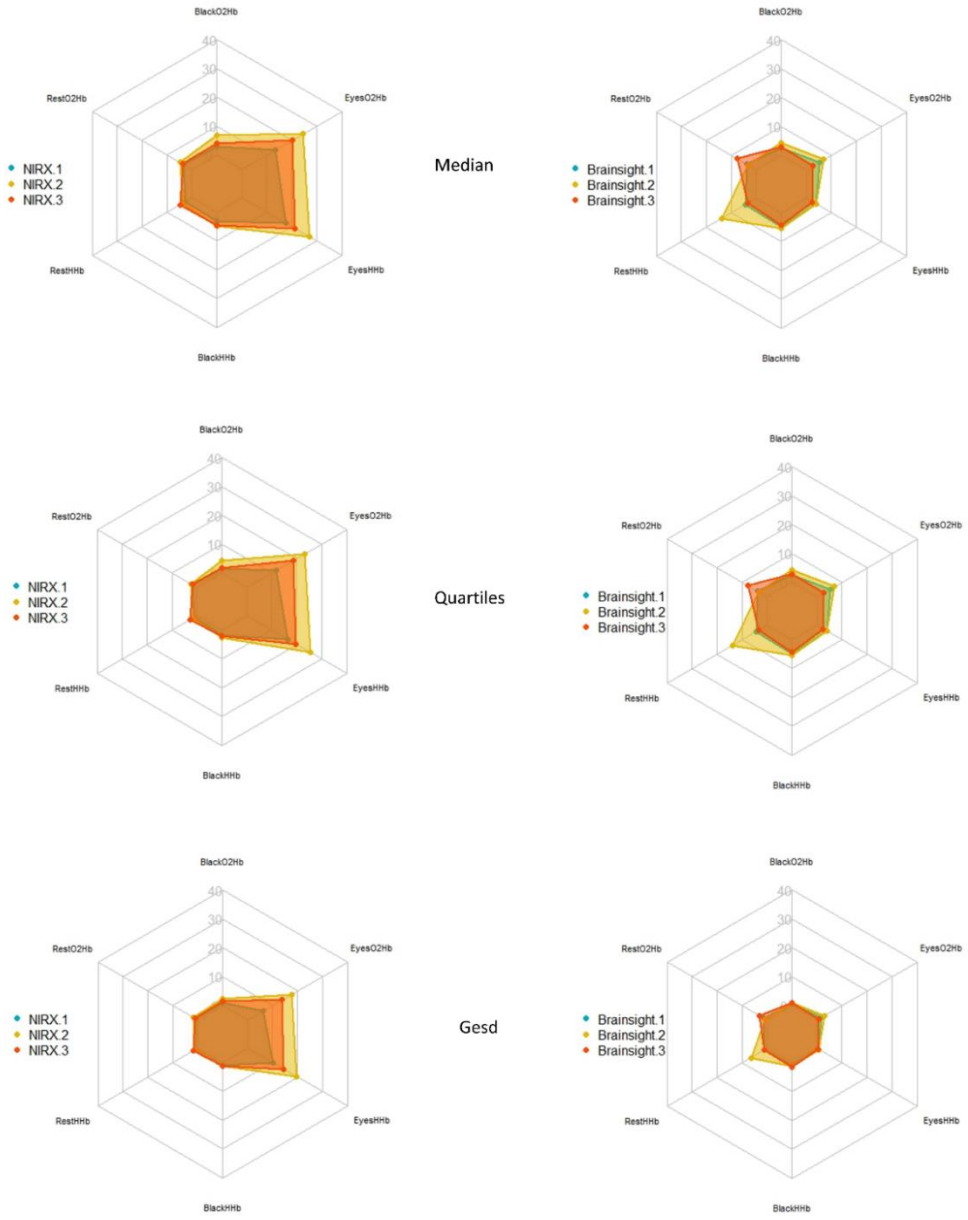

Figure I.6: *Radar plot representing the percentage of outliers detected over the 6633 features for the three trials (represented in blue, yellow and red overlapping colours) of the three conditions (Eye, Black and Rest) for the two IR wavelengths (each corner of the hexagram). Top panel shows the outlier detection based on the median, middle panel shows quartiles and bottom panel shows GESD. Left panels shows the results obtained for NIRSport2 data and right panels for Brainsight data.*

Step 6: Next, Fuzzy C-Mean was calculated based on the Z-scored HCTSA features (Figure I.7). Due to the huge number of dimensions, a principal component analysis (PCA) was applied to extract the linear combination of the two components that explain the largest part of the variance in the dataset (sum of PC1 and PC2 = 43.63%). As shown in the Figure I.7, data from the Eye condition with NIRSport2 are part of a different cluster than the other conditions. Also, the results show that there is not specific effect of wavelength.

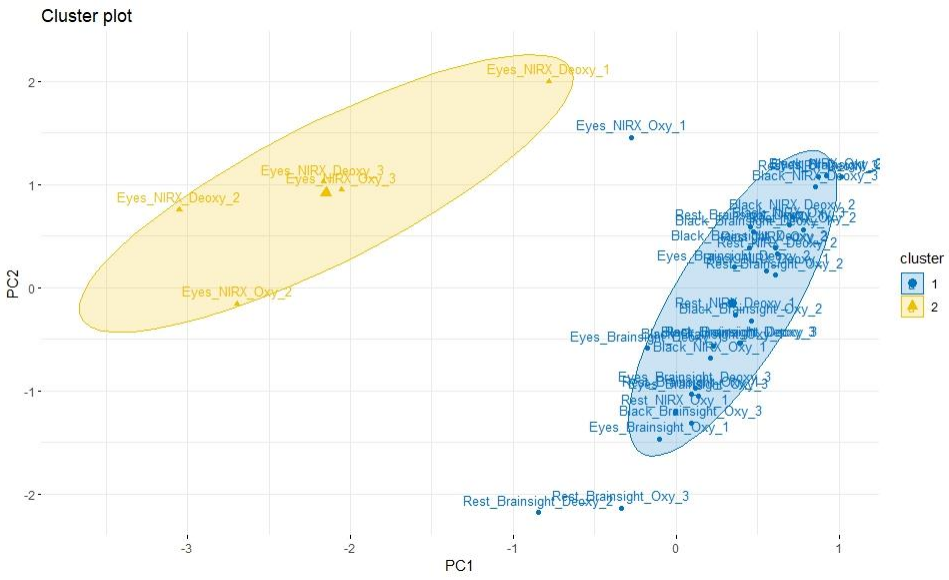

Figure I.7: *Representation of clusters obtain using Fuzzy C-Mean on the two principal components of the Z-scored HCTSA matrix. Colours reflect the principal membership to cluster 1 (blue) and 2 (yellow).*

To summarise, the main findings from the six steps of analysis suggest than the signal from the NIRSport2 in the Eye condition seems to stand out from the other conditions. However, with black material placed over the optode, this demarcation is no longer present. In fact, whatever the fNIRS system used, the current analyses did not distinguish between signals acquired in the

condition with black material and IR light from the EyeLink 1000 from those without the presence of IR light from the EyeLink 1000. These results suggest that there is a possibility that the fNIRS signal is impacted by the EyeLink IR illuminator, but this can be minimized in experimental testing with the Brainsight and NIRSport2 devices by covering the participant's head, and thus all optodes, with a piece of black material. However, while the main results of the six analysis steps seem consistent, a potential limitation must be considered as data from only one participant were analysed in this chapter.

Appendix II

MNI coordinate (x,y,z) for each channels of chapter 3 and estimated percentage of covering (%) of Brodmann areas (BA).

Channel	MNI	x	y	z	BA	%
1		46.8305	53.553	43.6895		
					9 - Dorsolateral prefrontal cortex	0.389978
					44 - pars opercularis, part of Broca's area	0.013072
					45 - pars triangularis Broca's area	0.232026
					46 - Dorsolateral prefrontal cortex	0.364924
2		28.799	69.4225	41.287		
					9 - Dorsolateral prefrontal cortex	0.404555
					10 - Frontopolar area	0.347072
					46 - Dorsolateral prefrontal cortex	0.248373
3		10.8195	75.4625	40.996		
					9 - Dorsolateral prefrontal cortex	0.398721
					10 - Frontopolar area	0.585288
					46 - Dorsolateral prefrontal cortex	0.015991
4		-11.9065	75.0315	40.218		
					9 - Dorsolateral prefrontal cortex	0.377014
					10 - Frontopolar area	0.56928
					46 - Dorsolateral prefrontal cortex	0.053706
5		-28.257	69.7315	39.6795		
					9 - Dorsolateral prefrontal cortex	0.332965
					10 - Frontopolar area	0.34292
					46 - Dorsolateral prefrontal cortex	0.324115
6		-44.1425	54.6685	42.8635		
					9 - Dorsolateral prefrontal cortex	0.347439
					44 - pars opercularis, part of Broca's area	0.004454
					45 - pars triangularis Broca's area	0.214922
					46 - Dorsolateral prefrontal cortex	0.433185
7		51.9255	56.81	29.0525		
					9 - Dorsolateral prefrontal cortex	0.053506
					10 - Frontopolar area	0.091328
					45 - pars triangularis Broca's area	0.333948
					46 - Dorsolateral prefrontal cortex	0.521218

8	33.894	72.6795	26.65		
				9 - Dorsolateral prefrontal cortex	0.087642
				10 - Frontopolar area	0.605609
				11 - Orbitofrontal area	0.011394
				46 - Dorsolateral prefrontal cortex	0.295355
9	54.9365	59.317	12.748		
				10 - Frontopolar area	0.222586
				11 - Orbitofrontal area	0.001637
				45 - pars triangularis Broca's area	0.293781
				46 - Dorsolateral prefrontal cortex	0.481997
10	34.683	75.9055	9.466		
				10 - Frontopolar area	0.618721
				11 - Orbitofrontal area	0.212329
				46 - Dorsolateral prefrontal cortex	0.157534
				47 - Inferior prefrontal gyrus	0.011416
11	10.7065	80.599	26.779		
				9 - Dorsolateral prefrontal cortex	0.075194
				10 - Frontopolar area	0.920484
				46 - Dorsolateral prefrontal cortex	0.004322
12	-12.0195	80.168	26.001		
				9 - Dorsolateral prefrontal cortex	0.075586
				10 - Frontopolar area	0.895743
				46 - Dorsolateral prefrontal cortex	0.028671
13	11.4955	83.825	9.595		
				10 - Frontopolar area	0.846621
				11 - Orbitofrontal area	0.153379
14	-11.5795	83.6285	8.895		
				10 - Frontopolar area	0.823016
				11 - Orbitofrontal area	0.176984
15	-34.9875	71.1615	25.562		
				9 - Dorsolateral prefrontal cortex	0.055304
				10 - Frontopolar area	0.533998
				11 - Orbitofrontal area	0.010879
				45 - pars triangularis Broca's area	0.009973
				46 - Dorsolateral prefrontal cortex	0.389846
16	-50.873	56.0985	28.746		
				9 - Dorsolateral prefrontal cortex	0.036087
				10 - Frontopolar area	0.05603
				45 - pars triangularis Broca's area	0.366572

				46 - Dorsolateral prefrontal cortex	0.541311
17	-34.5475	74.622	8.456		
				10 - Frontopolar area	0.564743
				11 - Orbitofrontal area	0.196568
				46 - Dorsolateral prefrontal cortex	0.224649
				47 - Inferior prefrontal gyrus	0.014041
18	-55.2325	57.0905	12.554		
				10 - Frontopolar area	0.147737
				45 - pars triangularis Broca's area	0.374893
				46 - Dorsolateral prefrontal cortex	0.47737

Appendix III

Bonferroni-corrected pairwise comparisons on main effect of Channel for local efficiency in Chapter 3 indicated the following differences:

Channel *1* lower ($p < 0.01$) than channel *3* (MD = 1.27e-02), *8* (MD = 1.29e-02), *11* (MD = 1.16e-02), *12* (MD = 1.20e-02), *13* (MD = 1.17e-02) and *14* (MD = 1.26e-02)

Channel *16* lower ($p < 0.05$) than channel *3* (MD = 1.77e-02), *4* (MD = 1.25e-02), *7* (MD = 1.04e-02), *8* (MD = 1.80e-02), *9* (MD = 9.88-03), *10* (MD = 1.41e-02), *11* (MD = 1.66e-02), *12* (MD = 1.70e-02), *13* (MD = 1.67e-02), *14* (MD = 1.77e-02), *15* (MD = 1.23e-02), *17* (MD = 1.04e-02).

Channel *6* lower ($p < 0.05$) than channel *2* (MD = 1.18e-02), *3* (MD = 2.02e-02), *4* (MD = 1.50e-02), *7* (MD = 1.30e-02), *8* (MD = 2.05e-02), *9* (MD = 1.24e-02), *10* (MD = 1.66e-02), *11* (MD = 1.91e-02), *12* (MD = 1.95e-02), *13* (MD = 1.93e-02), *14* (MD = 2.02e-02), *15* (MD = 1.48e-02), *17* (MD = 1.29e-02) and *18* (MD = 1.20e-02)

Channel *5* lower ($p < 0.05$) than channel *3* (MD = 1.15e-02), *8* (MD = 1.18e-02), *11* (MD = 1.04e-02), *12* (MD = 1.08e-02), *13* (MD = 1.05e-02) and *14* (MD = 1.15e-02).

Appendix IV

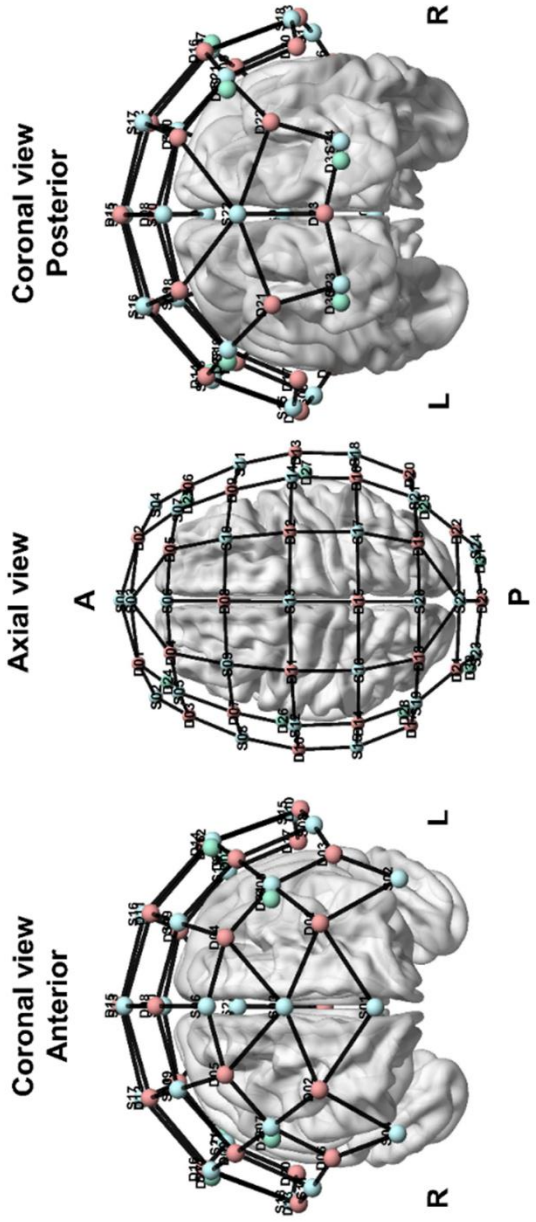

Figure IV.1: *Representation of channels included in each ROI (one colour per ROI)*

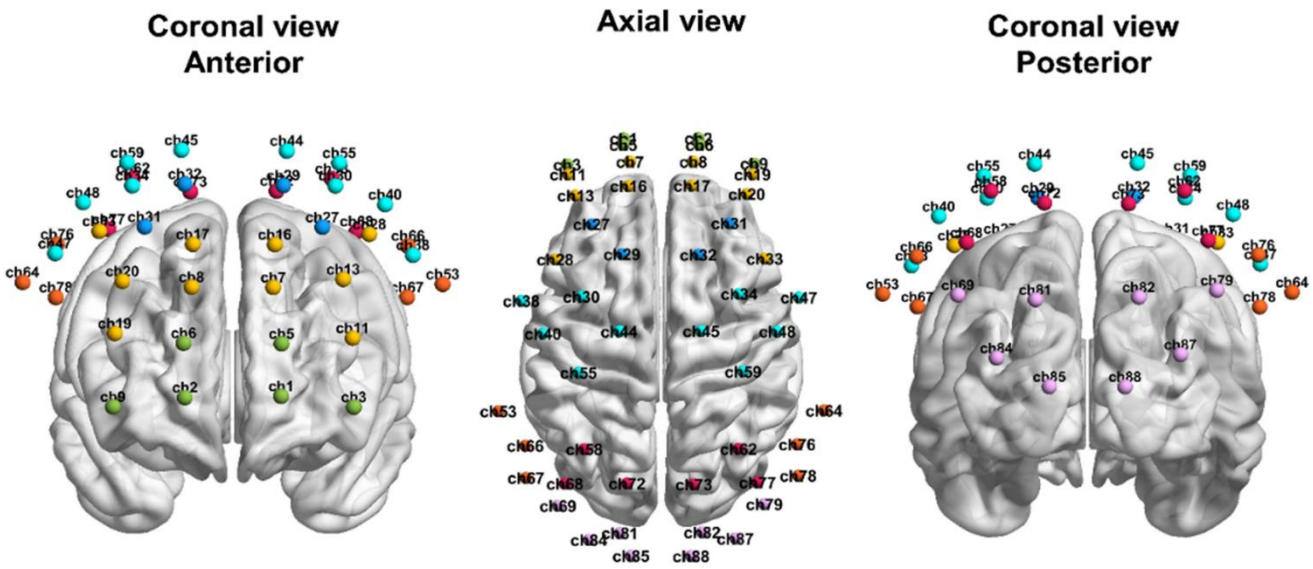

Figure IV.2: *Representation of the 24x24 full optode organisation (emitters = light red dots; receivers = light blue dots) and channels (black edges).*